



EnMAP Ground Segment

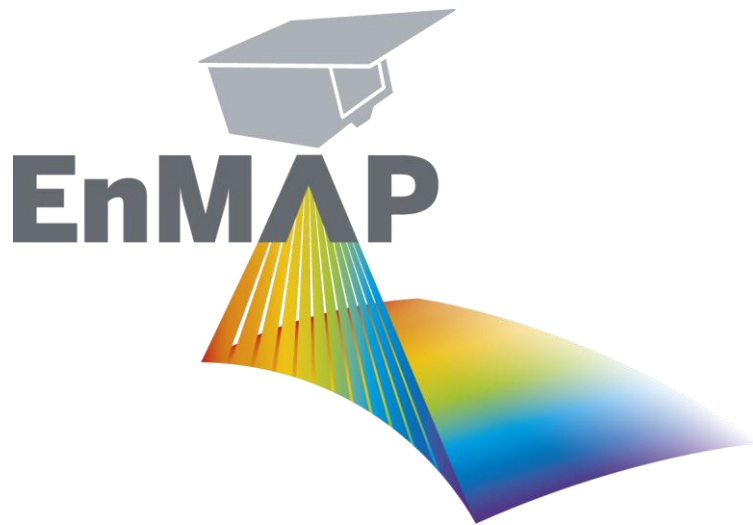
Mission Quarterly Report #09

01.07.2024 to 30.09.2024

Restriction: public

Doc. ID	EN-GS-RPT-1109
Issue	1.0
Date	09.01.2025

Configuration Controlled: Yes



German Remote Sensing Data Center (DFD)
Remote Sensing Technology Institute (IMF)
German Space Operations Center (GSOC)
German Research Centre for Geosciences (GFZ-Potsdam)
German Space Agency at DLR

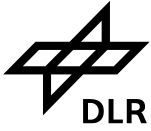


TABLE OF SIGNATURES

Prepared

Date Emiliano Carmona, (DLR MF-PBA, EnMAP OMM)

Date Sabine Chabrilat, (GFZ-Potsdam, EnMAP SciLead)

Reviewed

Date Daniel Schulze, (DLR RB-MIB, dep. EnMAP OMM)

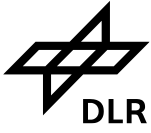
Date Sabine Engelbrecht, (DLR DFD-INF, EOC PAD)

Date Robert Größel, (DLR RB-CTA, GSOC PAD)

Date Karl Segl, (GFZ-Potsdam, dep. EnMAP SciLead)

Approved & Released

Date Laura La Porta, (DLR AR-AO, EnMAP MM)



DISTRIBUTION LIST

The document is publicly available via www.enmap.org.

CHANGE RECORD

Version	Date	Chapter	Comment
1.0	09.01.2025	All	First issue of Mission Quarterly Report #09 corresponding to 01.07.2024 to 30.09.2024. Corrected parameter in Table 7-18 (RID SE-KA-0004)

Custodian of this document is Carmona, Emiliano.



CONTENTS

Table of Signatures	2
Distribution List	3
Change Record	3
Contents	4
List of Figures	4
List of Tables	7
1 Introduction	9
1.1 Purpose	9
1.2 Scope	9
2 References	10
3 Terms, Definitions and Abbreviations	11
4 Mission	12
4.1 Mission Objectives	12
4.2 Mission Description	12
4.3 Mission Status Summary	13
5 Users and Announcements-of-Opportunities	15
5.1 Users	15
5.2 Announcements-of-Opportunities	16
6 Archived and Delivered Observations	18
6.1 Archived Observations	18
6.2 Delivered Observations	21
6.2.1 Delivered L2A products from the Download service (EOC Geoservice)	23
7 Detailed Status	24
7.1 User Interfaces	24
7.2 Satellite	24
7.2.1 Orbit	24
7.2.2 Life Limited Items	25
7.2.3 Redundancies	25
7.3 Ground Stations	26
7.3.1 S-Band	26
7.3.2 X-Band	26
7.4 Processors	26
7.5 Calibrations	27
7.5.1 Dead Pixels	28
7.5.2 Spectral Calibration	29
7.5.3 Radiometric Calibration	32
7.5.4 Geometric Calibration	39
7.6 Internal Quality Control	39
7.6.1 Archive	39
7.6.2 Level 1B	41
7.6.3 Level 1C	51
7.6.4 Level 2A	56
8 External Product Validation	69
9 Others	71

LIST OF FIGURES

Figure 5-1	Number of registered users per country	16
Figure 6-1	Geographic location of all Earth observation tiles archived, World	19
Figure 6-2	Geographic location of all Earth observation tiles archived, Europe	20
Figure 6-3	Cloud coverage in [%] of archived Earth observation tiles	21
Figure 6-4	Observation angle of archived Earth observation tiles	21
Figure 6-5	Levels of delivered Earth observation tiles from acquisition orders	22
Figure 6-6	Levels of delivered Earth observation tiles from catalog orders	22
Figure 7-1	Number of ACS Precise Modes per day during Q3 2024	25
Figure 7-2	Decay per day from Lamp (RAD), Linearity (LIN) and Spectral (SPC) measurements for low gain (top) and high gain (bottom)	28
Figure 7-3	Average percentage change in the VNIR radiometric coefficients for five selected bands since launch	28
Figure 7-4	VNIR Dead Pixel Mask	28
Figure 7-5	SWIR Dead Pixel Mask.....	29
Figure 7-6	VNIR (top) and SWIR (bottom) center wavelength in nm.....	30
Figure 7-7	Change in center wavelength per spectral pixel for VNIR (top) and SWIR (bottom). Left panels show the changes with respect to current spectral calibration table in use and right panels with respect to the previous measurements.	31
Figure 7-8	VNIR (top) and SWIR (bottom) FWHM in nm	32
Figure 7-9	VNIR (top) and SWIR (bottom) calibration coefficient in mW/cm ² /sr/μm.....	34
Figure 7-10	Percentage change in VNIR Calibration Coefficients (top) and SWIR Calibration Coefficients (bottom).....	34
Figure 7-11	VNIR (top) and SWIR (bottom) gain matching calibration coefficients	35
Figure 7-12	VNIR (top) and SWIR (bottom) response non-uniformity coefficients	36
Figure 7-13	SNR contour map for[VNIR high gain from the LED linearity observations observed on 12.09.2024. The reference radiance is shown with a blue line. Contour lines with SNR values of 150 and 500 are also shown in black.	37
Figure 7-14	SNR contour map for VNIR low gain from the LED linearity observations observed on 12.09.2024. The reference radiance is shown with a blue line. Contour lines with SNR values of 150 and 500 are also shown in black. The mission requirement is evaluated at 495 nm for a radiance value of 36 mW/cm ² /sr (marked with a black cross) and is expected to be greater than 500.....	37
Figure 7-15	SNR contour map for SWIR high gain from the LED linearity observations observed on 12.09.2024. The reference radiance is shown with a blue line. Contour lines with SNR values of 150 and 500 are also shown in black. The mission requirement is evaluated at 2200 nm for a radiance value of 0.5 mW/cm ² /sr (marked with a black cross) and is expected to be greater than 150.	38
Figure 7-16	SNR contour map for SWIR low gain from the LED linearity observations observed on 12.09.2024. The reference radiance is shown with a blue line. Contour lines with SNR values of 150 and 500 are also shown in black.	38
Figure 7-17	VNIR estimated spectral shift at 760 nm w.r.t the valid spectral calibration table (CTB_SPC), and relative spectral stability expressed at 1 sigma (Q3 2024, 17228 tiles)	44
Figure 7-18	Center wavelengths per cross-track pixel based on the spectral calibration table (VNIR band 62) in the calibration table (CTB_SPC).....	44
Figure 7-19	SWIR estimated spectral shift at 2050 nm w.r.t the valid spectral calibration table (CTB_SPC, shown below), and relative spectral stability expressed at 1 sigma (Q3 2024, 18226 tiles)	45
Figure 7-20	Center wavelengths per cross-track pixel based on the spectral calibration table (SWIR band 86).....	45
Figure 7-21	Datatake used (Tadschikistan)	45

Figure 7-22	Canada scene, band 80 (2005 nm) with standard (center) and new (right) DC correction. Color table "haze".	47
Figure 7-23	Canada scene, difference image between old and new processing	47
Figure 7-24	Canada scene, absolute difference statistics between the current and the new DC processing.	48
Figure 7-25	Canada scene, relative difference statistics between the current and the new DC processing.	48
Figure 7-26	Canada scene, single pixel spectra - current processing in red, new DC in white.	49
Figure 7-27	Libya 4, RGB (left), band 80 (2005 nm) with standard (center) and new (right) DC correction. Color table "haze".	50
Figure 7-28	Turkmenistan scene, relative difference statistics between the current and the new DC processing.	50
Figure 7-29	Turkmenistan scene, single pixel spectra - current processing in red, new DC in white.	.51
Figure 7-30	Assessment of RMSE values, calculated based on found ICPs, for all datatakes where ICP could be found	52
Figure 7-31	Mean deviation of EnMAP L1C products in pixel (left). RMSE value for EnMAP L1C products in pixel (right).	53
Figure 7-32	Mean deviation in pixel between VNIR and SWIR data of EnMAP L1C products (left). RMSE in pixel between VNIR and SWIR data of EnMAP L1C Products (right)	54
Figure 7-33	Development of co-registration accuracy based on the previous geometric QC reports	.55
Figure 7-34	Scene-ID 88772; RGB-Quicklook with Bands 611.02nm – 550.69nm – 463.73nm	57
Figure 7-35	Scene-ID 88772; Geomask with Land in green, shadow in red, clouds in brown, cirrus in blue	57
Figure 7-36	Scene-ID 86285; RGB-Quicklook with Bands 611.02nm – 550.69nm – 463.73nm	58
Figure 7-37	Scene-ID 86285; Signal sampled at location 'AC 1'; red: measured signal, blue: corrected signal	58
Figure 7-38	Scene-ID 86285; Signal sampled at location 'AC 2'; red: measured signal, blue: corrected signal	59
Figure 7-39	Scene-ID 86285; Quality mask in greyscale where white corresponds to 1, i.e. best overall quality	60
Figure 7-40	Normalized Water Leaving Reflectance of scene-ID 86285; Wavelengths for RGB: 611.02nm – 550.69nm – 463.73nm	60
Figure 7-41	Scene-ID 86285; nWLR sampled at location nWLR 1	61
Figure 7-42	Scene-ID 86285; nWLR sampled at location nWLR 2	61
Figure 7-43	EnMAP L2A false colour composites (bands 155-108-50) of scenes DT1849 Tile 14 and DT95871 Tile 24 and their corresponding masks (QL quality classes)	63
Figure 7-44	EnMAP L2A false colour composites (155, 108, 50) of scene 43267 Tile 7 and Tile 8 with zoom on the overlapping area.	63
Figure 7-45	Comparison of image spectra of the two neighbouring tiles (scene 43267 Tile 7 and Tile 8, solid and dashed lines resp.)	64
Figure 7-46	Typical image spectra (single pixel) of vegetation of the different years (white=2022, red=2023, green=2024)	64
Figure 7-47	Typical image spectra (single pixel) of of water bodies of the different years (white=2022, red=2023, green=2024)	65
Figure 7-48	Cloud mask, QL quality classes and EnMAP L2A false colour composite (155, 108, 50) of DT95871 Tile 24 showing misclassification of cloud shadow as water bodies (in white in the center image).	65
Figure 7-49	Image spectra of classified water bodies (DT95871 Tile 24), whereas only the white spectra corresponds to water, the other three correspond to cloud shadow over dense dark vegetation	66

Figure 7-50	Image spectra of classified water bodies (DT43267 Tile 7), whereas only the white, red and green spectra correspond to water, the other three correspond to cloud shadow over dense dark vegetation.....	66
Figure 7-51	Time series of EnMAP L2A CIR colour composites (bands 155-108-50), Wuerzburg area, Germany.	67
Figure 7-52	Typical image spectra (single pixel) of trees of the different years; each color represents a pixel within the 4 different times.....	67
Figure 7-53	Cloud mask, QL quality classes and EnMAP L2A CIR colour composite for the 4 years.	68

LIST OF TABLES

Table 2-1	References.....	10
Table 5-1	Number of registered users per continent (number of user countries during reporting period).....	15
Table 5-2	Number of registered and approved users per category (Cat-1 Science and Cat-1 Distributor)	16
Table 5-3	Number of released science proposals per Announcement-of-Opportunity (AOs#) and total number of requested and granted tiles per AO#.....	16
Table 5-4	Number of accepted science proposals and total number of requested and granted tiles per topic	17
Table 6-1	Number and size of archived and not archived products	18
Table 6-2	Number and size of delivered products	18
Table 7-1	Status of life-limited items.....	25
Table 7-2	S-Band Ground Station Passes.....	26
Table 7-3	X-Band Ground Station Passes.....	26
Table 7-4	Number and size of archived radiometric and spectral calibration observations	27
Table 7-5	Number and percent of dead pixels.....	28
Table 7-6	Number and size of archived spectral calibration observations	29
Table 7-7	Generated spectral calibration tables	32
Table 7-8	Number and size of archived radiometric calibration observations	32
Table 7-9	Generated radiometric calibration tables	39
Table 7-10	Generated new geometric calibration tables	39
Table 7-11	Overall quality rating statistics	39
Table 7-12	Overall quality rating in relation to Sun Zenith Angle (SZA)	40
Table 7-13	Reduced and low quality rating statistics.....	40
Table 7-14	QualityAtmosphere rating statistics	40
Table 7-15	QualityAtmosphere rating in relation to Sun Zenith Angle (SZA)	40
Table 7-16	QualityAtmosphere rating in relation to Cloud Cover and DDV availability	41
Table 7-17	Dead pixel statistics, VNIR.....	42
Table 7-18	Dead pixel statistics, SWIR.....	42
Table 7-19	Saturation statistics, VNIR	42
Table 7-20	Saturation statistics, SWIR	42
Table 7-21	Artifacts statistics (without striping), VNIR	43
Table 7-22	Artifact statistics (without striping), SWIR	43

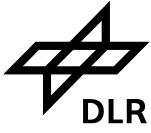


Table 7-23	Validated CTB_RAD	45
Table 7-24	Validated CTB_SPC	46
Table 7-25	Improvement of geometric performance	54
Table 7-26	Datatake IDs of analyzed water products	56
Table 7-27	Datatake ID of analyzed land products	62



1 Introduction

1.1 Purpose

This mission quarterly report (MQR) states information on the EnMAP mission status with regard to the registered user community, announcements-of-opportunities and observations as well as the status of the user interfaces, satellite (platform and payload), ground stations (S-band and X-band), processor (Archive, Level 1B, Level 1C, Level 2A (land and water)), calibration (spectral, radiometric, geometric), data quality control and validation of EnMAP.

Please visit www.enmap.org for further information on EnMAP.

1.2 Scope

This ninth Mission Quarterly Report (MQR) applies to the operations of EnMAP in the reporting period of Routine Phase (RP) from **01.07.2024 to 30.09.2024 (Q3 2024)**.

2 References

Reference Identifier	Document Identifier and Title
[1]	L. Guanter et al. (2015) The EnMAP Spaceborne Imaging Spectroscopy Mission for Earth Observation. Remote Sensing, Issue 7, pp. 8830-8857.
[2]	EN-GS-UM-6020 Portals User Manual, Version 1.4
[3]	EN-PCV-ICD-2009 Product Specification, Version 1.8
[4]	EN-PCV-TN-4006 Level 1B ATBD, Version 1.9
[5]	EN-PCV-TN-5006 Level 1C ATBD, Version 1.6
[6]	EN-PCV-TN-6007 Level 2A (land) ATBD, Version 2.2
[7]	EN-PCV-TN-6008 Level 2A (water) ATBD, Version 3.1
[8]	Chabrillat, S. et al. (2022) EnMAP Science Plan. EnMAP Technical Report, DOI: 10.48440/enmap.2022.001
[9]	Storch, T.; Honold, H.-P.; Chabrillat, et al. The EnMAP imaging spectroscopy mission towards operations. Remote Sens. Environ. 2023, 294, 113632. DOI: 10.1016/j.rse.2023.113632

Table 2-1 References



3 Terms, Definitions and Abbreviations

Terms, definitions and abbreviations for EnMAP are collected in a database which is publicly accessible via Internet on www.enmap.org.

An Earth observation of swath length $n \times 30$ km (and swath width 30 km) is separated into n tiles of size 30 km \times 30 km.

4 Mission

4.1 Mission Objectives

The primary goal of EnMAP (Environmental Mapping and Analysis Program) is to measure, derive and analyze quantitative diagnostic parameters describing key processes on the Earth's surface [1].

During the mission operations, with the successful launch on 1st of April 2022 and an expected operational mission lifetime of at least 5 years, EnMAP will provide valuable information for various application fields comprising soil and geology, agriculture, forestry, urban areas, aquatic systems, ecosystem transitions.

4.2 Mission Description

The major elements of the EnMAP mission are the EnMAP Space Segment, built by OHB System AG and owned by the German Space Agency at DLR, the EnMAP Ground Segment built and operated by DLR institutes DFD, MF, RB, and the EnMAP User and Science Segment represented by GFZ. The project management of the EnMAP mission is responsibility of the German Space Agency at DLR.

The EnMAP Space Segment is composed of

- the platform providing power and thermal stability, orbit and attitude control, memory, S-band uplink/downlink for TM/TC data transmission/reception, X-band downlink for payload data transmission, and
- the payload realized as a pushbroom imaging dual-spectrometer covering the wavelength range between 420 nm and 2450 nm with a nominal spectral resolution ≤ 10 nm and allows in combination with a high radiometric resolution and stability to measure subtle reflectance changes.

The EnMAP satellite is operated on a sun-synchronous repeat orbit to observe any location on the globe with comparable illumination conditions. This allows a maximum reflected solar input radiance at the sensor with an acceptable risk for cloud coverage.

The EnMAP Ground Segment is the interface between Space Segment and User and Science Segment. It comprises functionalities to

- perform planning of imaging, communication and orbit maneuver operations, provision of orbit and attitude data, command and control of the satellite, ground station networks (in particular: Weilheim, Germany, for S-band and Neustrelitz, Germany, for X-Band), receive satellite data, perform long-term archiving and delivery of products, and
- perform processing chain (for systematic and radiometric correction, orthorectification, atmospheric compensation), instrument calibration operations, and the data quality control of the products.

The EnMAP mission interfaces to the international science and user community through the EnMAP Portal www.enmap.org with official information related to EnMAP by DLR and GFZ-Potsdam (as the document in hand) and links for ordering observations and products.

The EnMAP Science Segment is represented by the EnMAP Science Advisory Group chaired by the mission principal investigator at the GFZ-Potsdam. The Science Segment addresses aspects such as

- supporting and performing validation activities to improve sensor performance and product quality
- developing scientific and application research to fully exploit the scientific potential of EnMAP [8] including provision of software tools for EnMAP data processing and analyses (EnMAP-Box) and provision of teaching and education materials (HYPERedu)
- Organizing workshops, summer schools and in general information, training and networking activities for the user community

The EnMAP User Segment is the community of German and international users ordering acquisitions and accessing products of EnMAP.

4.3 Mission Status Summary

The mission successfully finished the commissioning phase (CP) on 01.11.2022 [9] and entered its routine phase (RP) on 02.11.2022. In the reporting period, from 01.07.2024 to 30.09.2024, there have been no major issues affecting the instrument or the satellite. The mission has been operating normally with only one outage of 4 days duration (01-04 September 2024) caused by the known “DSHA SAFETY MODE”, that was followed by a VNIR SAFETY_MODE that required to be investigated in more detail before operations could resume. Additionally, other DSHA SAFETY MODES happened during this quarter during a high solar activity period without creating any serious challenge, except for the loss of observation time. No consequences for the mission or the data quality have been observed after these events and, like in previous quarters, the mission is regularly reaching and surpassing the initial maximum acquisition capacity of 5000 km / day thanks to the changes introduced during the last year. At the end of the period, the back-to-back mode is fully integrated and working without problem in the EnMAP planning system and it is used for 26.5% of the acquisitions performed.

In this period, 1819 Earth observations of 30 km swath width and up to 990 km swath length were successfully performed which resulted in 17288 archived Earth observation tiles of 30 km × 30 km and 27 calibration acquisitions. In addition, 17140 products were delivered from catalog orders. In total, 12592 Earth observations were performed until 30.09.2024 by the EnMAP team and the 3786 registered Science users. This results in 99455 archived Earth observation tiles (137174 products including the different versions of the re-processed products) and 181116 Earth products delivered to users from observations requests (98277) and catalogue orders (82839) since the start of the mission. More details are presented in Section 5 and 6.

The following limitations are applicable at 30.09.2024:

- Striping effects in SWIR data in the along-track direction more visible in uniform areas with a strong spectral gradient.

Other effects observed in the data by our Quality Control team are reported in section 7.6 while they are investigated in more detail.

The following changes were implemented in the reporting period:

- The path names of the files ordered through EOWEB have been shortened to improve the compatibility of the EnMAP products with Windows systems where there is a maximum path length of 256 characters.
- Re-processing of archived products is in progress. Priority processing is now assigned to the oldest data (commissioning phase). On these data the co-registration errors are larger, what makes the re-processing of the data more necessary for them. Reprocessed products can be identified with **archived version ≥ 01.03.01** in the EnMAP archive. Reprocessed products benefit from improved co-registration accuracy, improved absolute geometric performance and addition of VC-AUX products for improved data screening. The re-processing will continue over the coming months. For more details on geometric performance check Section 7.6.3.

In addition, in August 2024 it was announced the availability of EnMAP products through the EOC Geoservice (<https://geoservice.dlr.de/>) and the EOlab platform (<https://eo-lab.org/>). These possibilities allow the direct download of EnMAP L2A products generated by the EnMAP Ground Segment with a standard set of parameters. Since these L2A products are already processed, users can directly download these products without waiting times, allowing a fast way to get large amounts of EnMAP products from the mission archive. Notice that both EOC Geoservice and EOlab are not part of the standard services offered by the EnMAP mission and would require registration in these additional services. More information on the number of products downloaded through Geoservice can be found in section 6.2.1.

The following changes are expected to be performed in the next quarters:

- New processor version (V01.05.01) that shall introduce:
 - view angles in the metadata of L1C and L2A products
 - Fixes adjacency correction on L2A products around very small clouds
 - Implemented SWIR dark signal correction at L1B level

-
- Correction of radiometric striping in the along-track direction.
 - Complete re-processing of archived data (see note above concerning re-processed data improvements).
 - Implementation of measures to improve planning and acquisition activities, in particular the minimum size of a datatake will be changed from 1 tile to 3 tiles
 - Implementation of new linearity calibration (and updated calibration) to improve the VNIR-SWIR matching between spectrometers, specially at low radiances

5 Users and Announcements-of-Opportunities

5.1 Users

	Country/Continent (No of Countries)	Reporting Period 01.07.2024 to 30.09.2024	Since beginning of routine Phase until 30.09.2024 (end of reporting period)
<i>Total European Users</i>	<i>Europe (21)</i>	170	1903
European	• Germany	45	751
	• Italy	12	161
	• France	19	158
	• United Kingdom	16	121
	• Spain	21	98
	• Netherlands	8	82
	• Portugal	0	29
	• Turkey	5	55
	• Greece	4	38
	• Belgium	3	35
	• Poland	5	53
	• Austria	3	31
• Others (9)	29	251	
<i>Non European</i>	<i>North America (4)</i>	57	521
	<i>South America (5)</i>	38	198
	<i>Asia (19)</i>	141	859
	<i>Africa (12)</i>	20	153
	<i>Australia + New Zealand (2)</i>	18	152
	<i>Total (63)</i>	444	3786

Table 5-1 Number of registered users per continent (**number of user countries during reporting period**)

Decrease compared to previous values is caused by inhibition of user roles due to inconsistent or invalid UMS registration data.

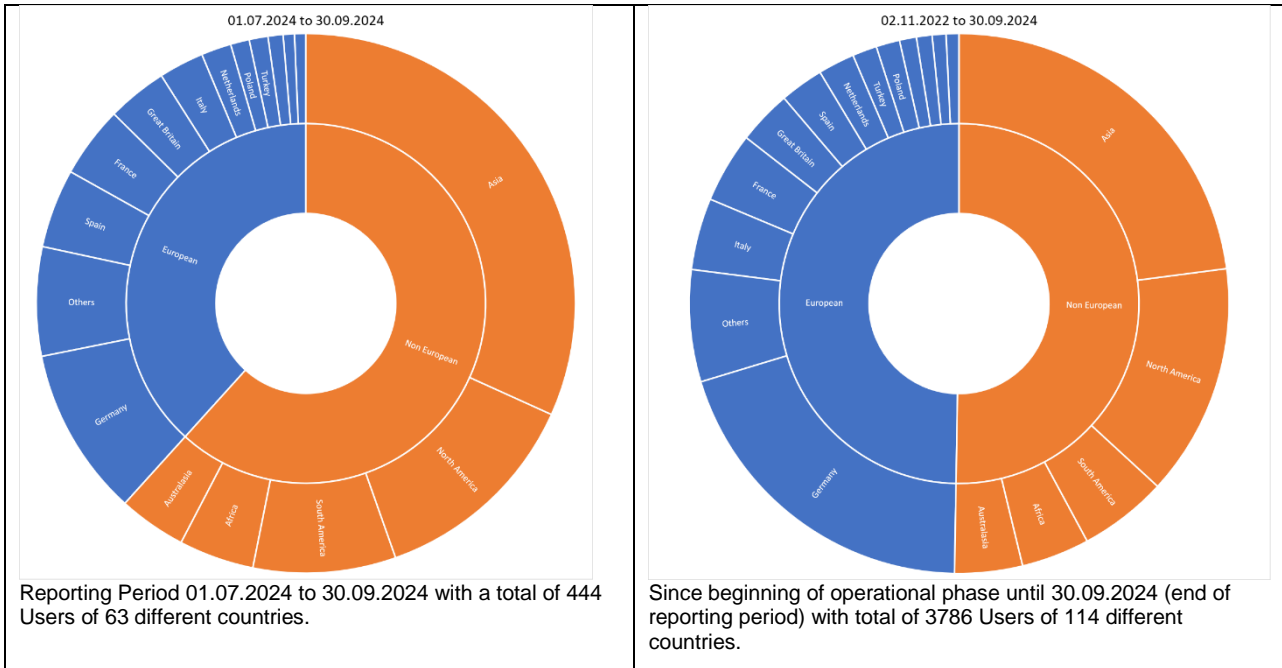


Figure 5-1 Number of registered users per country

Registered users belong to different categories, therefore e.g. All/World ≠ Science/World + Others/World.

User per Category		New within reporting period 01.07.2024 to 30.09.2024	Since beginning of routine phase start until 30.09.2024 (end of reporting period)
Registered users	Total	444	3786
	with role assignment*	357	2772
Cat-1 Science	Total	303	2233
	AO Process 00001*	303	2130
	AO Process 00002*	0	603
	AO Process 00003*	0	184
Cat-1 Distributor**	Total	288	2119

Table 5-2 Number of registered and approved users per category (Cat-1 Science and Cat-1 Distributor)

*Registered users with at least one active user role assignment

**Catalogue User, ordering EnMAP data from archive

5.2 Announcements-of-Opportunities

Announcement-of-Opportunity	New within reporting period 01.07.2024 to 30.09.2024			Since beginning of routine Phase until 30.09.2024 (end of reporting period)		
	Proposals	Total tiles requested	Total tiles granted	Proposals	Total tiles requested	Total tiles granted
A00001	66	12405	2684	507	41804	17435
A00002	2	130	46	125	20560	9385
A00003	0	0	0	4	151	97
Total	68	12535	2730	636	62515	26917

Table 5-3 Number of released science proposals per Announcement-of-Opportunity (AOs#) and total number of requested and granted tiles per AO#.










Icon	Topic	New within reporting period 01.07.2024 to 30.09.2024			Since beginning of routine Phase until 30.09.2024 (end of reporting period)		
		Proposal	Total tiles requested	Total tiles granted	Proposal	Total tiles requested	Total tiles granted
	VEGETATION	25	5294	1195	248	31609	12455
	GEO/SOIL	26	2693	285	197	9836	4523
	WATER	10	3410	180	81	8467	3027
	SNOW/ICE	0	0	0	14	1990	806
	URBAN	0	0	0	9	834	315
	ATMOSPHERE	5	127	59	28	3721	1369
	HAZARD/RISK	1	12	12	12	352	295
	METHODS	0	0	0	15	945	542
	CAL/VAL	1	999	999	32	4761	3585
	Total	68	12535	2730	636	62515	26917

Table 5-4 Number of accepted science proposals and total number of requested and granted tiles per topic

6 Archived and Delivered Observations

The following table shows the number of archived Earth Observation and Calibration products and their sizes within the specified time frames. Reason for “Archived = No” is that datatakes were commanded but no data arrived at the Processing System HSI.

Type	Archived		Reporting Period 01.07.2024 to 30.09.2024		Since beginning of Commissioning Phase until 30.09.2024 (end of reporting period)	
			Number Tiles / Observations	Size (in GB)	Number Tiles / Observations	Size (in GB)
Earth Observation (EO)	Yes	Total	17288 / 1819	8423.88	137174 / 12592	66840.49
		Average / Day	187.91 / 19.77	91.56	150.08 / 13.77	73.12
	No	Total	65		975	
		Average / Day	0.70		1.06	
Calibration (CAL)	Yes	Total	27	112.74	365	1524.13
		Average / Day	0.29	1.22	0.39	1.66
	No	Total	0		3	
		Average / Day	0.00		0.003	

Table 6-1 Number and size of archived and not archived products

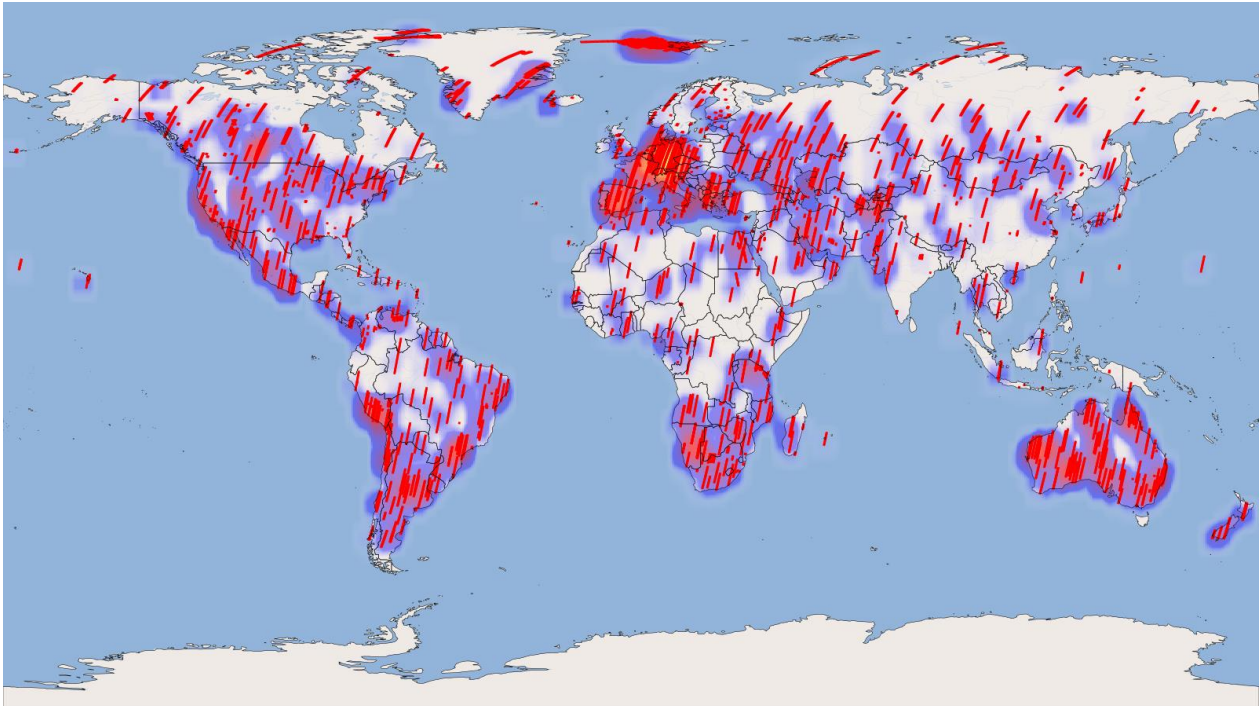
The following table shows the number of delivered products and their sizes within the specified time frames. Product deliveries result either directly from acquisition orders (“Observation”) or catalog orders (“Archive”).

Type	Delivered		Reporting Period 01.07.2024 to 30.09.2024		Since beginning of Commissioning Phase until 30.09.2024 (end of reporting period)	
			Number Tiles / Observations	Size (in GB)	Number Tiles / Observations	Size (in GB)
Earth Observation (EO)	Observation	Total	18108 / 1562	43301.77	98277 / 9724	8061.45
		Average / Day	196.82 / 16.97	47.37	107.52 / 10.63	87.62
	Archive	Total	17140	472689.67	82839	106186.11
		Average / Day	186.30	517.16	90.63	1154.19
Calibration (CAL)	Observation	Total	29	874.30	200	116.77
		Average / Day	0.314	0.95	0.215	1.26
	Archive	Total	0	3486.14	67	0.0
		Average / Day	0.0	3.81	0.07	0.0

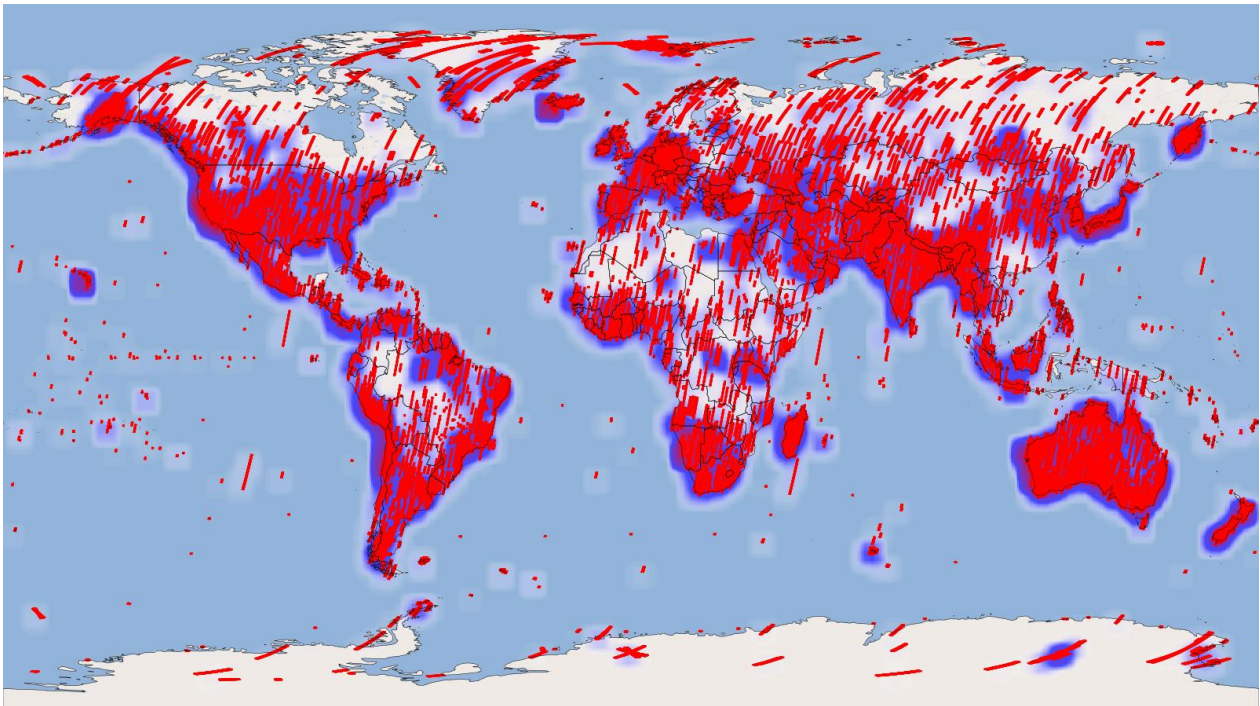
Table 6-2 Number and size of delivered products

6.1 Archived Observations

The following figures show the heatmaps for the whole world and for Europe within the specified time frames. The heatmaps represent the frequencies of products at a geographic location, where the number of products increases from blue over red to yellow.

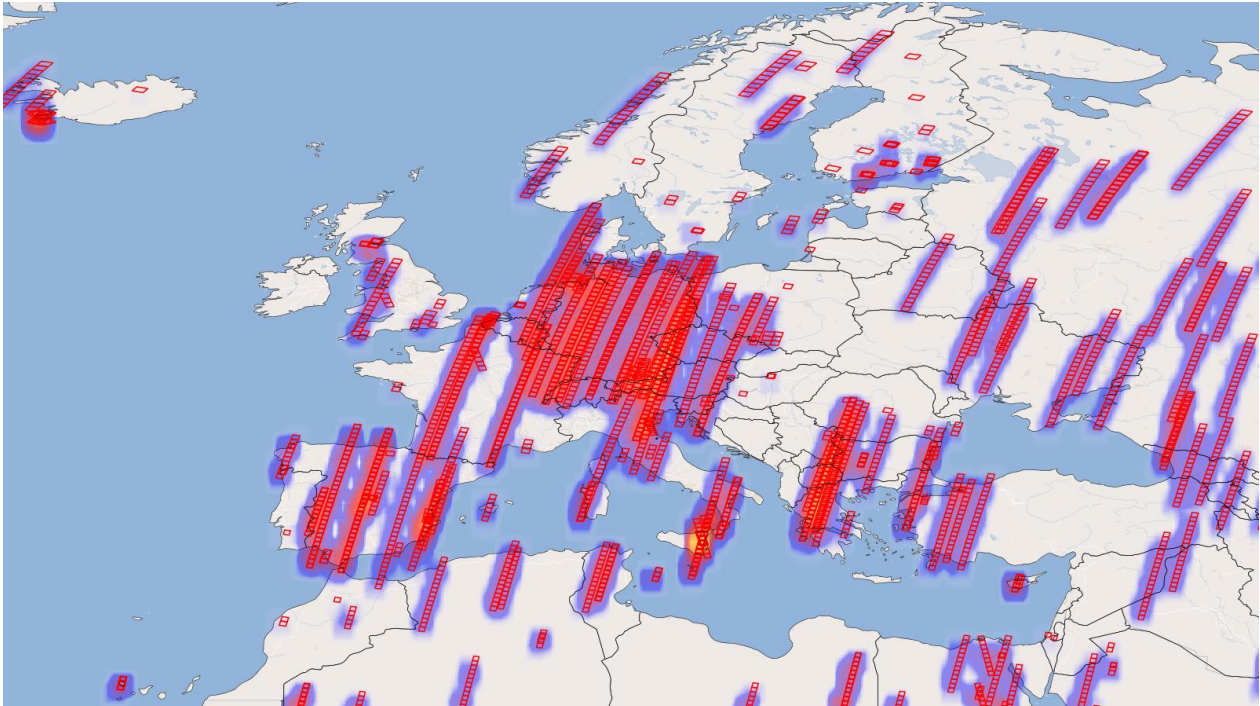


reporting period 01.07.2024 to 30.09.2024 with 17288 tiles

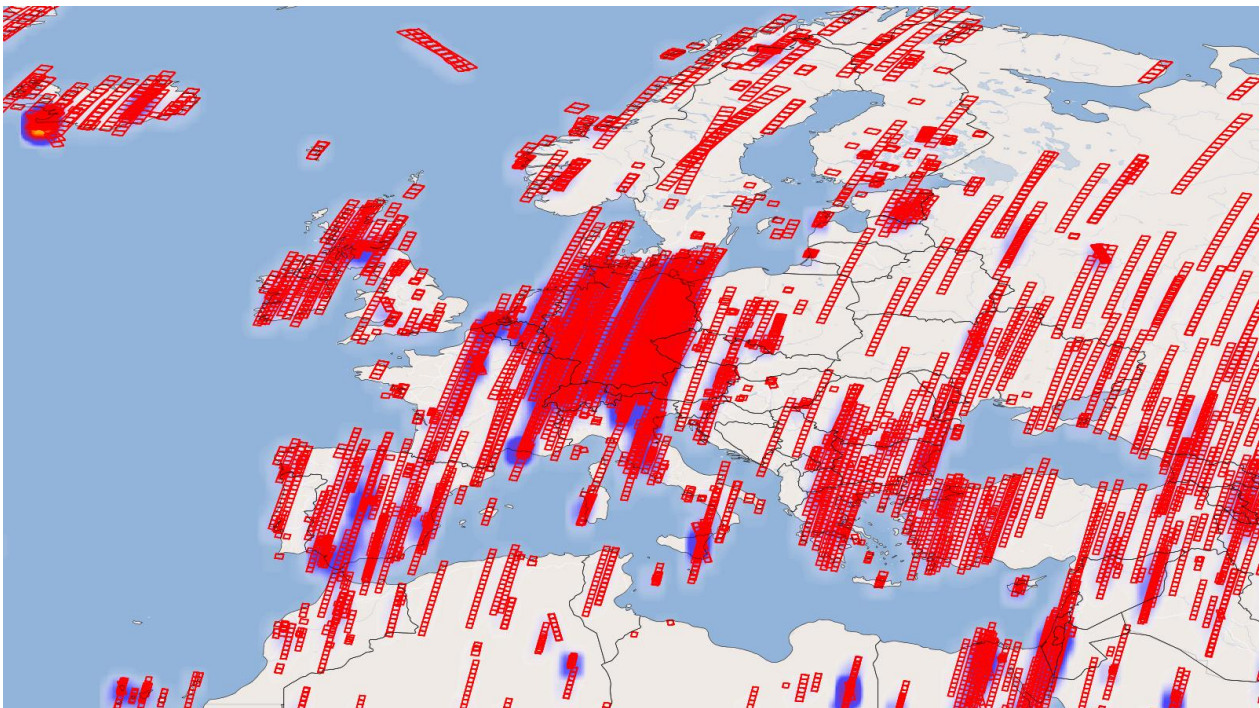


reporting period 2022-04-01 to 30.09.2024 with 137174 products (includes commissioning phase acquisitions and different versions of the same tiles)

Figure 6-1 Geographic location of all Earth observation tiles archived, World



reporting period 01.07.2024 to 30.09.2024 Europe

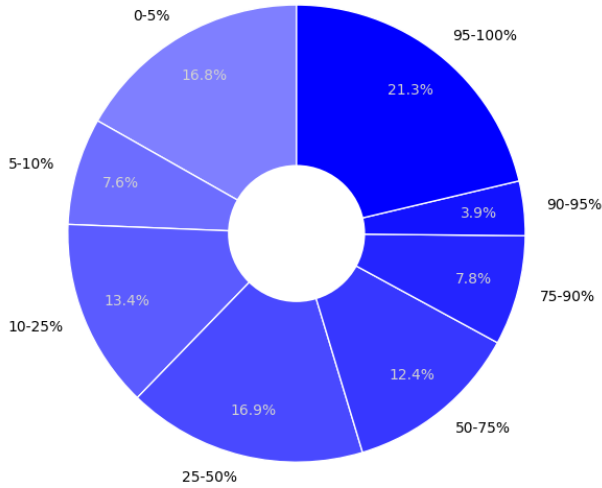


reporting period 2022-04-01 to 30.09.2024 Europe (includes commissioning phase acquisitions)

Figure 6-2 Geographic location of all Earth observation tiles archived, Europe

The following figures show the distribution of cloud coverage for the archived products.

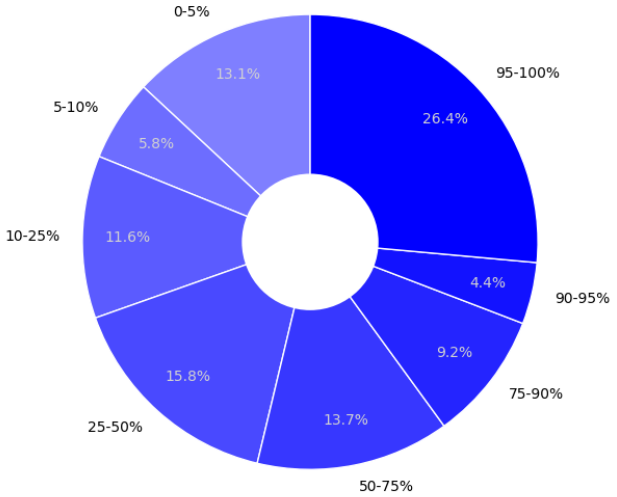
Cloud coverage in [%] of archived Earth observation tiles



reporting period 2024-07-01 - 2024-10-01 , tiles: 17288

period 01.07.2024 to 30.09.2024, tiles 17288

Cloud coverage in [%] of archived Earth observation tiles



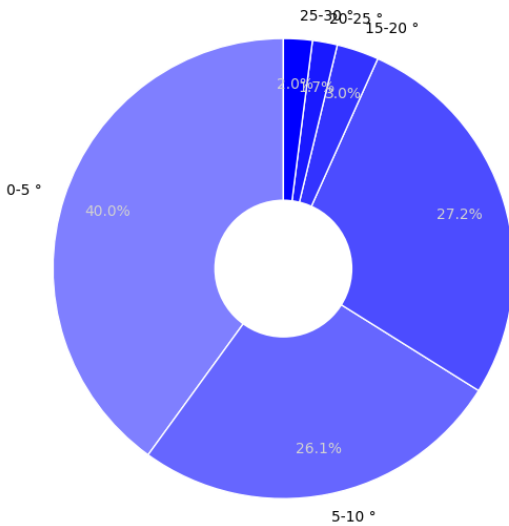
reporting period 2022-04-01 - 2024-10-01 , tiles: 137174

Until 30.09.2024, tiles 137174 (includes commissioning and all versions)

Figure 6-3 Cloud coverage in [%] of archived Earth observation tiles

The following figures show the distribution of observation angles for the archived products.

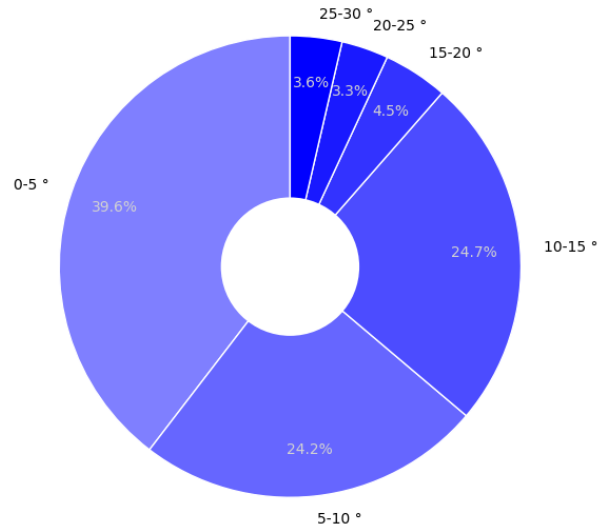
Observation angle in degrees [°] of archived Earth observation tiles



reporting period 2024-07-01 - 2024-10-01 , tiles: 17288

period 01.07.2024 to 30.09.2024, tiles 17288

Observation angle in degrees [°] of archived Earth observation tiles



reporting period 2022-04-01 - 2024-10-01 , tiles: 137174

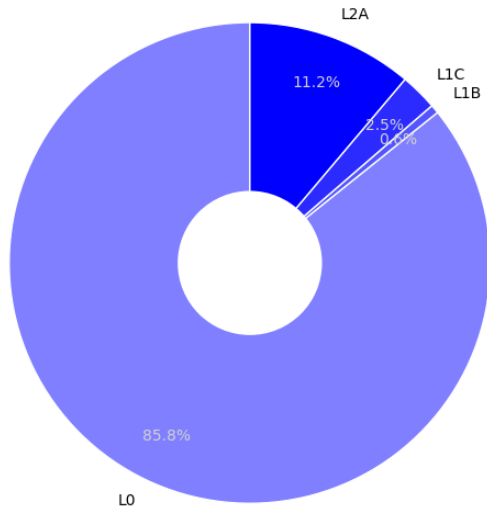
Until 30.09.2024, tiles 137174 (includes commissioning and all versions)

Figure 6-4 Observation angle of archived Earth observation tiles

6.2 Delivered Observations

The following figures show the distribution of processing level of the delivered products from acquisition orders.

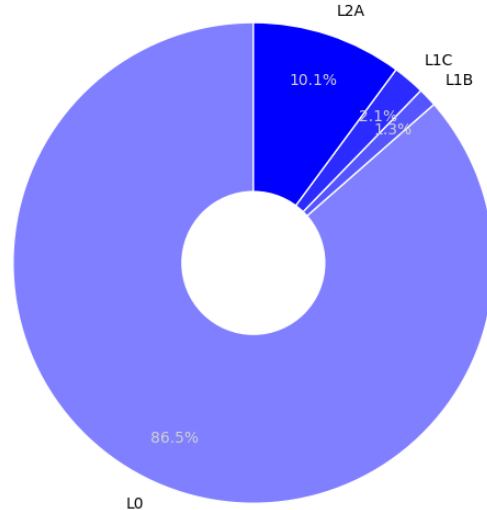
Processing Levels distribution from acquisition orders



reporting period: 2024-07-01 - 2024-10-01 , tiles: 18108

period 01.07.2024 to 30.09.2024, tiles 18108

Processing Levels distribution from acquisition orders



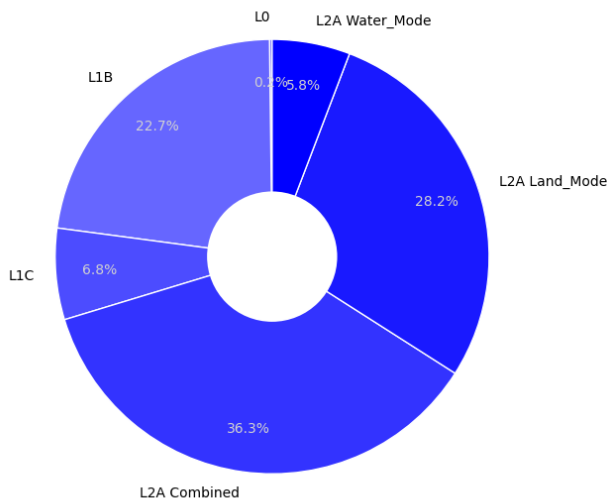
reporting period: 2022-04-01 - 2024-10-01 , tiles: 98277

Until 30.09.2024, tiles 98277 (includes commissioning)

Figure 6-5 Levels of delivered Earth observation tiles from acquisition orders

The following figures show the distribution of processing level and correction type (for L2A) of the delivered products from catalog orders.

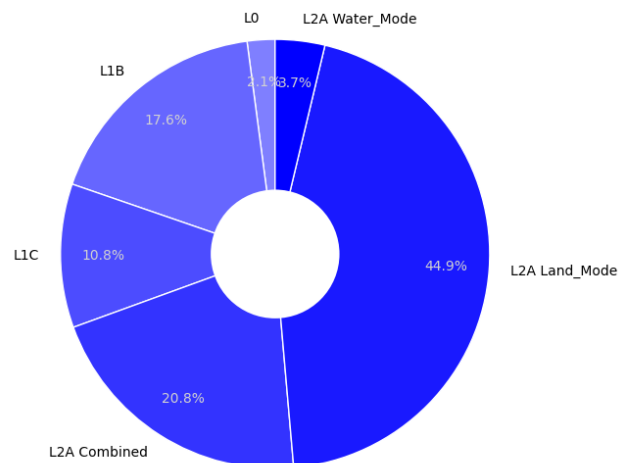
Processing Levels distribution from catalog orders



reporting period: 2024-07-01 - 2024-10-01 , tiles: 17140

period 01.07.2024 to 30.09.2024, tiles 17140

Processing Levels distribution from catalog orders



reporting period: 2022-04-01 - 2024-10-01 , tiles: 82839

Until 30.09.2024, tiles 82839 (includes commissioning)

Figure 6-6 Levels of delivered Earth observation tiles from catalog orders

6.2.1 Delivered L2A products from the Download service (EOC Geoservice)

In order to reduce the workload of the system, the Ground Segment produces L2A products already processed with standard parameters that are available for direct download using the EOC Geoservice and the EOLab platform.

This new way of getting the EnMAP L2A products saves a lot of computational time for the system, and at the same time offers the user a resource to obtain L2A products without processing waiting times.

The total number of downloaded L2A products using the EOC Geoservice is **272938** for this reporting period (01.07.2024 to 30.09.2024)

7 Detailed Status

7.1 User Interfaces

Further improvements to the user interfaces are continuously on-going and will be reported in this section.

The Instrument Planning tool did not receive any major update during the reporting period. Some changes are in progress like the possibility to download the planned flightlines of each acquisition as a geojson file will be implemented in Q4 2024.

During the reporting period the Ground Segment of EnMAP continues to update the information on future high priority observations of the EnMAP mission (*Foreground Mission*). The tool displaying this information is available at the EnMAP web site under: https://www.enmap.org/data_tools/foreground_mission/

With this tool the users can get informed weeks in advance about future priority observations with EnMAP. Initially, a set of 10 flight-lines over Germany have been identified together with the user community and will be regularly scheduled until Autumn 2024. New regular flight lines on other locations are also announced in the Foreground Mission page.

7.2 Satellite

No major satellite issues have been observed in the reporting period.

During the reporting period the HSI transitioned to SAFE_ERROR mode creating a mission outage starting 02. September 2024. Root cause was a detected bitflip during a VNIR configuration check that triggered a readback error. The anomaly could be recovered on 05.09.2024 after the VNIR was switched off and switched on again after one orbit of waiting time.

The VNIR had already entered the SAFE_ERROR mode on 09. July 2024. Similar errors have been observed already two times before.

The DSHA has transitioned in total three times into the SAFETY_MODE within the last quarter. This anomaly can be solved only through a DSHA power-cycle with the result that all acquisitions currently stored in the DSHA are lost. There were different reasons identified by the manufacturer for this anomaly that happens spontaneously.

The Back-2-Back imaging sequences are used with >5 sequences per day, allowing a fast acquisition of up to three ground targets within one large attitude maneuver. Issues observed on previous quarter with the Back-2-back planning are now completely solved and the system is operating as expected.

7.2.1 Orbit

The reference orbit is a Sun-synchronous polar orbit with a mean local time of descending node of 11:00 hrs and a repeat cycle of 398 revolutions in 27 days at an altitude of 643 km (lateral deviation of at most 22 km at equator and altitude deviation of at most 6 km).

During the reporting period, a total of 1676 ACS Precise Modes were executed on-Board, compared to 1118 during the previous quarter. Due to the implementation of Back-to-Back Image Acquisitions, the number of ACS Precise Modes does not represent the number if performed activities anymore. By executing two or three Images as one sequence, the total number of ACS Precise Modes decreases whereas the number of Image Acquisitions remains stable or increases.

During Q3 2024, a total of three in-plane and two out-of-plane maneuvers were executed. No collision avoidance maneuvers were required. The resulting performance error off all maneuvers was estimated by FDS to be between -0.5 % and +1.3 %.

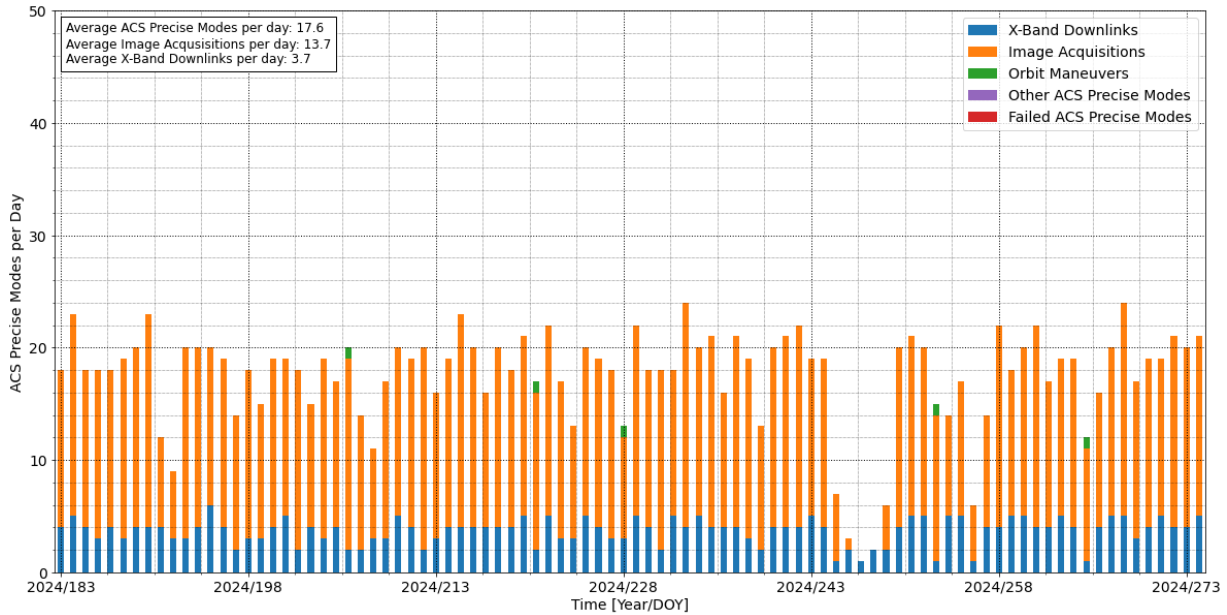


Figure 7-1 Number of ACS Precise Modes per day during Q3 2024

7.2.2 Life Limited Items

Life-Limited Item	01.07.2024 to 30.09.2024	until 30.09.2024	Estimated minimum total lifetime
Fuel	+0,6 kg	6,8 kg	>15 years
Battery and Solar Cells	nominal	nominal	nominal
Shutter Usage	+2,12%	14,73%	17,0 years (@ daily use)
FAD movements	+2,00%	24%	15,2 years (@ bimonthly use)
Diffuser exposure time based on sole measurement time	+3,33%	40,00%	8,5 years (@ bimonthly use)
Diffuser exposure time based on real cyclogram duration	+3,97%	47,70%	6,9 years (@ bimonthly use)
On-Board Calibration Equipment Usage	On-board calibration equipment:		
- OBCA SPC lamp 1	+1,41%	12,05%	19,3 years (@ biweekly use)
- OBCA RAD lamp 1/LED 1	+3,39%	23,22%	8,1 years (@ weekly use)
- FPA LEDs 1	+0,56%	6,00%	44,3 years (@ monthly use)

Table 7-1 Status of life-limited items

7.2.3 Redundancies

To date, the SWIR wavelength range is covered by SWIR-A (SWIR-B can be activated using a one-time switch mechanism).

All satellite subsystems are using nominal configurations.

7.3 Ground Stations

7.3.1 S-Band

S-Band Ground Stations	01.07.2024 to 30.09.2024		
	Total Passes	Non-Routine Passes (e.g. Anomaly Handling/SW Updates)	Failed Passes
All stations (Weilheim-Germany, Neustrelitz,-Germany, Inuvik,-Canada, O'Higgins-Antarctica, Svalbard-Norway)	553 (381 WHM, 148 INU)	11	7

Table 7-2 S-Band Ground Station Passes

7.3.2 X-Band

X-Band Ground Stations	01.07.2024 to 30.09.2024	
	Executed Passes	Successful Passes
All stations (Neustrelitz-Germany, Inuvik-Canada)	343 (250 NZ, 93 INU)	343 (250 NZ, 93 INU)

Table 7-3 X-Band Ground Station Passes

Inuvik (Canada) station is now part of the regular operations of the EnMAP Ground Segment for X-Band and S-Band downlinks. After integration, more data and more flexibility in S-band and X-band data reception is achieved, especially concerning image acquisitions over Europe.

7.4 Processors

Reference [3] provides the product specification and [4], [5], [6], [7] the algorithm theoretical basis for Level 1B, Level 1C and Level 2A (land / water).

During Q3 2024, the change log documenting the history of EnMAP processor updates continues to show the updates performed in the processing software. The document can be downloaded from the EnMAP website:

https://www.enmap.org/data/doc/EnMAP_processor_changelog.pdf

In the reporting period (01.07.2024 to 30.09.2024) the following processors version were introduced:

- Version **V01.05.00** (created on 09.09.2024). This new EnMAP processors version introduces:
 - Writing new metadata entries `viewingAzimuthAngle` and `viewingZenithAngle`
 - Fixed adjacency correction around very small clouds in L2A products
 - Implemented SWIR dark signal correction at L1B level (activated on 18.11.2024)
- Version **01.05.01** (created on 17.09.2024, available to users on 10.10.2024)
 - Small bugfix due to the changes in V01.05.00
 - Rest of changes in V01.05.00 are included in V01.05.01

Notice that V01.05.00 was not available to the users, it was replaced by V01.05.01 before it was updated on the operational environment. Also notice that although the SWIR dark signal correction was part of V01.05.01, this did not become active until 18.11.2024 with an update of the calibration tables.

The following limitations are applicable as of 30.09.2024:

- The SWIR-A compressor cooler produces a micro-vibration pattern of horizontal stripes on SWIR bands with strong spectral gradients. Still, all spectral and radiometric requirements are within

the specification of the mission.

The following changes are expected to be performed in the future quarters:

- Update of the linearity calibration to improve the matching between VNIR and SWIR spectrometers, specially at low radiance level.

7.5 Calibrations

Table 7-4 summarizes the radiometric calibration observations acquired in this quarter and which will be described in the rest of this section. The calibration acquisitions were generally acquired according to the routine operations plan.

Category	01.07.2024 to 30.09.2024	
	Number of Archived Observations	Size (in GB)
Total	27	113.2
Deep Space	2	2.6
Rel. Radiometric	13	50.7
Abs. Radiometric	2	2.6
Linearity	3	51
Spectral Calibration	7	6.3

Table 7-4 Number and size of archived radiometric and spectral calibration observations

The continuous degradation of the VNIR sensor was monitored and quantified. The rate of degradation is constantly decreasing as illustrated in Figure 7-2 and by the end of March 2023 it has reached the point where it is practically negligible and has been kept that way during the reporting period. The effect on the radiometric calibration coefficients of a few selected bands is shown in Figure 7-3.

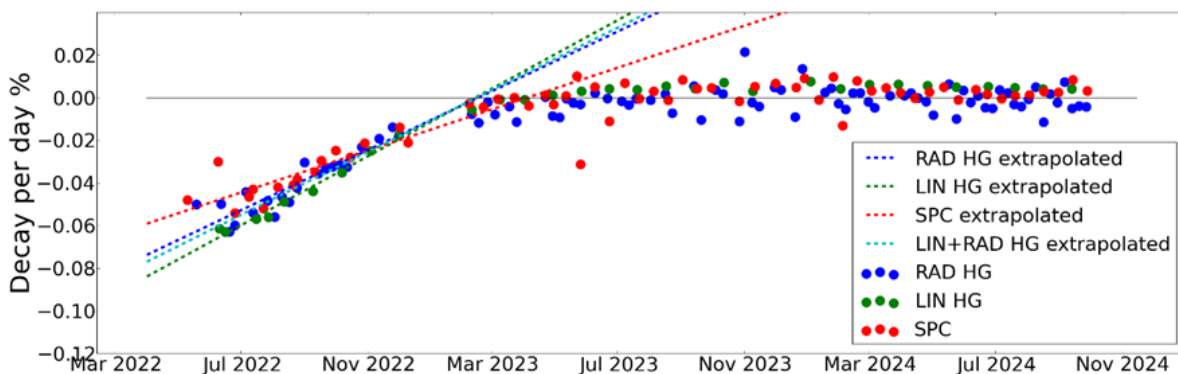
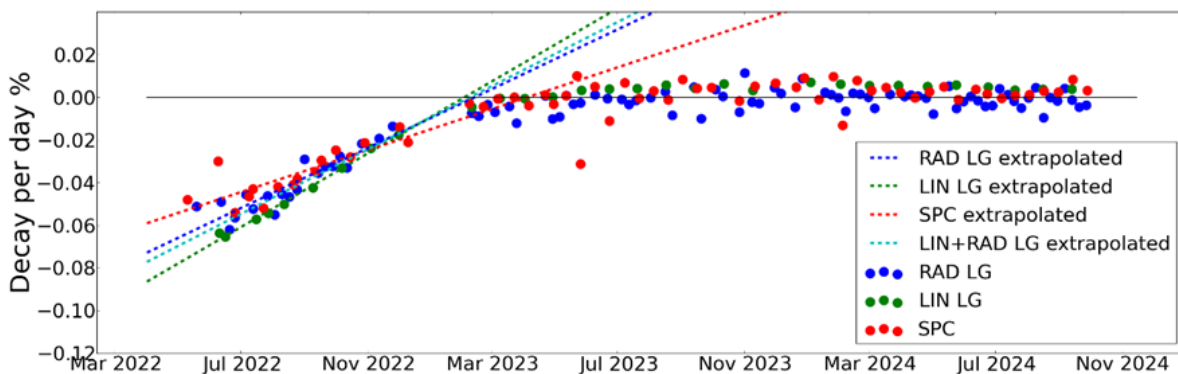


Figure 7-2 Decay per day from Lamp (RAD), Linearity (LIN) and Spectral (SPC) measurements for low gain (top) and high gain (bottom)

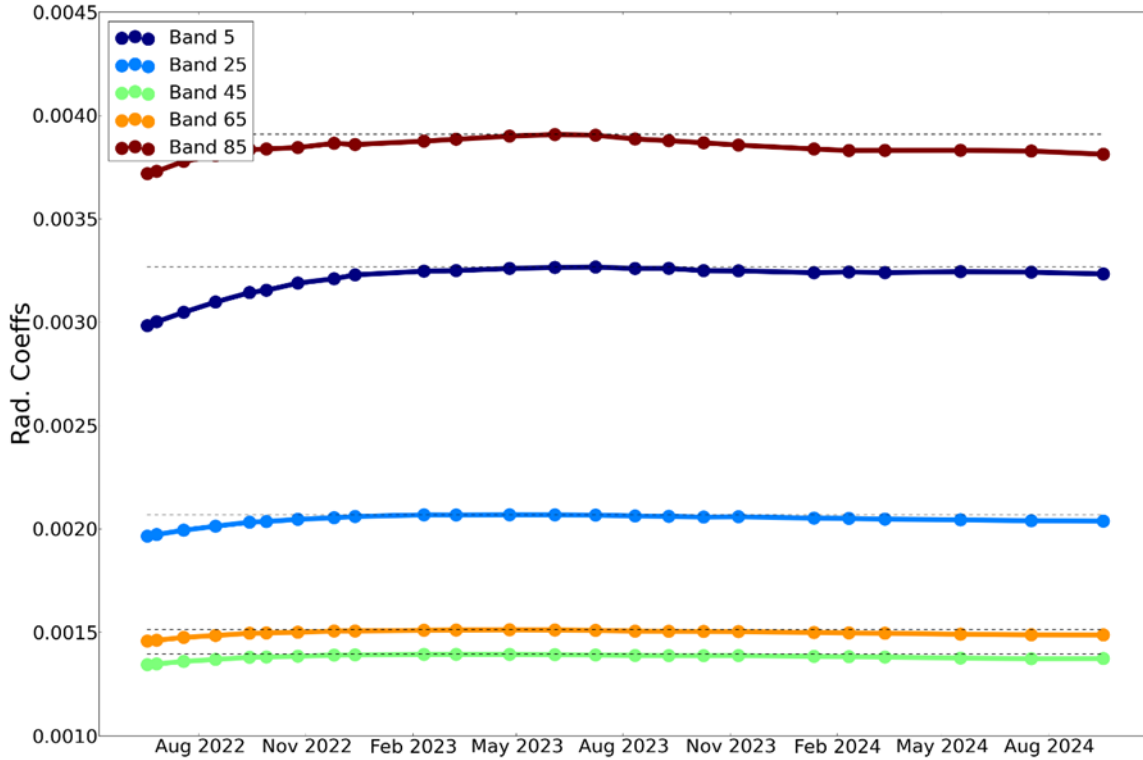


Figure 7-3 Average percentage change in the VNIR radiometric coefficients for five selected bands since launch

7.5.1 Dead Pixels

The following table shows the number and percentage of dead pixels. Figure 7-4 and Figure 7-5 show the position of the dead pixels in the focal plane of VNIR and SWIR sensors respectively. There have been no updates since 31.08.2022.

Defect Pixels	01.07.2024 to 30.09.2024	
	Number of Pixels	Percent
Total	1921	0.8
VNIR	137	0.2
SWIR	1784	1.2

Table 7-5 Number and percent of dead pixels

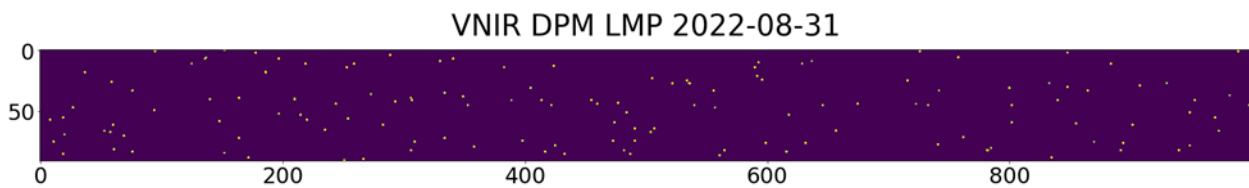


Figure 7-4 VNIR Dead Pixel Mask

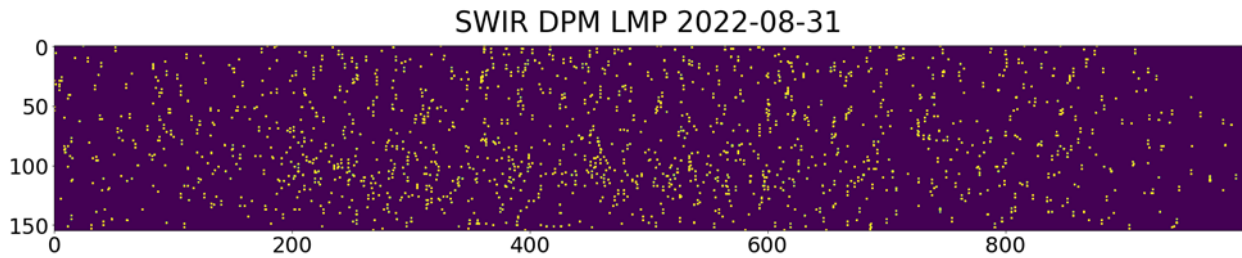


Figure 7-5 SWIR Dead Pixel Mask

There are no clusters of more than three spectrally or spatially adjacent dead pixels.

7.5.2 Spectral Calibration

Remark: In the following figures, OBCA is abbreviation for On-Board Calibration Assembly for spectral and radiometric calibrations.

Category	01.07.2024 to 30.09.2024	
	Number of Archived Observations	Size (in GB)
Total	7	6.3
Spectral Calibration	7	6.3

Table 7-6 Number and size of archived spectral calibration observations

The spectral properties – in particular center wavelength (CW) (see Figure 7-6 and Figure 7-7) and full width at half maximum (FWHM) (see Figure 7-8) for each band (spectral coordinate) and pixel (spatial coordinate) – have been characterized, considering all bands and pixels provided in Level 1B, Level 1C and Level 2A products.

The major conclusions of the monitoring of the spectral performance is summarized as follows:

- During the reporting period, 7 spectral calibration measurements were made which took place on: 06.07.2024, 20.07.2024, 02.08.2024, 16.08.2024, 31.08.2024, 13.09.2024 and 27.09.2024.
- The VNIR spectral range in this reporting period was found to be 418.4 – 993.3 nm over 91 bands (Figure 7-6). The average spectral sampling distance was 6.4 nm with a total range of 4.7 – 8.2 nm. This meets the requirement for overall wavelength coverage [HSI-POSS-0210], average spectral sampling distance [HSI-POSS-0310] and spectral sampling distance range [HSI-POSS-0320].
- The SWIR spectral range in this reporting period was found to be 902.1 – 2445.4 nm over 155 bands (Figure 7-6). The average spectral sampling distance was 10.0 nm with a total range of 7.5 – 12.0 nm. This meets the requirement for overall wavelength coverage [HSI-POSS-0210], average spectral sampling distance [HSI-POSS-0310] and spectral sampling distance range [HSI-POSS-0320].
- The spectral calibration measurements from this quarter show good temporal stability – measurements showed an absolute <0.2 nm change from the VNIR sensor and <0.55 nm change in SWIR (Figure 7-7). All changes were below 0.5 nm between measurements for VNIR and below 0.5 nm SWIR. This meets the requirement for consecutive spectral stability [HSI-POSS-0510] and overall spectral stability [HSI-POSS-0520].
- FWHM for VNIR and SWIR (Figure 7-8) are shown below but are not recalculated inflight.
- A VNIR degradation pattern is not clearly visible between consecutive spectral reference measurements acquired in this period, but there are positive and negative changes across the detector and on average the signal appears to have increased by 0.26% across all pixels from 22.06.2024 to 27.09.2024. A slightly smaller change was reported in the previous quarter (0.18%). Although small, the monitoring of this behavior will continue in the next reporting period.

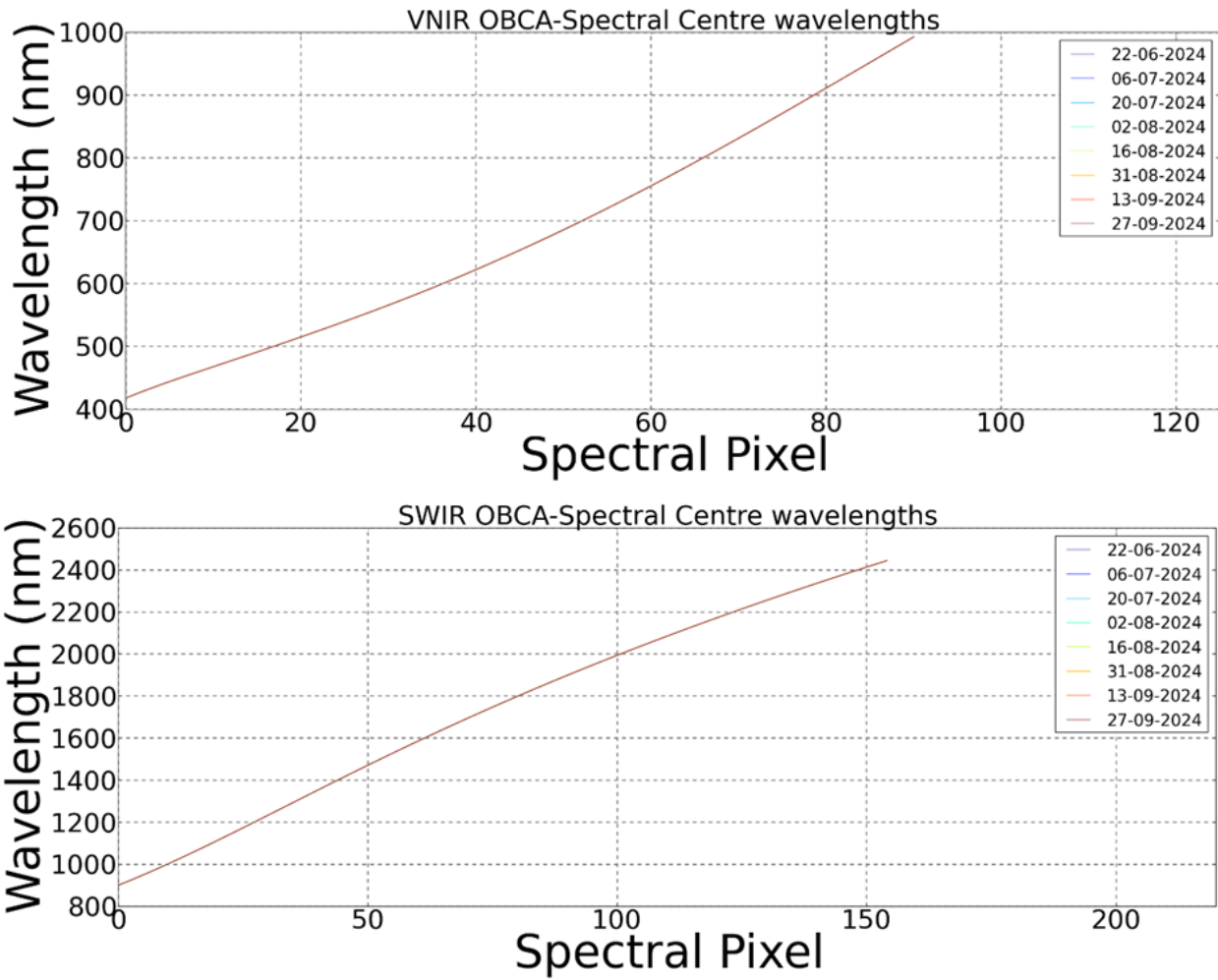


Figure 7-6 VNIR (top) and SWIR (bottom) center wavelength in nm

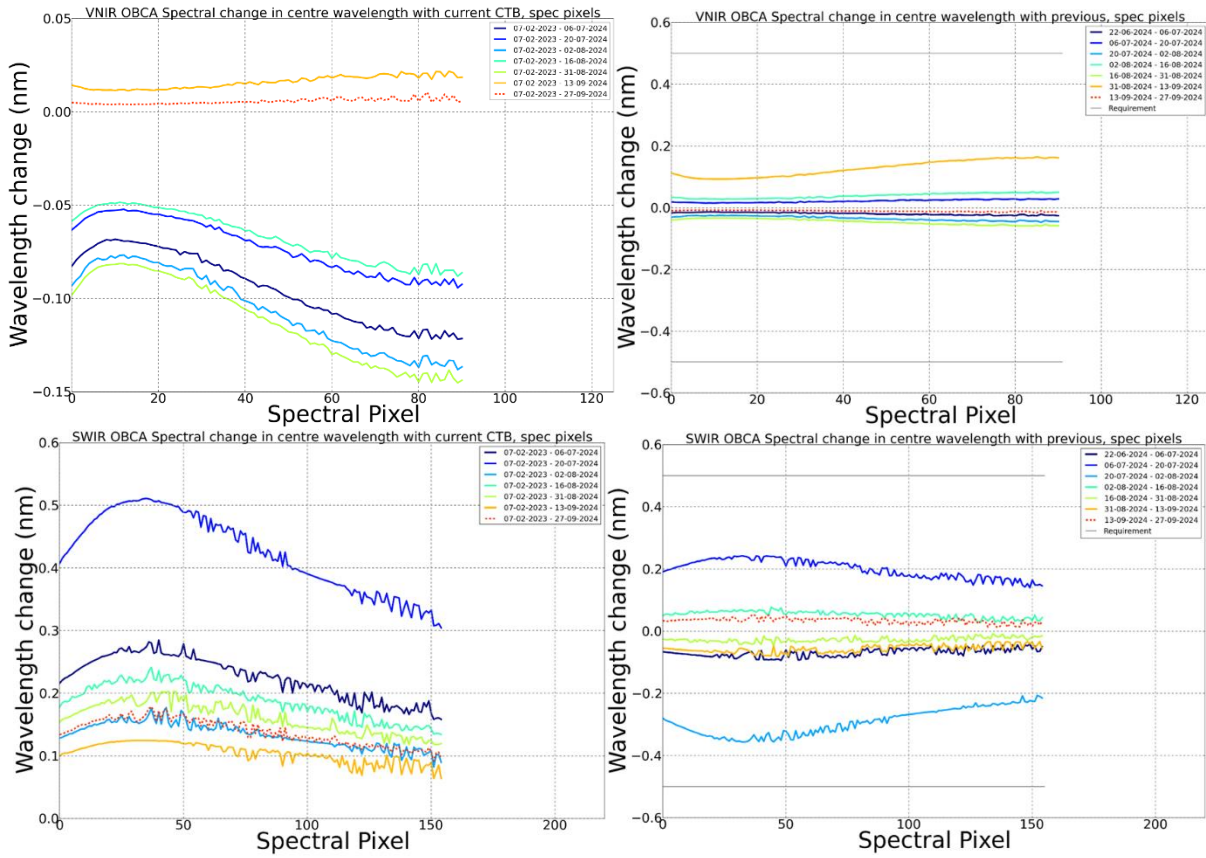
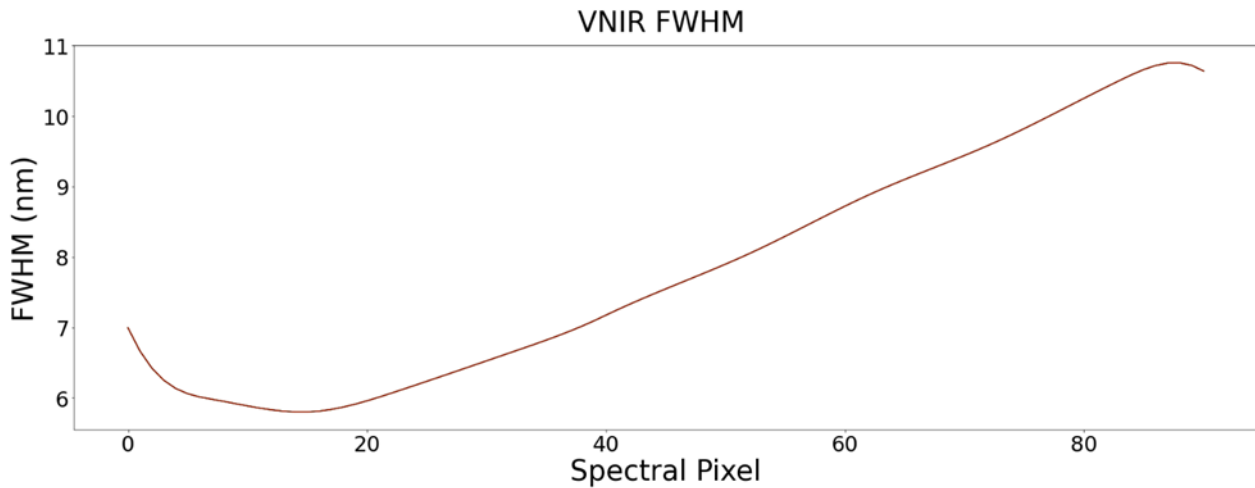


Figure 7-7 Change in center wavelength per spectral pixel for VNIR (top) and SWIR (bottom). Left panels show the changes with respect to current spectral calibration table in use and right panels with respect to the previous measurements.



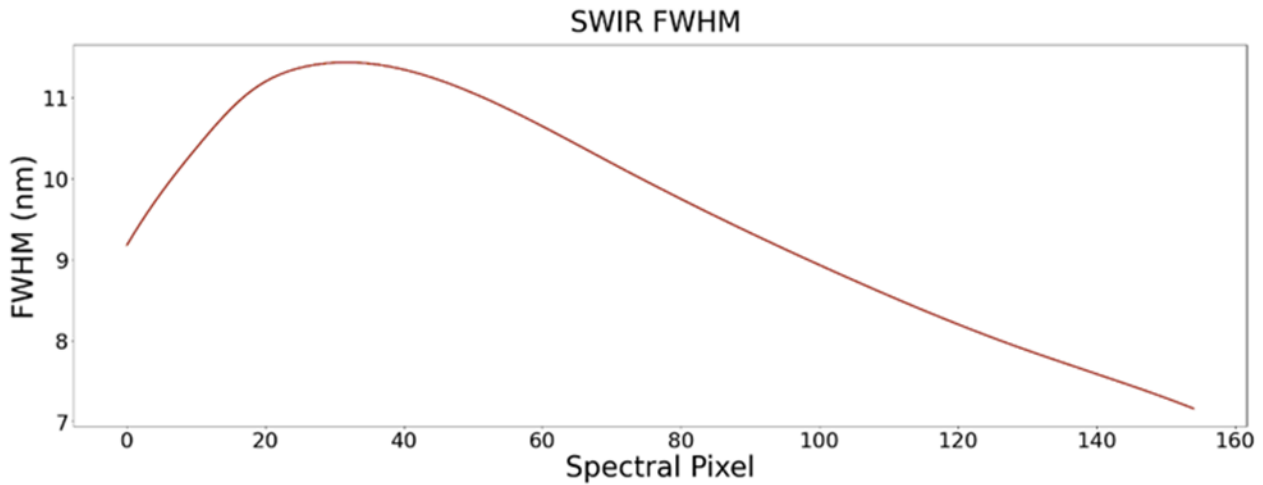


Figure 7-8 VNIR (top) and SWIR (bottom) FWHM in nm

CW and FWHM are available in the spectral calibration tables (see Table 7-7) and System Response Functions (SRF) per band are modelled by a Gaussian shape using those parameters.

No new calibration products were generated and delivered during the reporting period.

Product	Type	Date of Generation	Date of Validity Start	Date of Validity End	Delivered to

Table 7-7 Generated spectral calibration tables

7.5.3 Radiometric Calibration

Category	01.07.2024 to 30.09.2024	
	Number of Archived Observations	Size (in GB)
Total	20	106.9
Deep Space	2	2.6
Rel. Radiometric	13	50.7
Abs. Radiometric	2	2.6
Linearity	3	51

Table 7-8 Number and size of archived radiometric calibration observations

The radiometric properties – characterized in particular by the calibration coefficient for each band (spectral coordinate) and pixel (spatial coordinate) and radiance – during this reporting period are investigated, considering all bands and pixels and radiances provided in Level 1B, Level 1C and Level 2A products.

Both sensors feature two gain settings each. VNIR applies a quantization of 13 bits using a pixel-individual automatic gain switching, where the low gain value is automatically selected, if the signal exceeds a defined threshold. SWIR applies a fixed gain setting, where bands below 1980 nm take the low gain value and bands above 1980 nm take the high gain value.

Radiometric calibration coefficients (see Figure 7-9, Figure 7-10 and Table 7-9) and VNIR RNU (response non-uniformity, see Figure 7-12) were affected by the degradation of the VNIR sensor during commissioning but have stabilized from Q1 2023. In-flight, the gain matching coefficients (see Figure 7-11), the SWIR calibration coefficients, and the SWIR RNU (response non-uniformity, see Figure 7-12) have been stable.

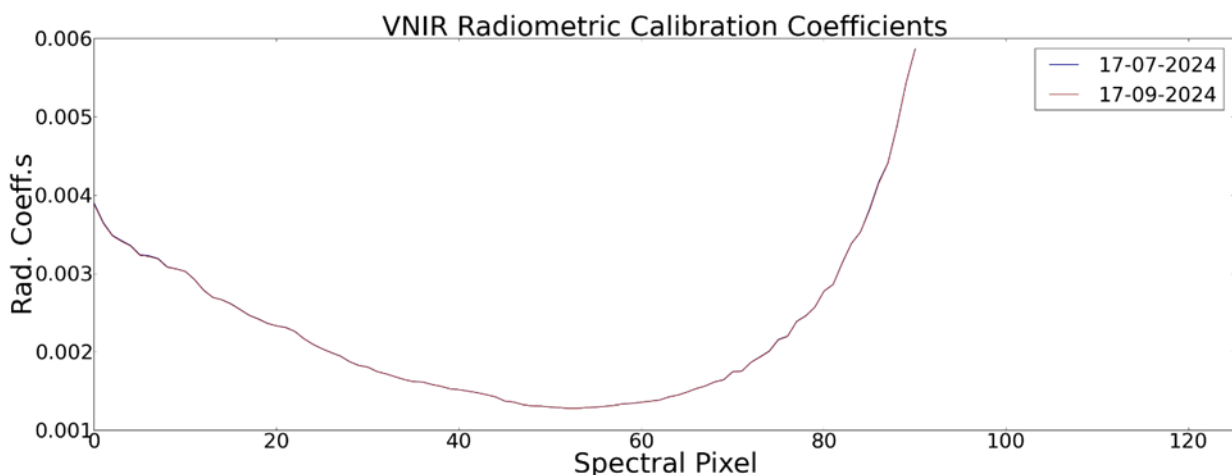
During the reporting period, 2 Absolute Radiometric calibration measurements was obtained. This took place on: 17.07.2024 and 17.09.2024.

Albeit now relatively small in magnitude, changes in the VNIR sensor have led to the creation of new calibration and reference tables for the new absolute radiometric measurement.

Although the VNIR degradation has almost stopped, the overall effects are visible in the reference measurements of the sun. However geometric conditions (sun-earth distance, pointing angle) also play a role in the absolute magnitude so the degradation cannot be quantified with these reference measurements.

The major conclusions of the monitoring of the absolute performance is summarized as follows:

- Changes in the VNIR sensor have affected the absolute Radiometric calibration coefficients: the increasing signal in the VNIR sensor, although not homogeneous, has resulted in decreasing radiometric coefficients. In this reporting period, the calibration coefficients decreased by about -0.28% to offset the increase in absolute (Figure 7-9 and Figure 7-10). Regarding RNU, the degradation features are still visible in the focal plane (Figure 7-12). Lastly, the Gain Matching correction has been relatively stable during this reporting period (Figure 7-11).
- The SWIR sensor has shown good stability during this reporting period, with no significant changes in the gain matching, RNU or radiometric calibration coefficients (Figure 7-9 and Figure 7-10).
- Regarding the total change in calibration corrections as a result of the VNIR degradation, almost all pixels experienced a change of less than 2.5% between consecutive measurements as set in requirement [HSI-POSR-0410]. The only pixels which exceeded this value were already marked as dead during inflight assessment. No SWIR pixels experienced a change of more than 2.5% between consecutive absolute calibration measurements.
- New VNIR and SWIR calibration and reference tables were created for both absolute radiometric measurements, mainly due to the changes in the VNIR sensor. The VNIR radiometric calibration coefficients have decreased in this reporting period to offset the increasing VNIR signal. The changes are small, and within requirements, so the dynamic coefficients are not calculated and calibration coefficients are taken directly from the most recent calibration table as envisioned at the beginning of the mission.
- Since April 2024, Absolute Radiometric calibration measurements are made at intervals of two months, following the stable performance of both sensors, and to allow for the extension of the lifetime of the solar diffuser.



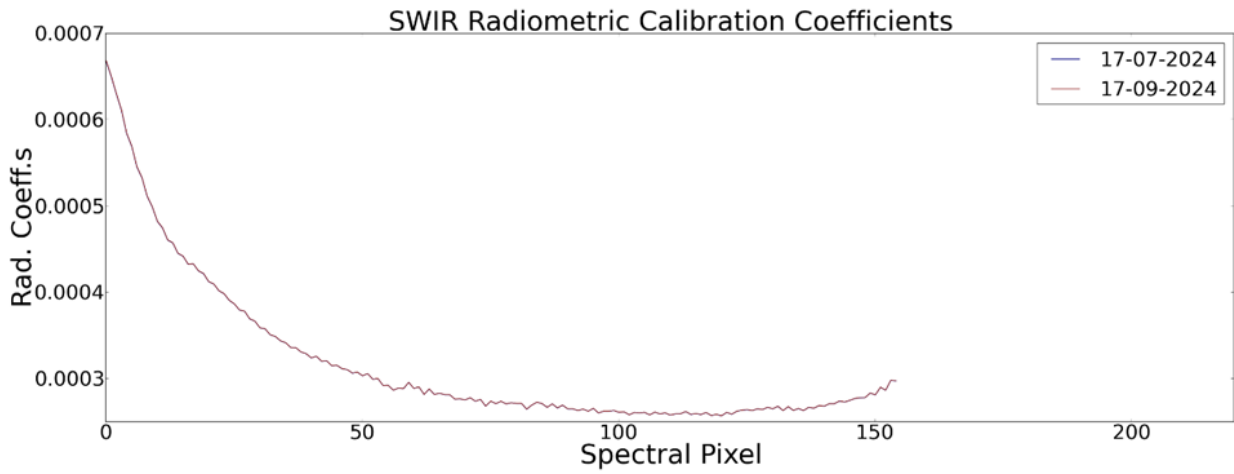


Figure 7-9 VNIR (top) and SWIR (bottom) calibration coefficient in $\text{mW}/\text{cm}^2/\text{sr}/\mu\text{m}$

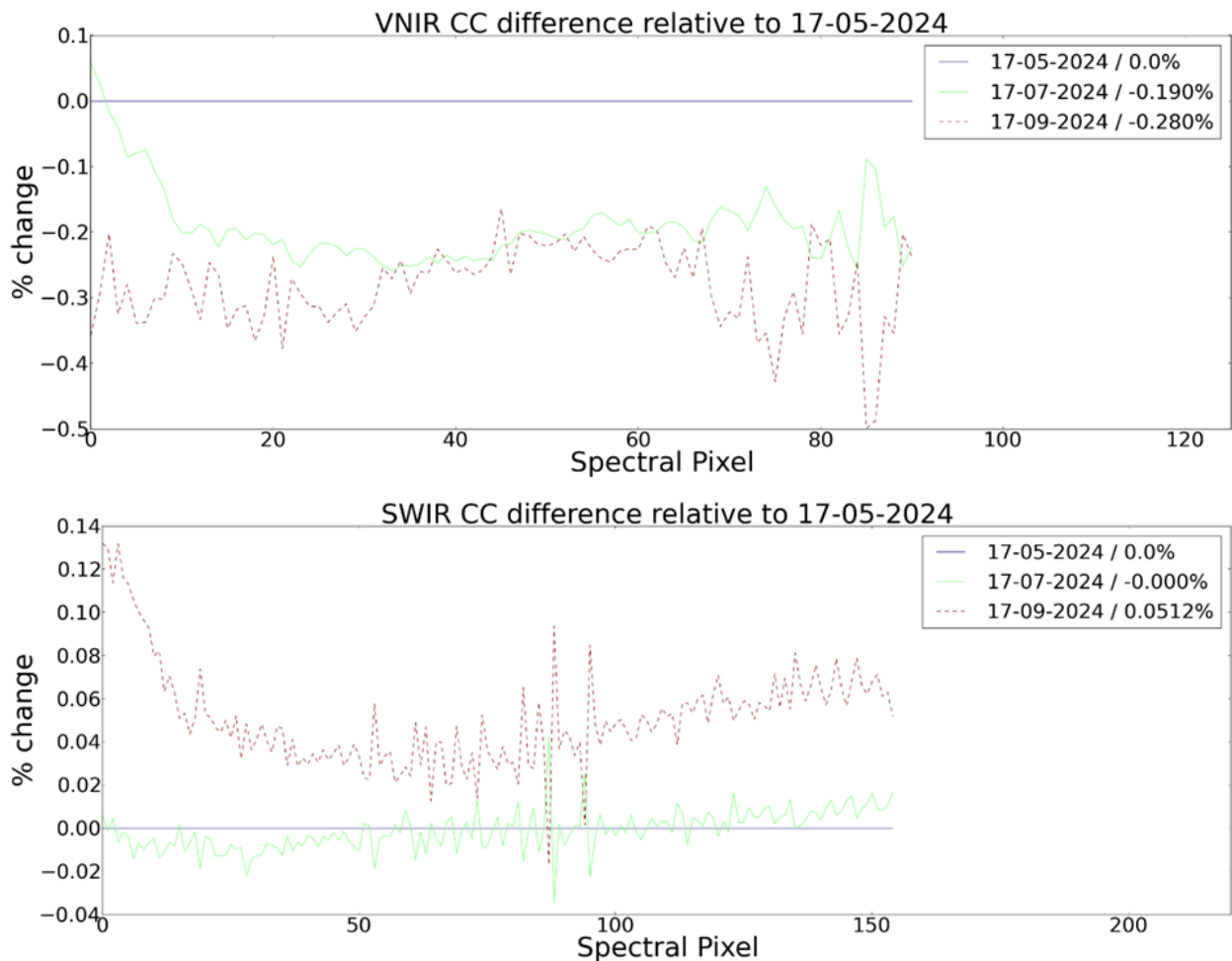


Figure 7-10 Percentage change in VNIR Calibration Coefficients (top) and SWIR Calibration Coefficients (bottom)

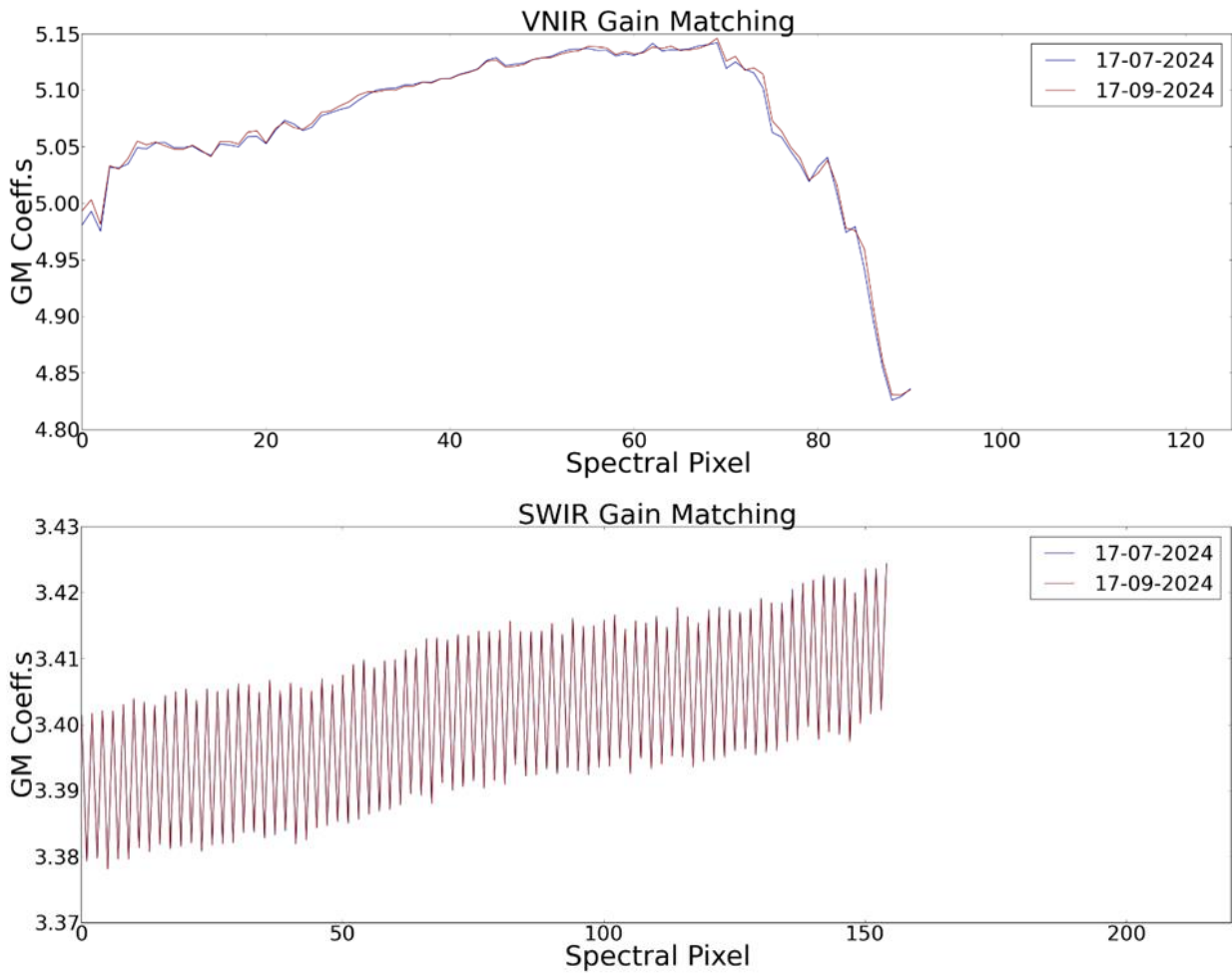
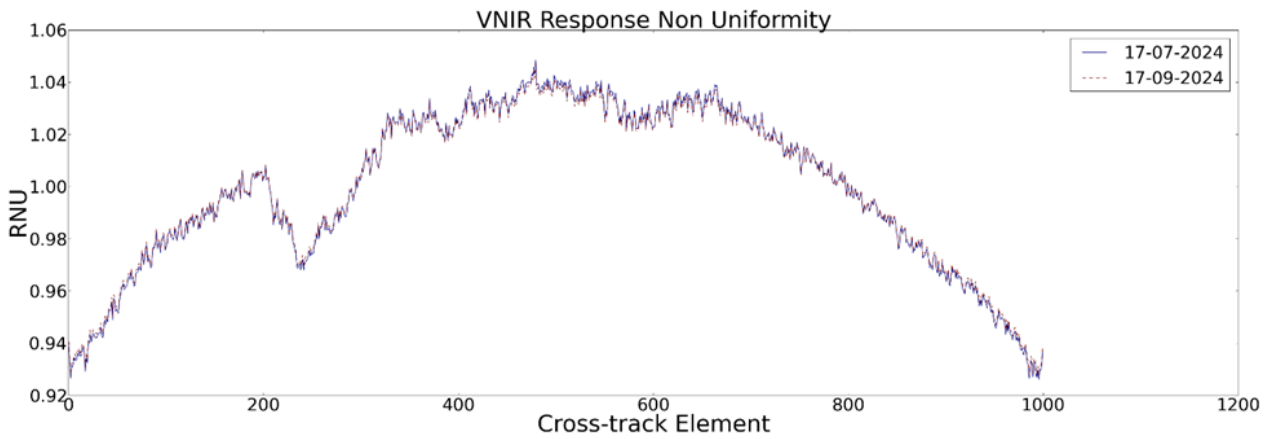


Figure 7-11 VNIR (top) and SWIR (bottom) gain matching calibration coefficients



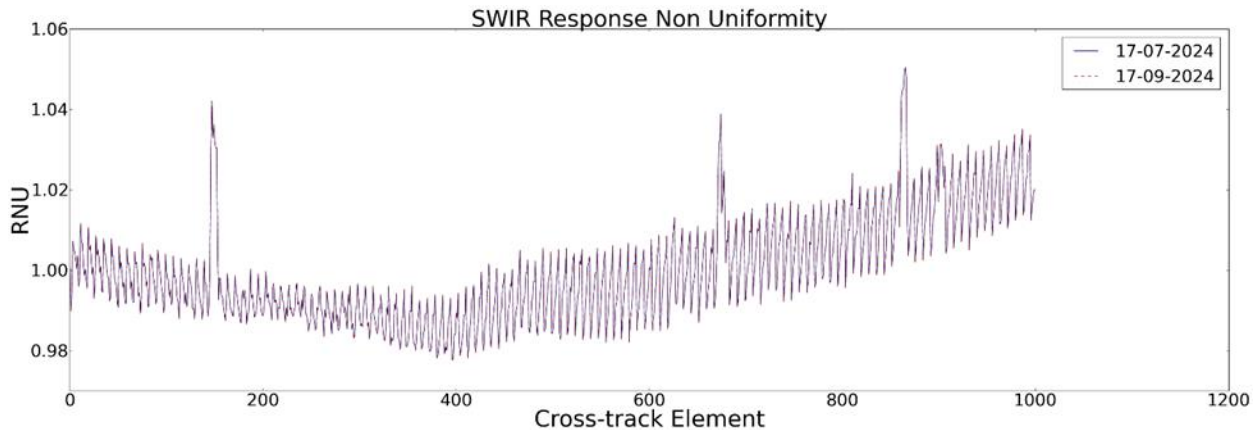


Figure 7-12 VNIR (top) and SWIR (bottom) response non-uniformity coefficients

Signal-to-Noise Ratio

The Signal-to-Noise Ratio (SNR) is derived from the Linearity reference measurements. This is not a perfect set-up for the assessment of the SNR as the linearity measurements only cover a single wavelength and light level at increasing integration times. However, it is well constrained, covering a wide range of radiances including the levels of the reference radiance spectrum that is used to evaluate the requirements (30% reflectance, 30° sun incidence angle, 21 km visibility, target 500 m above sea level). The lamp reference measurements are not used, as the reference spectrum is not well covered at the radiances of the lamp and extrapolation would be required to test the performance at the SNR requirements. Those requirements are: SNR greater than 500 at 495 nm in VNIR for the reference spectrum value given a 10 nm pixel; and SNR greater than 150 at 2200 nm in SWIR for the reference spectrum given a 10 nm pixel.

For the VNIR sensor, SNR is computed from the linearity calibration measurement. SNR values are shown as a contour map with the reference radiance spectrum as a blue line. Contour lines with SNR values of 150 and 500 are also shown in black. The plot in low gain mode includes the mission requirement which is evaluated at 495 nm for a radiance value of 36 mW/cm²/sr and is expected to be greater than 500: the calculated value here is 594. The radiance value used here for the evaluation is the value at 495 nm of the reference radiance spectrum after bandwidth normalization to a 10 nm pixel (see Figure 7-14).

For the SWIR sensor, SNR is also computed from the linearity calibration measurement. SNR values for the high gain mode are shown as a contour map with the reference radiance spectrum as a blue line. Contour lines with SNR values of 150 and 500 are also shown in black. The plot in high gain mode includes the mission requirement which is evaluated at 2200 nm for a radiance value of 0.5 mW/cm²/sr and is expected to be greater than 150: the calculated value here is 200. The radiance value used here for the evaluation is the value at 2200 nm of the reference radiance spectrum after bandwidth normalization to a 10 nm pixel (see Figure 7-15).

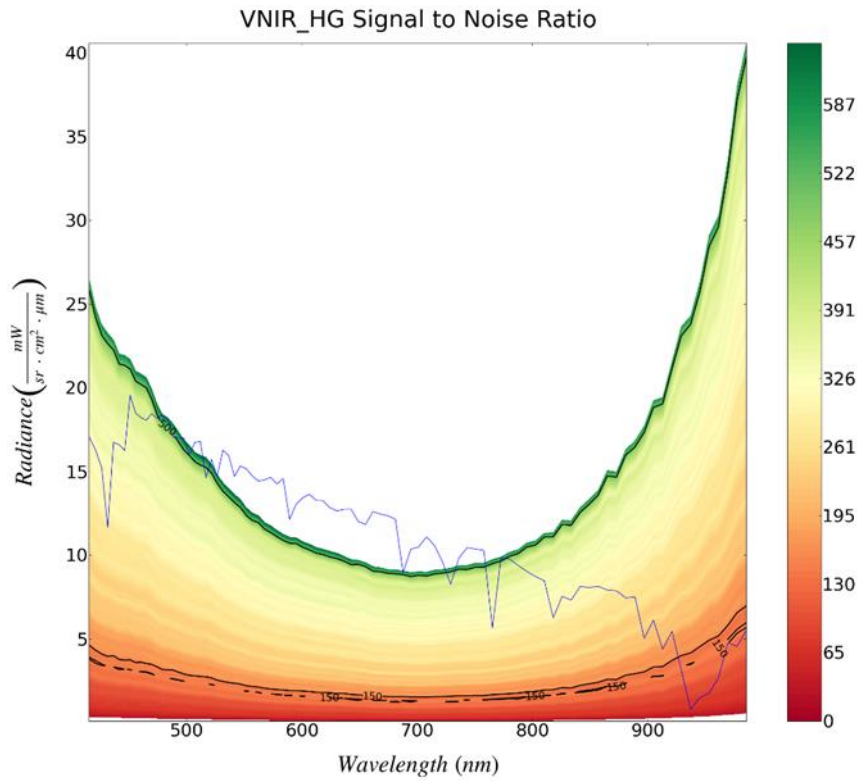


Figure 7-13 SNR contour map for VNIR high gain from the LED linearity observations observed on 12.09.2024. The reference radiance is shown with a blue line. Contour lines with SNR values of 150 and 500 are also shown in black.

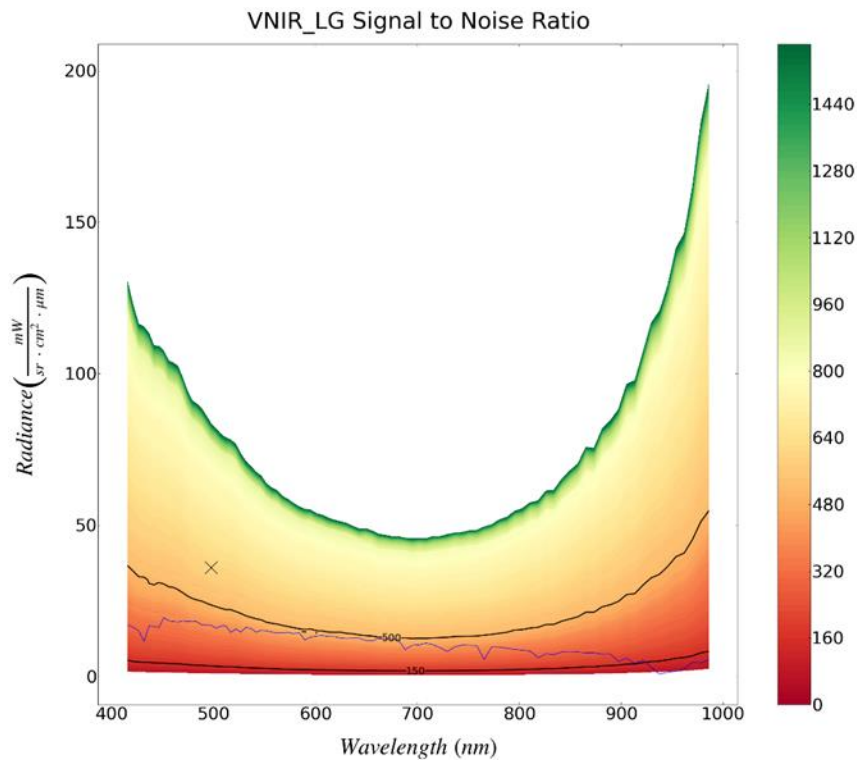


Figure 7-14 SNR contour map for VNIR low gain from the LED linearity observations observed on 12.09.2024. The reference radiance is shown with a blue line. Contour lines with SNR values of 150 and 500 are also shown in black. The mission requirement is evaluated at 495 nm for a radiance value of 36 mW/cm²/sr (marked with a black cross) and is expected to be greater than 500.

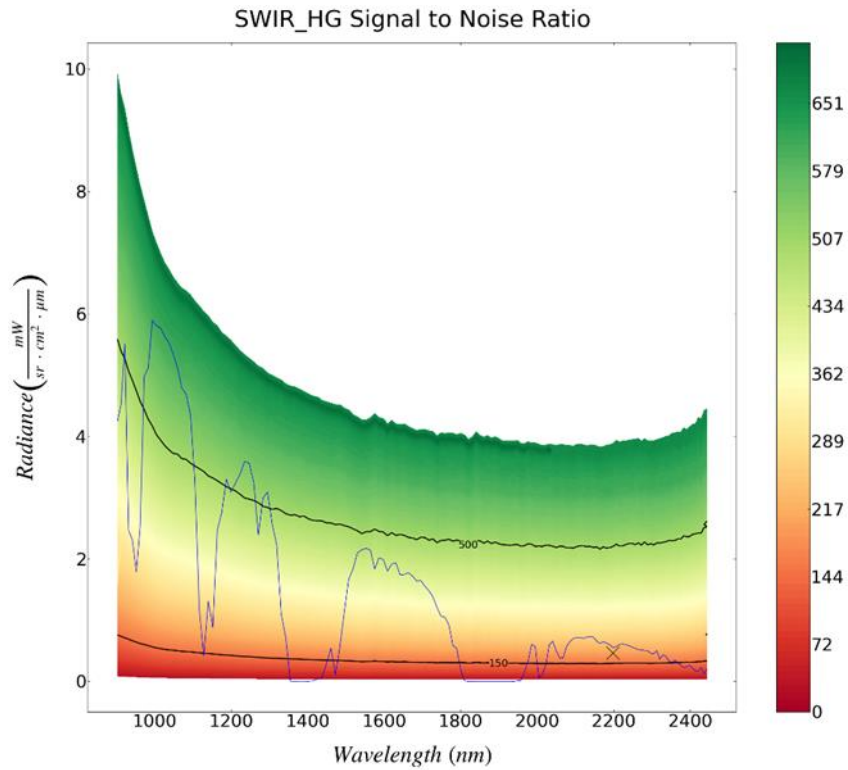


Figure 7-15 SNR contour map for SWIR high gain from the LED linearity observations observed on 12.09.2024. The reference radiance is shown with a blue line. Contour lines with SNR values of 150 and 500 are also shown in black. The mission requirement is evaluated at 2200 nm for a radiance value of 0.5 mW/cm²/sr (marked with a black cross) and is expected to be greater than 150.

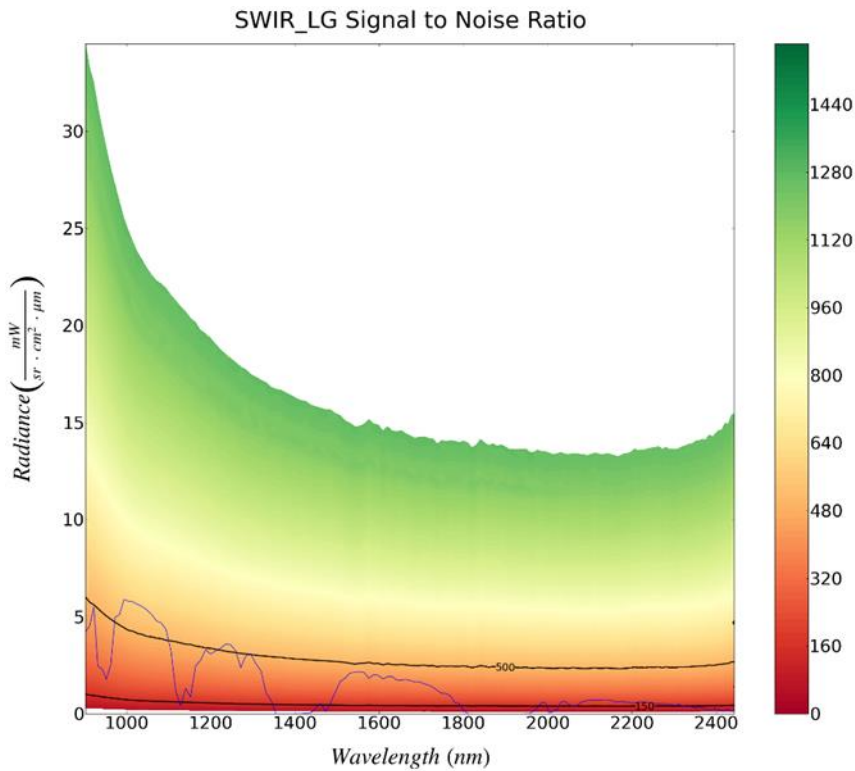


Figure 7-16 SNR contour map for SWIR low gain from the LED linearity observations observed on 12.09.2024. The reference radiance is shown with a blue line. Contour lines with SNR values of 150 and 500 are also shown in black.

The following calibration products were generated and delivered:

Product	Type	Date of Generation	Date of Validity Start	Date of Validity End	Delivered to
ENMAP01-CTB_RAD-20240729T000000Z_V040100_20240718T061952Z	CTB_RAD	18.07.2024	29.07.2022	28.09.2022	DIMS
ENMAP01-CTB_RAD-20240929T000000Z_V040100_20240917T141722Z	CTB_RAD	17.09.2024	29.09.2023	-	DIMS
ENMAP01-REF_SUN-20240729T000000Z_V040100_20240718T061952Z	REF_SUN	18.07.2024	29.07.2022	28.09.2022	DIMS
ENMAP01-REF_SUN-20240929T000000Z_V040100_20240917T141722Z	REF_SUN	17.09.2024	29.09.2023	-	DIMS

Table 7-9 Generated radiometric calibration tables

7.5.4 Geometric Calibration

There have been no new geometric calibration tables generated in the reporting period.

Type of Calibration Table	ID of Calibration Table	Date of Generation	Date of Validity Start	Date of Validity End
None				

Table 7-10 Generated new geometric calibration tables

The performance of the geometric calibration table is assessed in chapter 7.6.3.

7.6 Internal Quality Control

7.6.1 Archive

Within the given time period (01.07.2024 to 30.09.2024), 1819 datatakes with a total of 17288 tiles were acquired and archived (remark: additional datatakes acquired during this period but for which the archiving is pending might be missing in the statistics).

The overall quality rating statistics are listed in Table 7-11, and in relation to the Solar Zenith Angle (SZA) in Table 7-12. Also these ratings are further detailed for the VNIR and SWIR detector in Table 7-13, showing a nominal performance rating for the given quality thresholds.

In addition, the rating for the atmospheric conditions for the scenes are depicted in Table 7-14. When setting the atmospheric quality rating in relation to the illumination conditions (i.e., large SZA) during data acquisition (Table 7-15), 11% of the “reduced quality” ratings and 12% of the “low quality” ratings can be related to low Sun angles / night time acquisitions. In addition, the “low qualityAtmosphere” rating can be further related to high cloud cover (51% of the low qualityAtmosphere tiles) and the unavailability of enough DDV pixels (65%) (see Table 7-16). Consequently, the rating is absolutely reasonable and can be explained.

Parameter	Value	Percentage	Number of tiles
overallQuality	Nominal	98,6%	17053
	Reduced	<1%	11
	Low	1,3%	224

Table 7-11 Overall quality rating statistics

Parameter	Number of tiles	Sub-Parameter	Number of tiles
overallQuality = Low	224		
		Thereof with SZA > 70°	224

Table 7-12 Overall quality rating in relation to Sun Zenith Angle (SZA)

Parameter	Number of tiles	Sub-Parameter	Number of tiles
overallQuality = Reduced	11		
		Thereof with qualityVNIR nominal	0
		Thereof with qualitySWIR nominal	11
overallQuality = Low	224		
		Thereof with qualityVNIR nominal or reduced	6
		Thereof with qualitySWIR nominal or reduced	224

Table 7-13 Reduced and low quality rating statistics

Parameter	Value	Percentage
QualityAtmosphere	Nominal	45%
	Reduced	14%
	Low	42%

Table 7-14 QualityAtmosphere rating statistics

Parameter	Number of tiles	Sub-Parameter	Number of tiles
overallAtmosphere = Reduced	2341		
		Thereof with SZA > 60°	280
		Thereof with SZA > 70°	38
		Thereof with SZA > 80°	7
overallAtmosphere = Low	7228		
		Thereof with SZA > 60°	870
		Thereof with SZA > 70°	410
		Thereof with SZA > 80°	236

Table 7-15 QualityAtmosphere rating in relation to Sun Zenith Angle (SZA)

Parameter	Number of tiles	Sub-Parameter	Number of tiles
overallAtmosphere = Low	7228		
		Thereof with Cloud Cover > 66%	3719

	Thereof with DDV warnings	4766
--	---------------------------	------

Table 7-16 QualityAtmosphere rating in relation to Cloud Cover and DDV availability

Remark about definition of EnMAP low quality collection

The quality rating of EnMAP products is based on image parameters, such as illumination conditions (i.e., sun elevation angle) and image defects, and on possible anomalies in the image data or instrument telemetry. These parameters are retrieved during the pre-processing and are added to the metadata and quality layers for every archived L0 product. In EOWEB GeoPortal two collections of EnMAP L0 products are available: “EnMAP-HSI (L0)” and “EnMAP-HSI (L0), Low Quality”. An L0 product is assigned to the low-quality collection if the corresponding metadata item qualityFlags.overallQuality is equal to 2 (low quality). This happens for products with a significant number of striping, saturation, artefact or dead pixels, when the screening of data and instrument indicates non-nominal behavior or, in the majority of cases, when the sun elevation angle is less than or equal to 0 (e.g., night scenes). A detailed definition of qualityFlags.overallQuality is given in Sec. 4.4.9 in the L1B ATBD (EN-PCV-TN-4006).

7.6.2 Level 1B

7.6.2.1 Radiometric Performance

Defective / de-calibrated detector elements

Using the Detector Map components, an offline check of possibly defective or de-calibrated detector elements is conducted. In particular, a detector element is identified as “possibly defective” if it is suspicious in at least 75% of the useful tiles. Note that this analysis is based on L1B_RAD data, so no dead / defective pixel interpolation was carried out. Within the given reporting period, the following indications for defective pixels are found for the VNIR and the SWIR camera:

VNIR (total of 17288 tiles, with 17002 suitable for analysis):

Newly found suspicious pixels in **green**, previously detected in **black**, no longer present ones in **red**.

Band	Cross-track element
77	600
85	14
89	395

Note that the band index starts at 1.

SWIR (total of 16380 tiles, with 16101 suitable for analysis):

Newly found suspicious pixels in **green**, previously detected in **black**, no longer present ones in **red**.

Band	Cross-track element	Band	Cross-track element	Band	Cross-track element
2	235, 286, 593, 673	48	511	96	341, 819
3	381	50	311, 344, 395	100 — 513	
4	362, 363, 418	53	97, 98	101	318
5	687	54	602, 941	106	107
7	910	56	221, 965	107	265, 764
8	801	58	632, 922	108	886
8	124	59	89, 90	111	315
11	715	61	312	118	837
14	29, 684	63	123		
16	535	69	864		
19 — 84		72	801, 844, 845		



28	104	75	737
29	855, 928	85	525
30	360, 855	91	973
31	360	92	677, 973
33	560		
38	241		
39	486		

Dead detector elements

Within the given reporting period, the statistics for dead pixels are provided in Table 7-17 and Table 7-18. When comparing these numbers to the estimates in Ch. 7.5.1, one must bear in mind that the latter is based on the full detector readout configuration, while the numbers provided in the following are related to the standard readout configuration as provided in the user product. Because of the smaller readout area, these following dead pixel numbers are lower in comparison.

Parameter	Number of dead pixels	Percentage of tiles in reporting period
DeadPixelsVNIR	137	100%

Table 7-17 Dead pixel statistics, VNIR

Parameter	Number of dead pixels	Percentage of tiles in reporting period
DeadPixelsSWIR	1509	100%

Table 7-18 Dead pixel statistics, SWIR

Saturation and radiance levels

Within the given reporting period, no indications for increased saturation defects are found for the VNIR and the SWIR camera (see Table 7-19 and Table 7-20).

Parameter	Value (per mille of scene)	Percentage of tiles
SaturationCrosstalkVNIR	0	93%
	> 0 per mille	7.5%
	> 10 per mille	1.1%

Table 7-19 Saturation statistics, VNIR

Parameter	Value (per mille of scene)	Percentage of tiles
SaturationCrosstalkSWIR	0	93%
	> 0 per mille	6.6%
	> 10 per mille	0.2%

Table 7-20 Saturation statistics, SWIR

Other radiometric artifacts

Within the given reporting period, the striping performance is similar to the one encountered during the Commissioning Phase. Within PCV, different de-striping approaches were tested, and the selected one by M. Brell (GFZ) is implemented in processor version V01.02.00 (07.03.2023).

Apart from this, no indications for an increase in general radiometric artifacts are found for the VNIR and the SWIR camera (see following tables).

Parameter	Value (number of pix)	Percentage of tiles
generalArtifactsVNIR	0	0%
	> 0	100%
	> 10	5.4%
	> 100	1.5%
	> 1000	0%

Table 7-21 Artifacts statistics (without striping), VNIR

Parameter	Value (number of pix)	Percentage of tiles
generalArtifactsSWIR	0	0%
	> 0	100%
	> 10	100%
	> 25	7.3%
	> 100	1.9%
	> 1000	0%

Table 7-22 Artifact statistics (without striping), SWIR

7.6.2.2 Spectral Performance

For the analysis of the spectral stability, the Detector Maps of all Earth datatakes acquired in the reporting period were used. Note that no smile correction was applied, so the analysis shows only on the instrument characteristics. At the wavelengths of stable atmospheric features (760 nm Oxygen absorption and CO2 absorption at ~2050 nm), simulations of spectral shifts were carried out by resampling the absorption in the interval of +/- 3.0 nm with steps of 0.05 nm. Then the signal of the Detector Maps and the simulated shifted absorptions were normalized, and a least-square fit was used where the sensed absorption matches the simulations. Also an additional polynomial fitting was applied, as especially the CO2 absorption band region has low signal and is thus significantly influenced by noise.

For the VNIR, when aggregating the shifts (Figure 7-17) the mean derivation is almost constant in across-track direction and -as before- around 0.5 nm towards shorter wavelengths, underpinning the consistency with the in-orbit spectral calibration and especially regarding the shape of the spectral smile. Note that of course these results are consistent within the limitations of this vicarious approach. Additionally, the variability of the vicariously estimated spectral calibration can be expressed as the standard deviation at 1 sigma is below 0.4 nm, which includes the spectral stability of EnMAP and as well the variations of the used Earth datatakes and the limitations of the method.

In summary, for the VNIR the estimated differences to the CTB_SPC consistent with the results of previous reporting periods, confirming the validity of the spectral calibration and the spectral stability of the instrument taking into accounts the limitations of the vicarious approach.

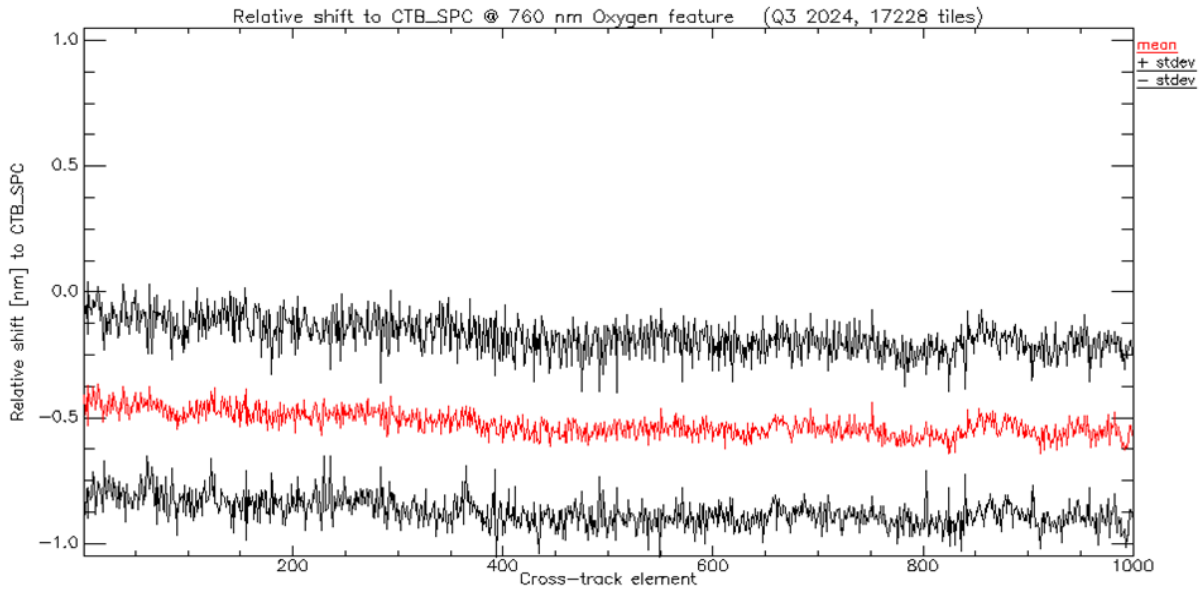


Figure 7-17 VNIR estimated spectral shift at 760 nm w.r.t the valid spectral calibration table (CTB_SPC), and relative spectral stability expressed at 1 sigma (Q3 2024, 17228 tiles)

For this analysis, the reference is thus not the nominal center wavelengths (i.e., a single number per band), but the CW per cross-track pixel, thus explicitly including the spectral smile (see Figure 7-18).

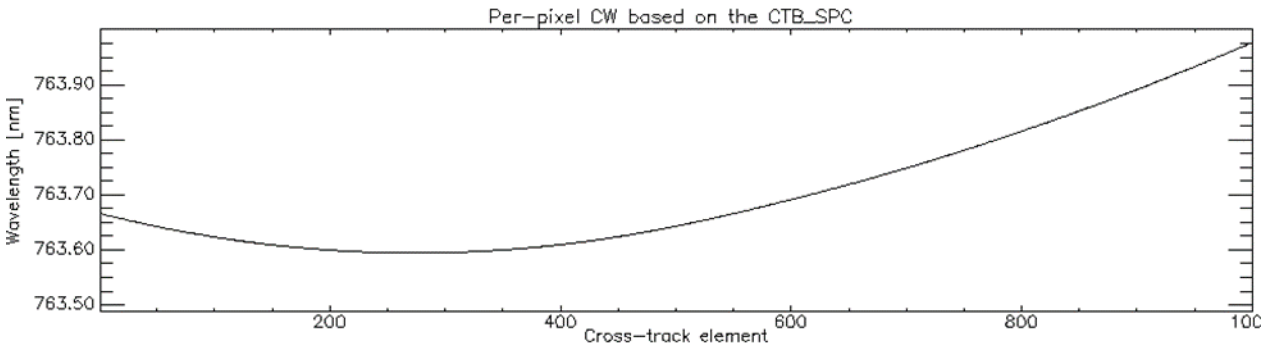


Figure 7-18 Center wavelengths per cross-track pixel based on the spectral calibration table (VNIR band 62) in the calibration table (CTB_SPC).

For the SWIR having less pronounced atmospheric absorption features, more influence of the background and a much lower signal level, the fitting also results in more clutter, as shown in Figure 7-19.

In order to demonstrate that the mean derivation to the CTB_SPC is within the spread of the data, the mean and standard deviation are calculated using the relative values, as shown in Figure 7-19. Here the differences to the CTB_SPC (Figure 7-20) are well within 1 standard deviation, confirming the validity of the spectral calibration. Note that for Q3 2024, the spread is also slightly increased in the SWIR w.r.t. Q2 2024, with the mean and median of the stdev of 0.65 nm (1 sigma) being the same as Q2. This is very likely an effect of more clutter within the acquire datatakes, as also the histograms generated with additional clutter removal are highly similar to Q1 2024.

Considering the EnMAP bandwidths of ~8.5 nm (FWHM), the spread of the vast majority of successful fits is within 3 nm, which agrees with the estimated overall stdev of ~0.65 nm (1 sigma) shown in Figure 7-19. To conclude, also for the SWIR the spectral calibration and the instrument stability can be confirmed, and no significant changes to previous reporting periods were found.

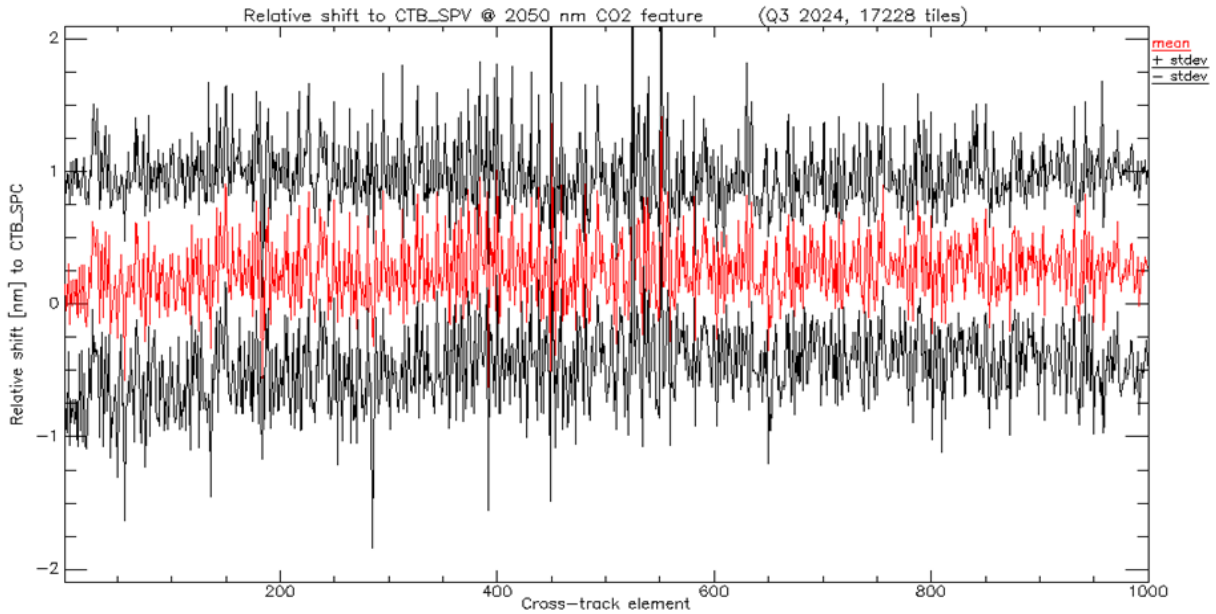


Figure 7-19 SWIR estimated spectral shift at 2050 nm w.r.t the valid spectral calibration table (CTB_SPC, shown below), and relative spectral stability expressed at 1 sigma (Q3 2024, 18226 tiles)

For this analysis, the reference is thus not the nominal center wavelengths (i.e., a single number per band), but the CW per cross-track pixel, thus explicitly including the spectral smile (see Figure 7-20).

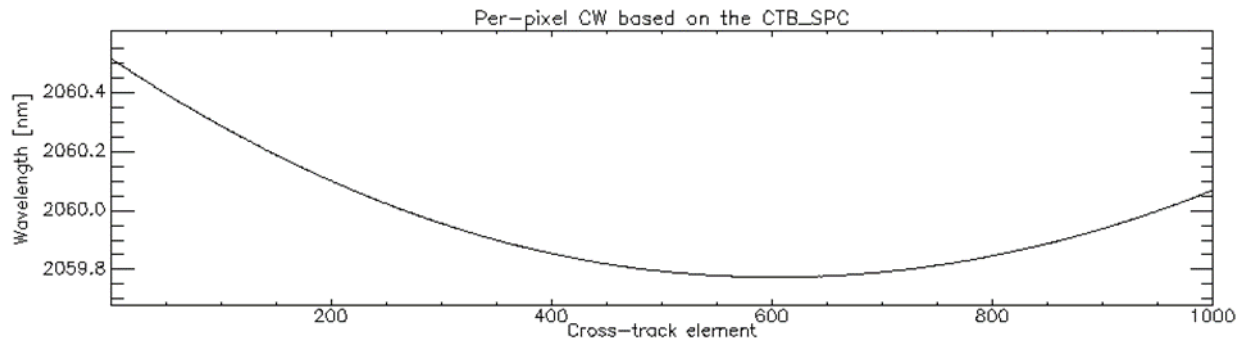



Figure 7-20 Center wavelengths per cross-track pixel based on the spectral calibration table (SWIR band 86).

7.6.2.3 Routine check of scenes in context of updates in CTB_RAD, CTB_SPC calibration tables

7.6.2.3.1 CTB_RAD

In the context of routine checks after radiometric calibration update, Table 7-23 shows the summary.

Table 7-23 Validated CTB_RAD

Validated CTB	ENMAP01-CTB_RAD-20240729T000000Z_V040100_20240718T061952Z
Datatake used	ENMAP01-___L1B-DT0000085062_20240801T065323Z_012  Figure 7-21 Datatake used (Tadschikistan)
Summary of result	New CTB_RAD confirmed

	<ul style="list-style-type: none"> • VNIR: for the given scene, <ul style="list-style-type: none"> • relative changes to P30 are similar as between periods before (below 0.2%) • for given scene, the absolute change is between -0.005 and +0.02 • for the given scene, no VNIR fringing is visible • as before, for bands above ~450 nm differences are slightly higher at center than towards edges of detector, with the stable “fingerprint” showing up. • SWIR: for the given scene: <ul style="list-style-type: none"> • relative and absolute change to P30 are very small (below 0.05%), smaller than the previous period • for given scene, no SWIR fringing is visible
--	--

7.6.2.3.2 CTB_SPC

In the context of routine checks after spectral calibration update, Table 7-24 shows the summary.

Table 7-24 Validated CTB_SPC

Validated CTB	None
Datatake used	
Summary of result	

7.6.2.3.3 Preparation checks for improved SWIR DC Correction

Along Q4 2024 a new processor version and calibration table update will deliver a significant improvement in the handling of very low signals in SWIR sensor.

Datatake IDs	Processor Version	Comment
DT4147 tile 2 (2022-10-02) Turkmenistan, Methane emission	Internal V01.05.00 with experimental CTBs	<p>Overall improvement with new DC correction:</p> <ul style="list-style-type: none"> - Overall radiance level does not change significantly - Shape of radiance spectra is not significantly altered - Relative change is scene-dependent: <ul style="list-style-type: none"> - Change in low gain range always <1% - Change in high gain range of ~2% - For SWIR low-rad scenes (Canada, Russia, Amazon) changes of 5% up to 10% - For high SWIR radiance scenes (Libya and Turkmenistan) changes of max. 2% - As expected, spatial patten of change resembles the „blocking“ structure in the DC which is thus successfully removed - Comparison of single bands show the removal of the striping effects after the correction in dark areas. - Bright areas are not effected by striping and are not visibly changed after DC-correction <p>See below for examples from the detailed QC report on the topic.</p>
DT69724 tile 18 (2024-04-19) Canada, low light		
DT78058 tile 10 (2024-06-16) Russia, low light		
DT78723 tile 02 (2024-06-22) Amazon, dark dense vegetation		
DT80327 tile 09 (2024-06-30) Libya 4, bright homogeneous desert		

Using the internal version of the processor V01.05.00 with the improved DC correction enabled and including the related experimental CTBs, tests were conducted to check the quality of these scenes w.r.t. the current baseline processing. The selected scenes range from low-light scenes and scenes with low reflectance in the SWIR to “normal” scenes with typical mid-latitude conditions to bright and highly reflectance scenes.

Additionally, various dates of the mission lifetime are used to check if the new DC correction is valid also for older scenes.

As expected, the influence of the new SWIR DC correction is largest for scenes with low SWIR signals, as shown in the following for the Canada scene.

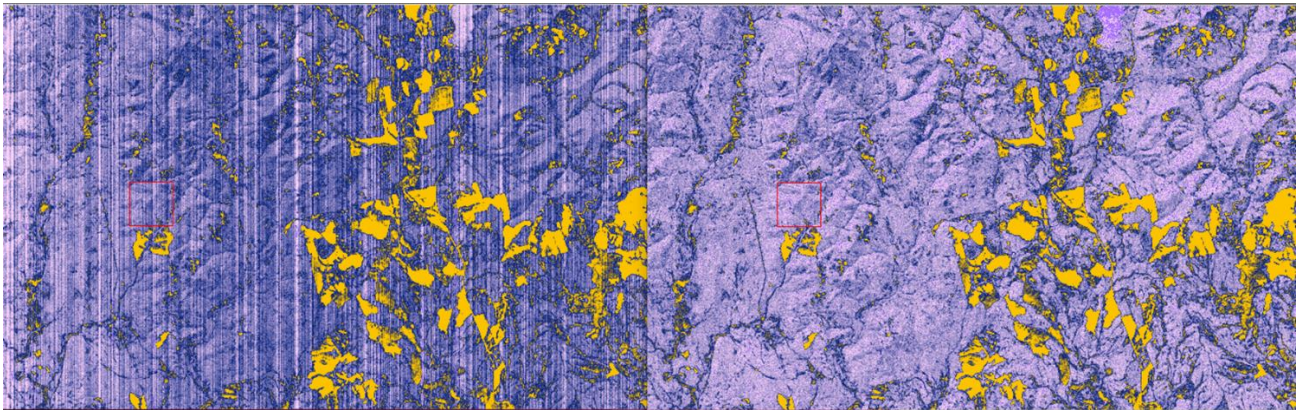


Figure 7-22 Canada scene, band 80 (2005 nm) with standard (center) and new (right) DC correction. Color table “haze”.

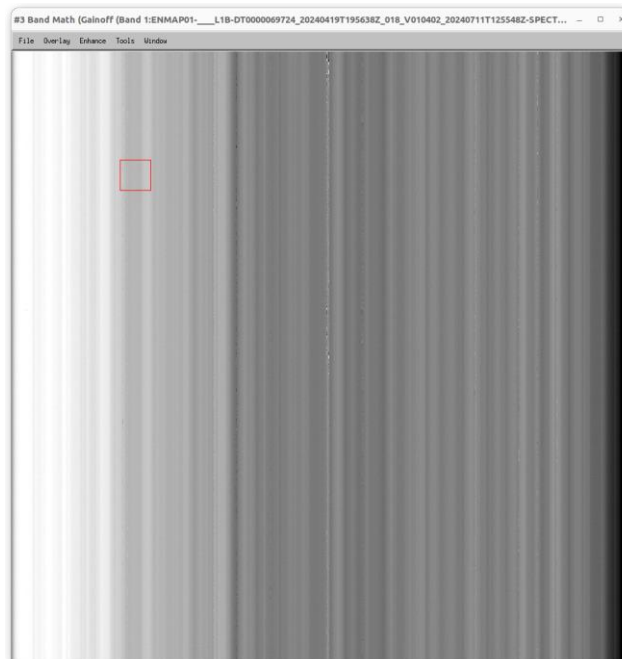


Figure 7-23 Canada scene, difference image between old and new processing

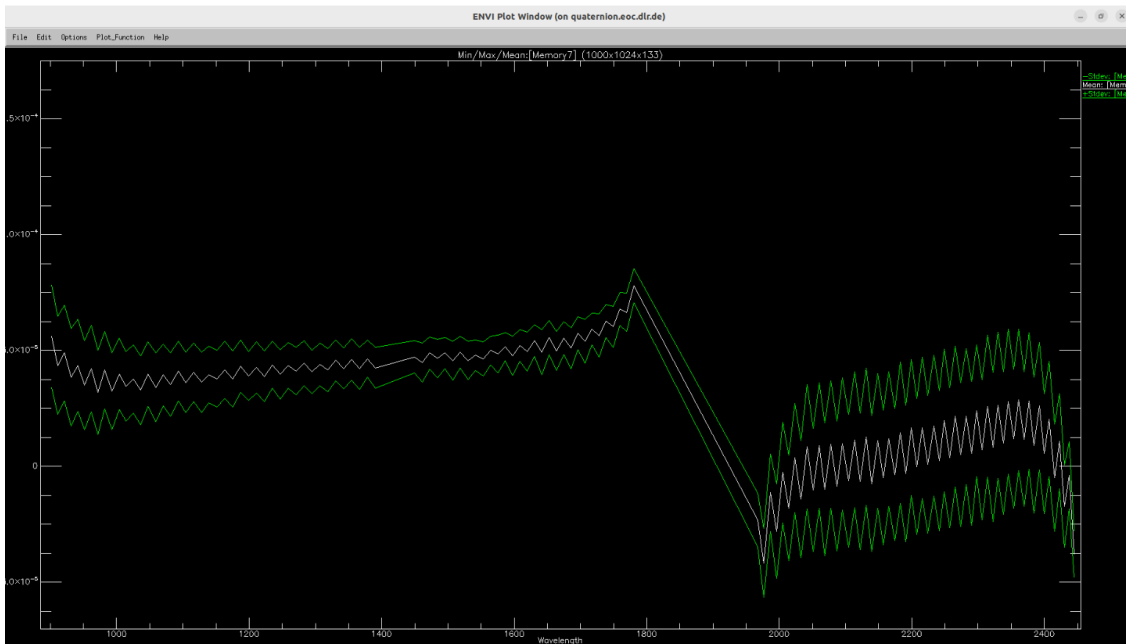


Figure 7-24 Canada scene, absolute difference statistics between the current and the new DC processing.

As shown in the difference image (current – new correction) in Figure 7-23 and the corresponding per-band statistics in Figure 7-24, the changes represent the “spiky” cross-track striping pattern. For the magnitude, the overall influence difference between DC corrections is close to zero, with the low gain range in the new processing having slightly lower radiances (thus a positive value) and the high gain range being close to zero. Considering the relative changes as depicted in Figure 7-25 low gain range are small outside the atmospheric absorption features (0.02% up to 1300 nm, and below 2% up to 1600 nm); for the high gain range, the changes are significantly higher ranging from ~4% up to ~10%. But when having a look at the single pixel spectra (Figure 7-26), the spectra are still close to identical and the high relative changes above 2000 nm can be explained by the overall very low signal. When having a look at one of these bands with a high relative change depicted above in Figure 7-22, then the improvement of the new DC correction is obvious for this low radiance scene.

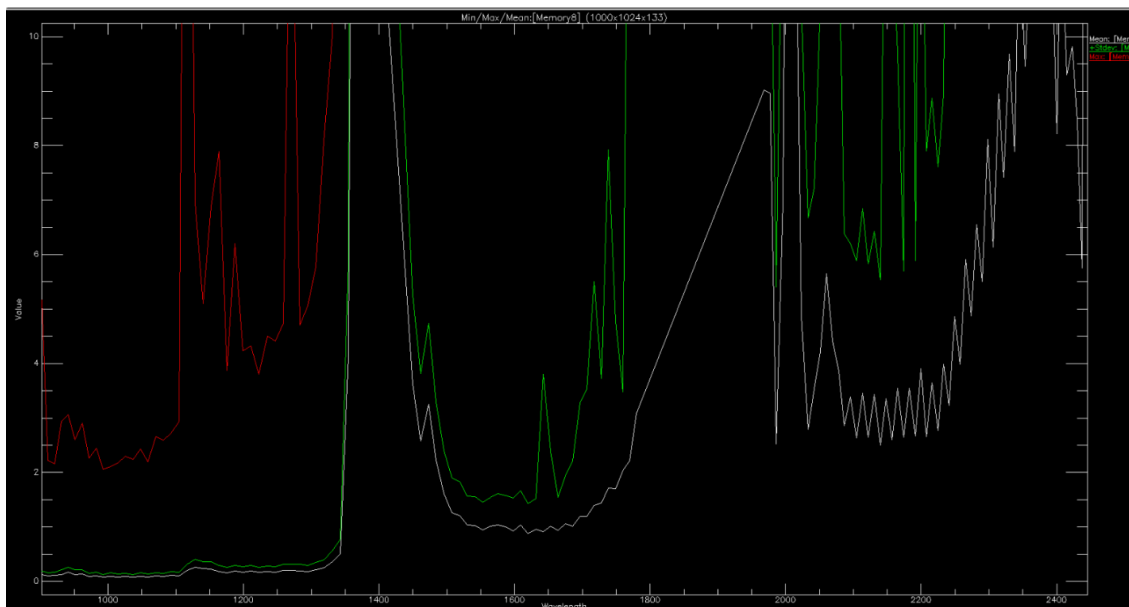


Figure 7-25 Canada scene, relative difference statistics between the current and the new DC processing.

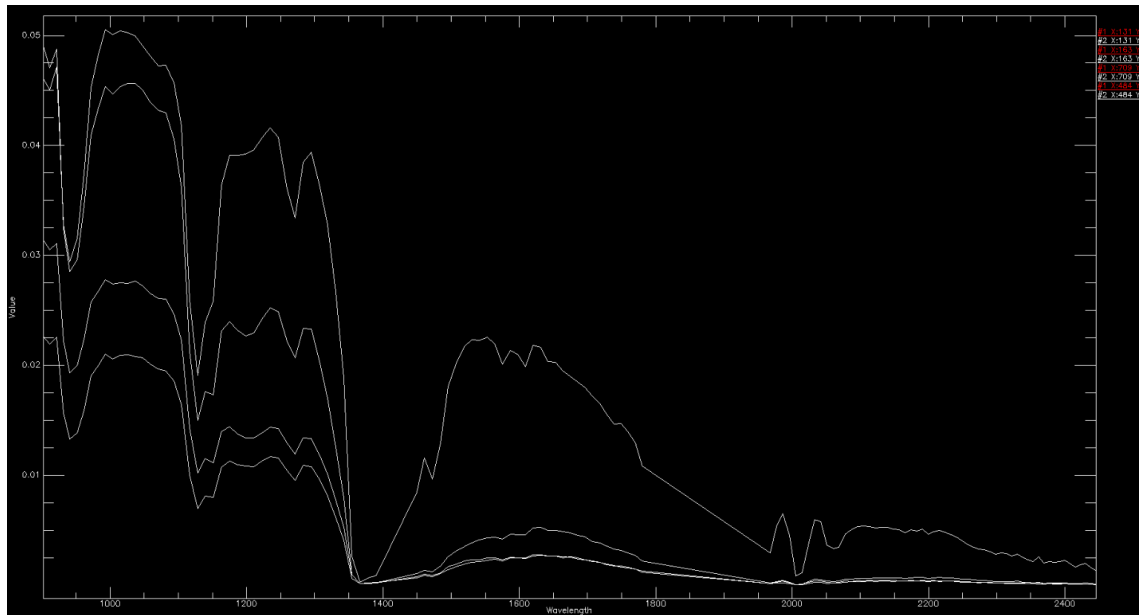


Figure 7-26 Canada scene, single pixel spectra - current processing in red, new DC in white.

To summarize the results for the shown Canada example and all other scenes with low SWIR radiance,

- Cross-track striping artefacts and gradients are successfully removed using the new SWIR DC correction, with the most impact on low-radiance pixels and small impact on high radiance pixels
- The spectral shape in all SWIR bands is maintained, and the radiance level in absolute units is only very slightly changed
- The relative changes are very small in the low gain range (up to ~1800 nm), always below 1%
- For the high gain range above ~1800 nm, the relative impact is significantly larger with 4% - 10% changes, but this is related to the removal of the striping artefacts at very low radiance levels.

When checking the influence on bright high radiance scenes (Libya, Turkmenistan), the influence of the new DC is smaller, but can still be seen as shown for Libya (Figure 7-27) where the striping is also removed. And as shown for the Turkmenistan scene, the relative change between the two processing versions (Figure 7-28) is below 0.5% for the full low gain range, and only higher at flanks of atm. absorptions. For the very last SWIR bands in the high gain range, the relative change increases up to 1%. Also the resulting single pixel spectra are close to identical in spectral shape and magnitude (Figure 7-29).

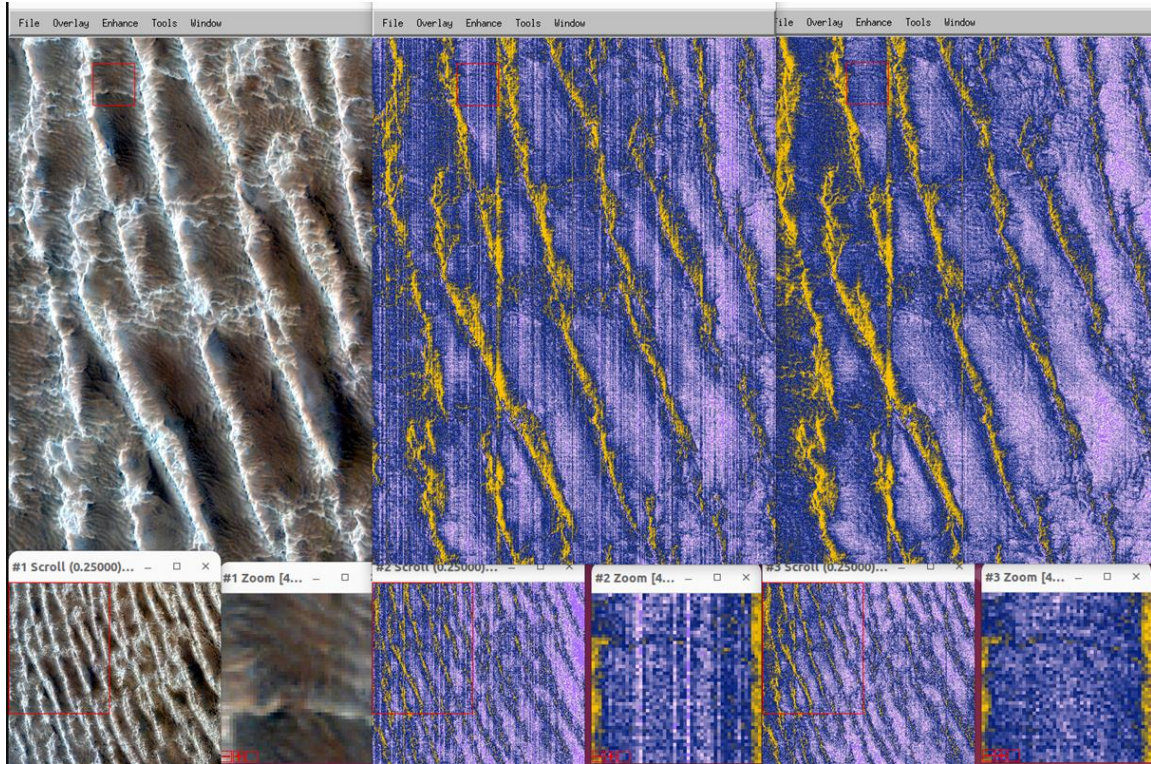


Figure 7-27 Libya 4, RGB (left), band 80 (2005 nm) with standard (center) and new (right) DC correction. Color table "haze".

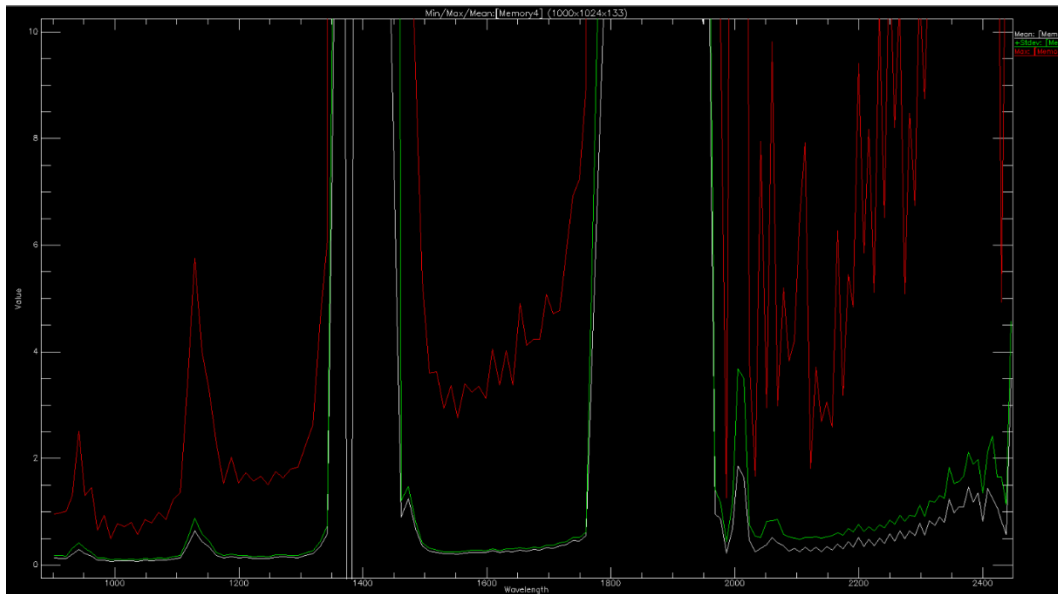


Figure 7-28 Turkmenistan scene, relative difference statistics between the current and the new DC processing.

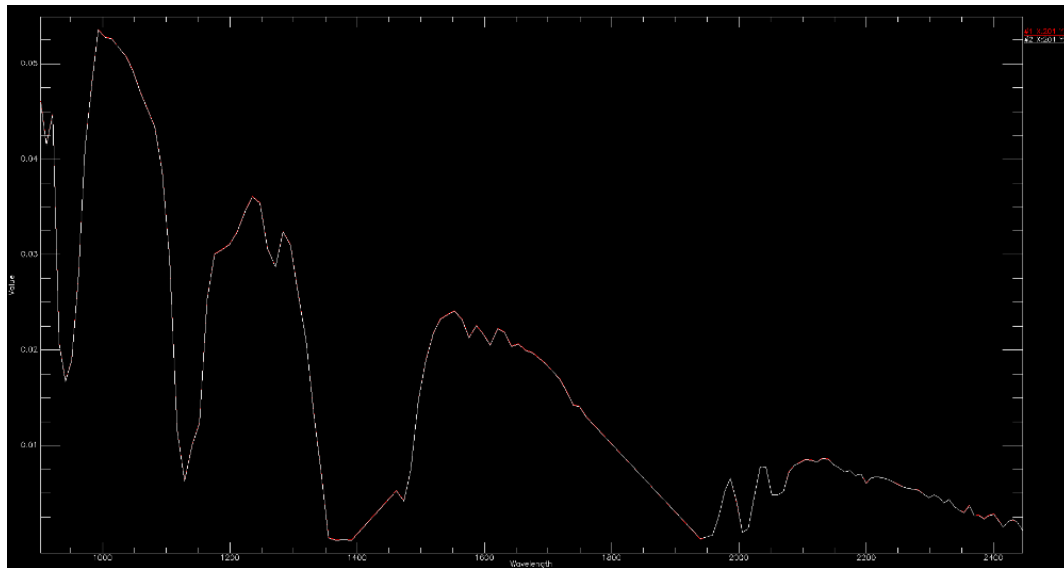


Figure 7-29 Turkmenistan scene, single pixel spectra - current processing in red, new DC in white.

To summarize the results for the high SWIR radiance scenes,

- Also for these scenes, the cross-track striping artefacts and gradients are successfully removed using the new SWIR DC correction, but the influence is smaller.
- The spectral shape in all SWIR bands is maintained, and the radiance level in absolute units is only very slightly changed
- The relative changes are very small in all the SWIR, and only up to 1% in the very last SWIR bands with low signal.

It is worth pointing out that one of these scenes (Turkmenistan) includes methane emission sources; checking the results, the new SWIR DC correction does not change the scene statistics significantly and thus is expected not to interfere with the methane retrieval methods.

7.6.3 Level 1C

This report covers the timeframe from 01.07.2024 to 30.09.2024. No geometric calibration was performed during this period.

In the timeframe of this report, 1819 datatakes have been acquired. In 1273 of those datatakes (~70 %), enough ground control points (GCP) and independent check points (ICP) were found to perform a geometric accuracy assessment. The datatakes without enough GCPs were not assessed quantitatively, but a random subset of them was inspected visually. The vast majority of those datatakes was either almost fully covered with clouds or showing only water, desert or rain forest. The behavior is thus as expected.

The assessment of the RMSE values in the metadata is shown below in Figure 7-30.

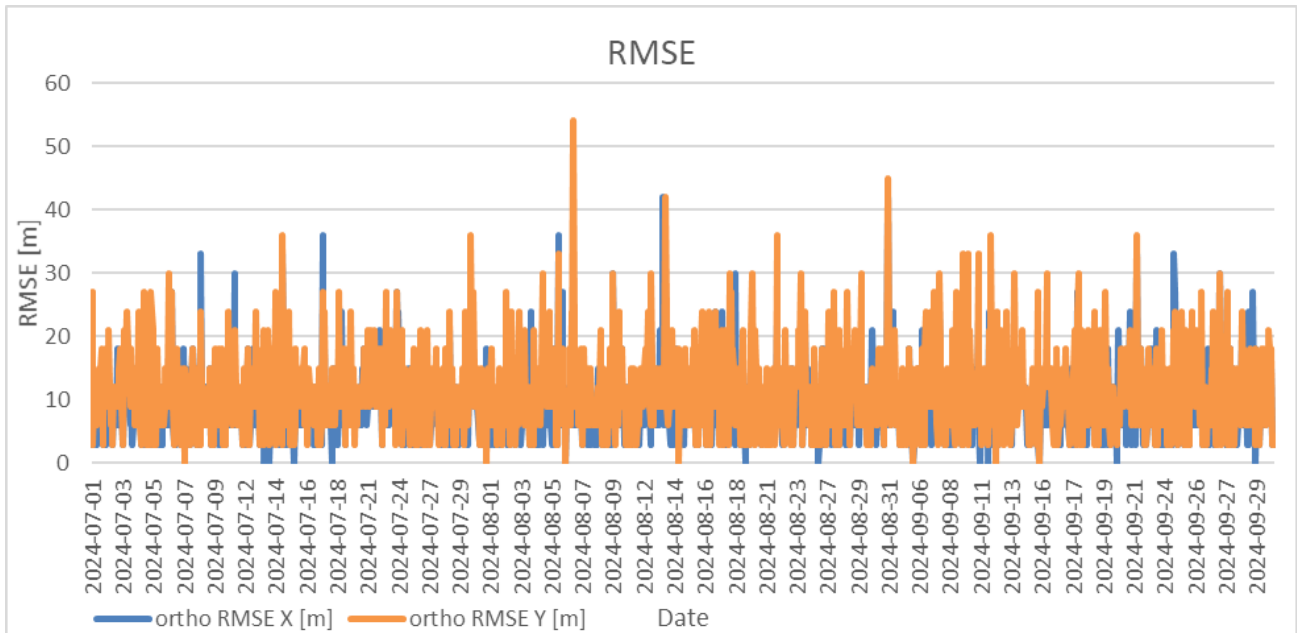


Figure 7-30 Assessment of RMSE values, calculated based on found ICPs, for all datatakes where ICP could be found

In x-direction, 8 datatakes (~0.6%) had an RMSE value above 30 m (1 GSD), whereas in y-direction, 12 datatakes (~0.9%) are above this threshold. For most of those datatakes, only very few GCP and ICP could be found during processing, making the results less reliable. The mean values are 9.01 m in x-direction and 11.30 m in y direction. This shows a very high geolocation accuracy for the datatakes where matching was possible. The requirement GRD-PCV-0155 (1 GSD) is thus fulfilled.

The average boresight angles, which can be interpreted as the correction and thus the error of the scene if no GCPs could have been found, correspond to approximately -15 m in x direction with a standard deviation of approximately 21 m and -29 m in y direction with a standard deviation of approximately 20 m on ground. It is reasonable to assume that the scenes where no GCPs could be found are in the same accuracy range and thus well within the requirement of 100 m (GRD-PCV-0150). Note that the x and y direction mentioned in this report are not in the image coordinate system but in UTM, as the evaluation is done on L1C products.

7.6.3.1 Geometric accuracy

EnMAP L1C products are matched against a reference image (Sentinel-2 data, if not stated otherwise) by using image matching techniques to assess the geometric accuracy. At the obtained checkpoints (CP), statistics are calculated to provide mean and RMSE values (Figure 7-31) for each scene. Note that the obtained accuracy in the analysis is always w.r.t. the reference image. This report covers EnMAP data from 01.07.2024 to 30.09.2024. A random sample of 471 L1C tiles was selected based on visual inspection of the catalogue quicklooks (e.g. to avoid cloudy images).

The requirement GRD-PCV-0155 shall be fulfilled:

The geolocation accuracy at nadir look direction of level 1C and 2A products shall be better than 1 GSD (1 sigma) in each direction with respect to reference images provided that reference images are available and sufficient similarity.

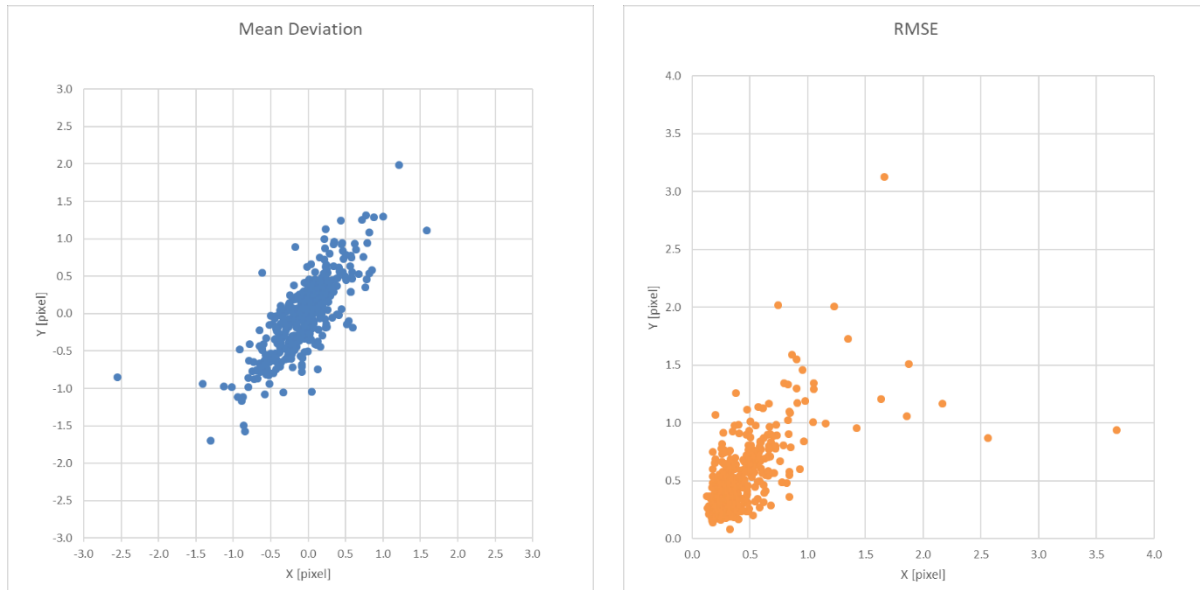


Figure 7-31 Mean deviation of EnMAP L1C products in pixel (left). RMSE value for EnMAP L1C products in pixel (right)

Note, that during processing the boresight angles and the geometric accuracy related quality flags are calculated on datatake level while in the figures and tables above, the accuracy is assessed per tile. The mean values over all 471 L1C tiles are -0.03 and 0.00 pixel in mean deviation with a standard deviation of 0.42 and 0.49 pixel while the mean RMSE values are 0.45 and 0.53 pixel, all in x and y direction respectively. The data show, that for the vast majority of scenes the accuracy wrt. reference image is better than one pixel and thus the requirements are fulfilled. Compared to the last geometric QC report, the values are very stable (see Figure 7-33).

7.6.3.2 Co-registration accuracy

In this chapter, the co-registration accuracy is checked against the Space Segment requirement SRDS-PIM-0050 (EN-KT-RFW-003 is also to be considered here):

*The HS-Imager shall be designed such, that the geometric co-registration is $\leq 20\%$ of the nominal Ground Sampling Distance ($0.2 * GSD$ linear displacement in both directions).*

For the assessment of co-registration accuracy, the SWIR data of EnMAP L1C products are matched against the corresponding VNIR data and the mean deviation values shown in this section (Figure 7-32).

This report covers EnMAP data from 01.07.2024 to 30.09.2024. A random sample of 474 L1C tiles was selected based on visual inspection of the catalogue quicklooks (e.g. to avoid cloudy images).

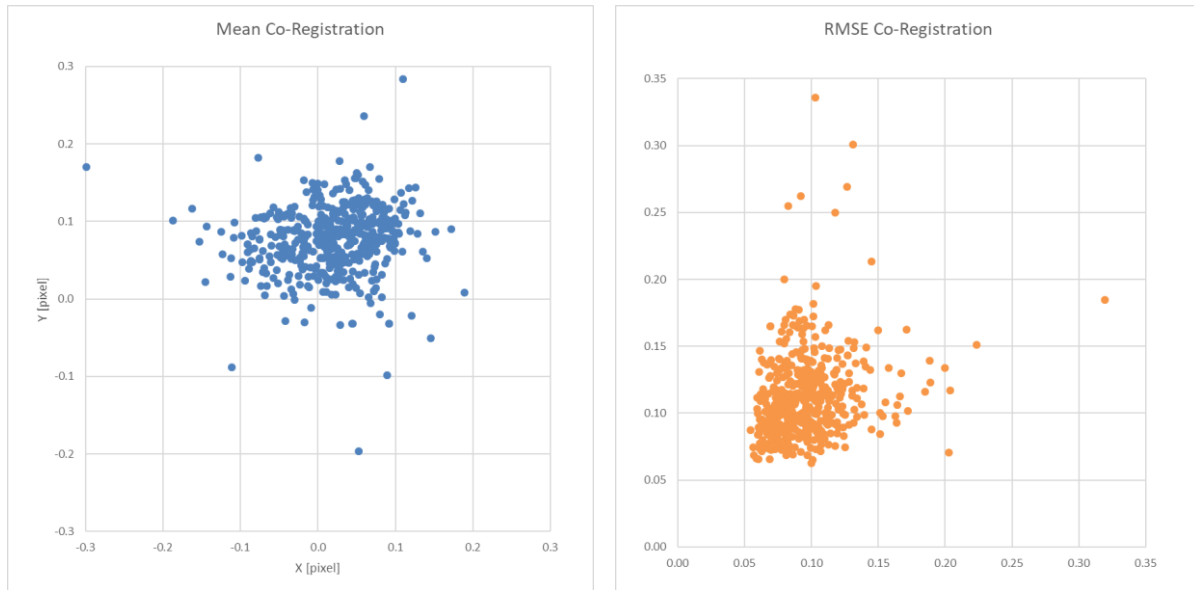


Figure 7-32 Mean deviation in pixel between VNIR and SWIR data of EnMAP L1C products (left). RMSE in pixel between VNIR and SWIR data of EnMAP L1C Products (right)

The data show, that the mean co-registration is well within the requirement. Note that the theoretical accuracy of the used matching algorithm is 0.1 pixel, and as can be seen in the RMSE values, still some mismatches were not removed by the blunder detection techniques that were applied. The mean deviation over all analyzed tiles are 0.02 pixel in x-direction with a standard deviation of 0.06 pixel and 0.08 pixel in y direction with a standard deviation of 0.04 pixel. Compared to the results in the previous geometric QC report, the values are very stable as can be seen in Figure 7-33.

7.6.3.3 Development of geometric performance

Since the launch of EnMAP on April 1st 2022, the geometric performance has been improved significantly. This was achieved by different geometric calibrations and processor updates. Table 7-25 shows the measures performed, their date and their effect.

Date	Measure	Effect
01.08.2022	Fix of attitude processing	Improvement of absolute geolocation (w/o matching)
20.09.2022	Boresight Calibration	Improvement of absolute geolocation (w/o matching)
03.11.2022	1 st Geometric Calibration	Improvement of absolute geolocation (w/o matching) Improvement of VNIR/SWIR co-registration (~0.8 pix -> ~0.4 pix)
11.02.2023	2 nd Geometric Calibration	Improvement of VNIR/SWIR co-registration (~0.4 pix -> ~0.15 pix)
29.03.2023	Processor update (v01.02.00)	Improvement of VNIR/SWIR co-registration (~0.15 pix -> ~0.06 pix)
05.05.2023	Processor update (v01.03.01)	Improvement of geolocation accuracy

Table 7-25 Improvement of geometric performance

Figure 7-33 shows the development of the co-registration accuracy, measured as described in previous section. Again, after a significant improvement since commissioning phase, over the last report periods the accuracy has been very stable.

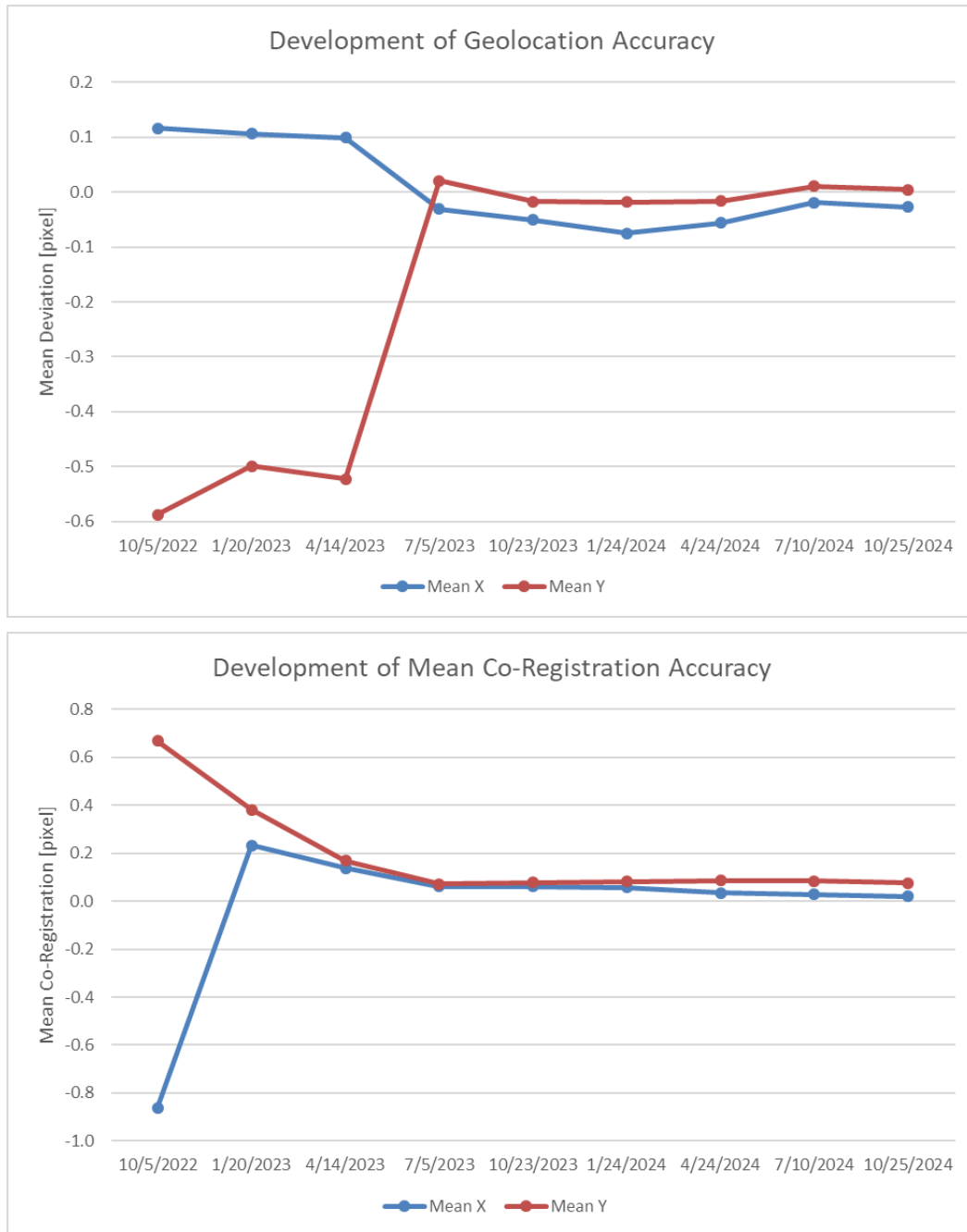


Figure 7-33 Development of co-registration accuracy based on the previous geometric QC reports

As most of the geometric processing – especially the matching against a reference image – is done on datacube level during L0 processing, the geometric accuracy and co-registration of data acquired earlier during the mission is not automatically improved when higher level products (L1B, L1C, L2A) are processed with the current processor version. However, during the currently ongoing L0 reprocessing of the whole archive, the geometric processing is executed with the latest processor version and geometric calibration table to make sure that the best geometric quality and co-registration is reached also for the reprocessed data. Users can recognize reprocessed data by checking the metadata tag **archivedVersion**: if the version is 01.03.00 or higher, then the geometric performance should be as analyzed in this report.

7.6.4 Level 2A

7.6.4.1 Validity of generated L2A “water” data

7.6.4.1.1 Analyzed scenes

The following scenes were taken into consideration:

DataTake - ID	Tile - ID	Location	L2A Option	Cirrus / Haze Removal	Overall Quality
85753	1	Wapusk, CAN	Water mode, water type “clear”	Cirrus	Nominal
83436	1	Gloucester Island, AUS	Water mode, water type “clear”	Cirrus	Nominal
83811	1	Wapusk, CAN	Water mode, water type “clear”	Cirrus	Nominal
86285	19	Venice, ITA	Water mode, water type “clear”	Cirrus	Nominal
88772	1	Birkholm, DEN	Water mode, water type “clear”	Cirrus	Nominal
88772	3	Kiel, DE	Water mode, water type “clear”	Cirrus	Nominal
89067	5	Tijuana, MEX	Water mode, water type “clear”	Cirrus	Nominal
89067	6	Rosarito, MEX	Water mode, water type “clear”	Cirrus	Nominal
91102	3	Briebie Island, AUS	Water mode, water type “clear”	Cirrus	Nominal

Table 7-26 Datatake IDs of analyzed water products

The below listed parameters were checked for above mentioned scenes by EOMAP:

Parameter	Check
Masking (Land, Water, Clouds, etc.)	No issues found.
Adjacency correction	No issues found.
Retrieval of atmospheric properties	No issues found.
Cirrus – correction	No issues found.
Retrieval of water leaving reflectance	No issues found.
Quality Mask	No issues found.

7.6.4.1.2 Data Checks

- Masking

First, the water mask is checked. The water body and the clouds, as well as shadows over land, are correctly masked (see Figure 7-34 and Figure 7-35).

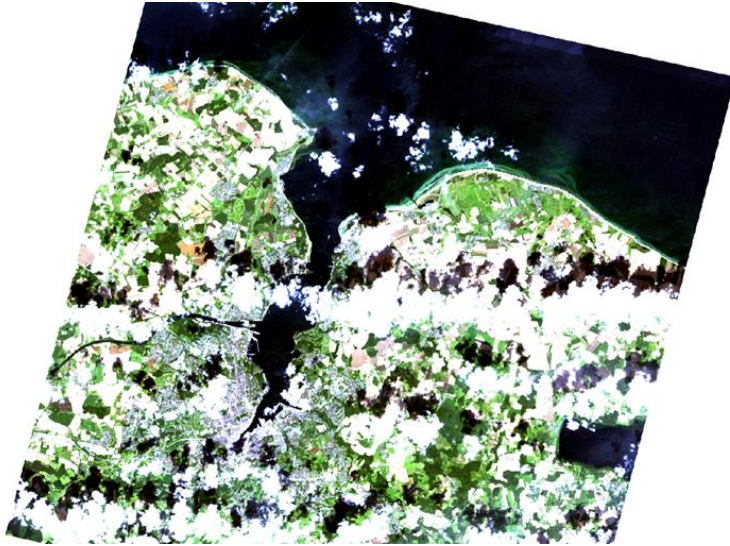


Figure 7-34 Scene-ID 88772; RGB-Quicklook with Bands 611.02nm – 550.69nm – 463.73nm

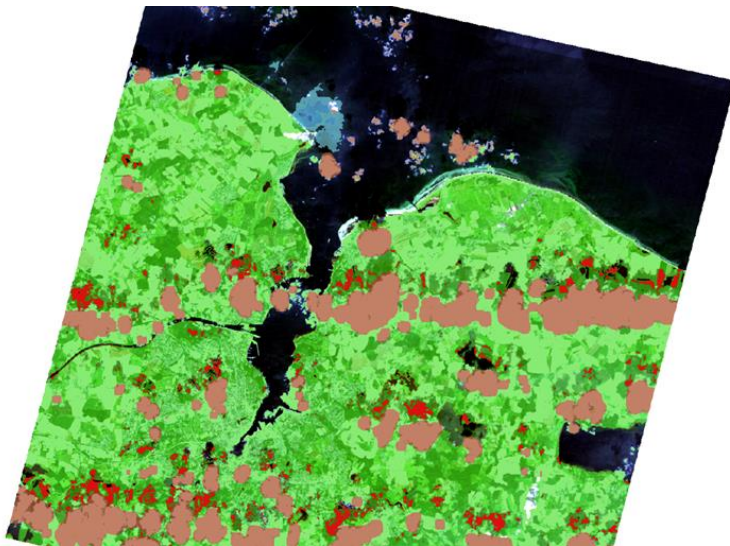


Figure 7-35 Scene-ID 88772; Geomask with Land in green, shadow in red, clouds in brown, cirrus in blue

- Adjacency Correction

Next, we check for the adjacency correction using the two sites 'AC1' and 'AC2' showed in Figure 7-36.



Figure 7-36 Scene-ID 86285; RGB-Quicklook with Bands 611.02nm – 550.69nm – 463.73nm

The coordinates of the sample locations are as follows:

AC 1: LAT 45.45182673 | LON 12.28019108

AC 2: LAT 45.38271273 | LON 12.30075479

To evaluate the adjacency correction, we choose a scene covering the Venice Bay. As sample locations, AC 1 near the coast line was chosen, as well as AC 2, not surrounded by any high reflective terrestrial feature (see Figure 7-36 for the sample locations).

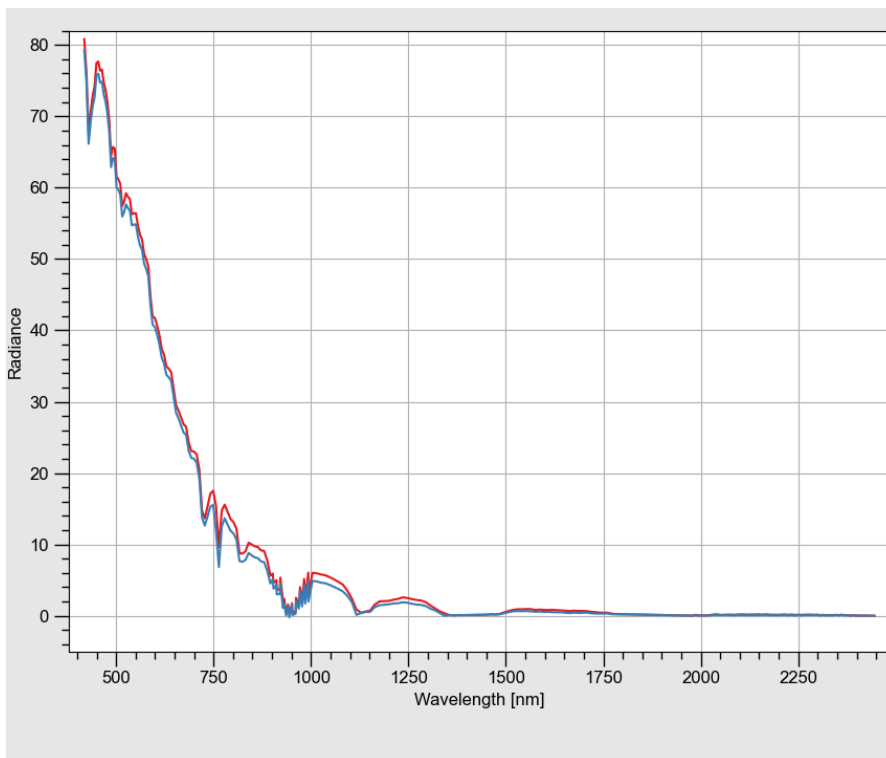


Figure 7-37 Scene-ID 86285; Signal sampled at location 'AC 1'; red: measured signal, blue: corrected signal

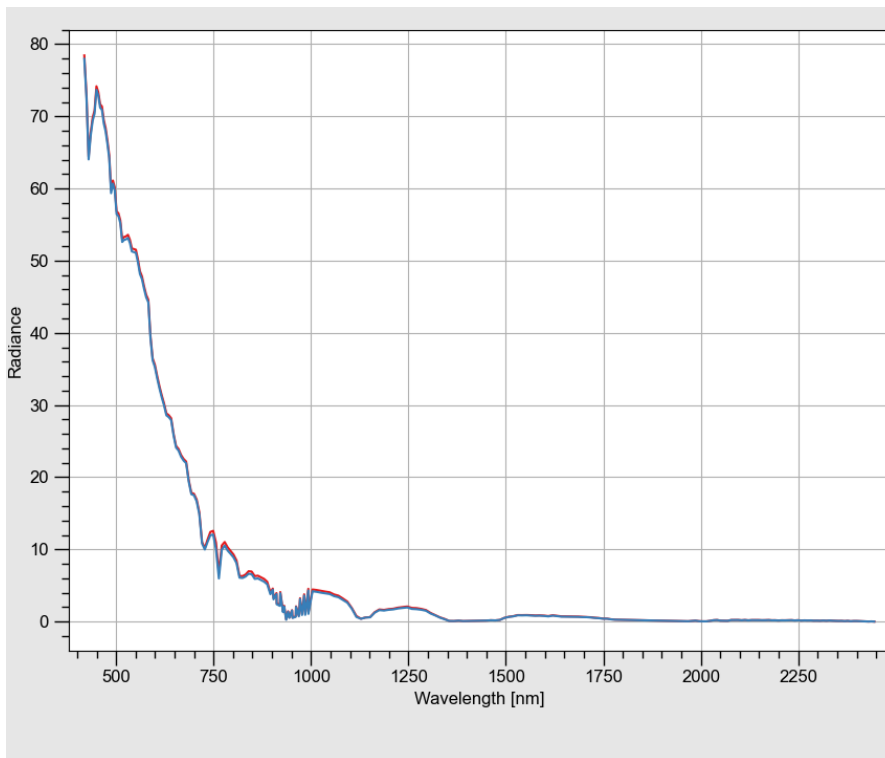


Figure 7-38 Scene-ID 86285; Signal sampled at location 'AC 2'; red: measured signal, blue: corrected signal

In Figure 7-37 and Figure 7-38, respectively, the influence of the adjacency correction on the spectrum is depicted. As expected, the amplitude of the applied correction is high for AC 1. Since this sampling location is neighbored by high reflective terrestrial features, this example pretty clearly shows the intention of applying adjacency correction and its importance for locations near shore. If not applied here, the absolute signal would be far too high, and any analysis would suffer from this. On the contrary, when sampling at location 'AC 2' we see that the amplitude of correction is much reduced and in parts of the spectrum not even noticeable anymore.

Thus, the adjacency correction works as we expect it to.

- Quality Mask

Figure 7-39 provide you with the quality mask of the scene, shown already in Figure 7-36. As depicted, most parts of the scene were found to be of good quality. Areas with low quality tend to have high values of AOT (Aerosol Optical Thickness), which hamper the proper correction of the corresponding atmospheric effects.

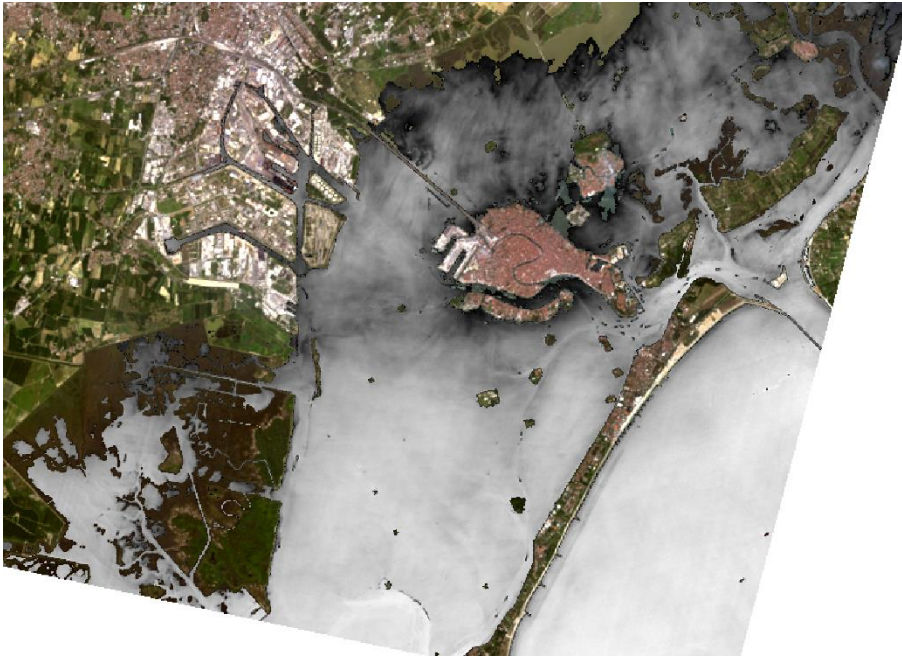


Figure 7-39 Scene-ID 86285; Quality mask in greyscale where white corresponds to 1, i.e. best overall quality

- Reflectance Product

To get a better impression of the product normalized water leaving reflectance as the final one, Figure 7-40 shows the reflectance using the RGB channels 611.02nm, 550.69nm and 463.73nm.



Figure 7-40 Normalized Water Leaving Reflectance of scene-ID 86285; Wavelengths for RGB: 611.02nm – 550.69nm – 463.73nm

For the two labeled locations in Figure 7-40, the sampling coordinates are as follows:

nWLR 1: LAT 45.42941373 | LON 12.28100917

nWLR 2: LAT 45.36704577 | LON 12.38238510

The following two plots, Figure 7-41 and Figure 7-42 depict the normalized water leaving reflectance (nWLR), sampled at the locations nWLR 1 and nWLR 2 (see Figure 7-40). nWLR 1 is located in some shallow area, where a high concentration of suspended matter can be found according to the Quicklook (Figure 7-39). At location nWLR 2, the water is deeper, and the water column seems to be much clearer. When taking a look at the two corresponding spectra, we see those expectations being confirmed. Summing up, the normalized water leaving reflectance, as the final product, represents a highly appropriate dataset for further investigations, like retrieving details on the water content and much more. The applied correction algorithms, e.g. the correction for adjacency effects on pixels near shore, ensure to suppress disturbing parts of the at-sensor radiance.

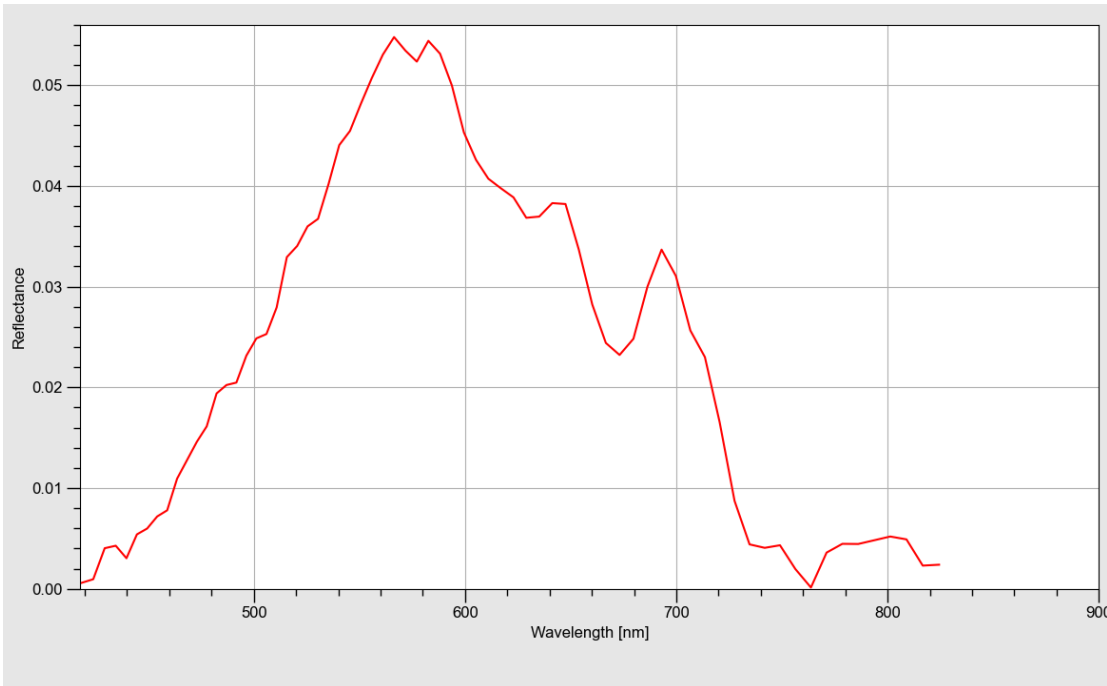


Figure 7-41 Scene-ID 86285; nWLR sampled at location nWLR 1

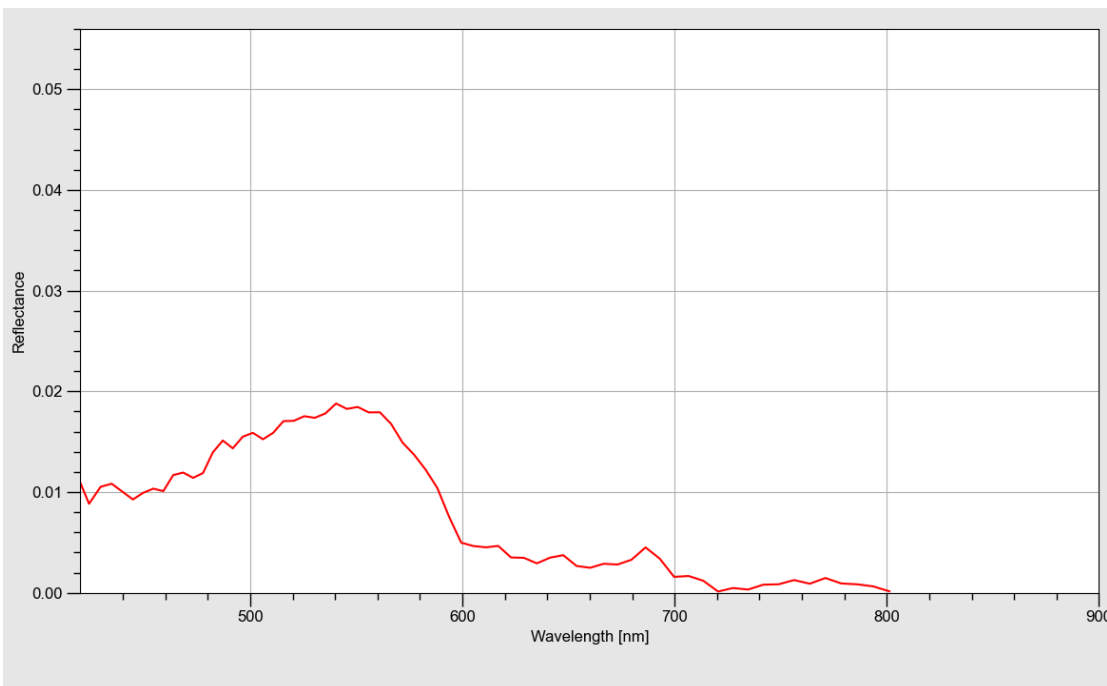


Figure 7-42 Scene-ID 86285; nWLR sampled at location nWLR 2

7.6.4.2 Validity of generated L2A “land” data

7.6.4.2.1 Analyzed scenes

Within the time interval between 01.07.2024 to 30.09.2024, an interactive in-depth analysis has been conducted for the following scenes:

datatakel D	tileID	date	location	L2A option	cirrus and haze removal	Archived Version	processor version	Overall Quality	Quality Atm
43167	07	2023-09-10	Germany	Land	No	01.03.03	V010501	Nominal	Nominal
43167	08	2023-09-10	Germany	Land	No	01.03.03	V010501	Nominal	Nominal
1849	14	2022-07-20	Germany	Land	No	01.04.01	V010501	Nominal	Nominal
95871	24	2024-09-21	Germany	Land	No	01.04.02	V010501	Nominal	Nominal
42020	22	2023-09-14	Germany	Land	Yes	01.03.03	V010501	Nominal	Nominal
90192	21	2024-08-30	Germany	Land	Yes	01.04.02	V010501	Nominal	Nominal
85508	22	2024-08-03	Germany	Land	Yes	01.04.02	V010501	Nominal	Nominal
73100	22	2024-05-14	Germany	Land	Yes	01.04.02	V010501	Nominal	Nominal

Table 7-27 Datatake ID of analyzed land products

For the selection of L2a data, care was taken to ensure a high degree of variety with respect to the geographical location of the data, external conditions (cloud cover) during the data take and processing parameters.

7.6.4.2.2 Data Checks

In the following, the tiles acquired over the Bavarian Forest acquired in 2022, 2023 and 2024 were checked for the shape and magnitude of the BOA_ref spectra. Also, the quality of the generated masks is evaluated.

For all tiles the visual image impression is fine. The geometric (relative) accuracy is within one pixel. For the masking (Figure 7-44), only haze was detected over a few patches of the scene; visual inspection shows that this masking is plausible. The BOA_ref spectra (Figure 7-46) over vegetation, soil and shallow water all show the typical shape and magnitude, indicating the correct L2A correction. As expected, the overlapping region between VNIR and SWIR includes the band-to-band changes (“jumps”) but outside this region the overall shape and magnitude of the BOA_ref between VNIR and SWIR is accurate.

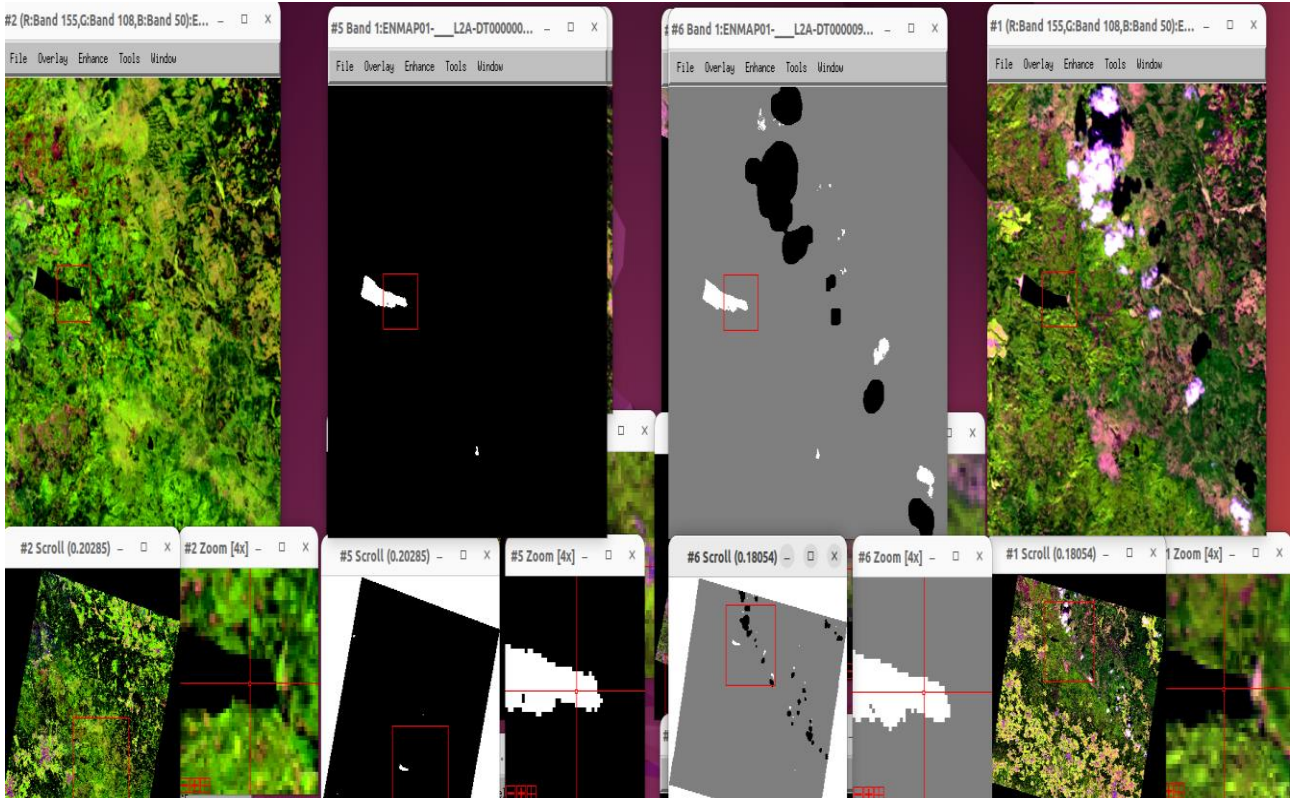


Figure 7-43 EnMAP L2A false colour composites (bands 155-108-50) of scenes DT1849 Tile 14 and DT95871 Tile 24 and their corresponding masks (QL quality classes)

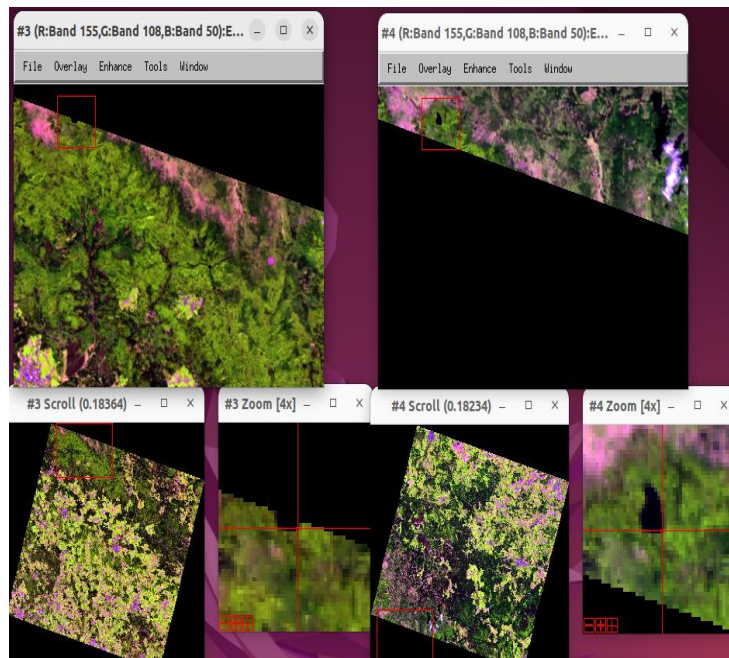


Figure 7-44 EnMAP L2A false colour composites (155, 108, 50) of scene 43267 Tile 7 and Tile 8 with zoom on the overlapping area.

The seamless processing between tiles was also checked, and as shown in no visual borders exist in the image when stitching, and the spectra (Figure 7-45) for similar surfaces in both tiles matches for all of these scenes. And when checking for the spatial continuity between the tiles, also the geometry matches.

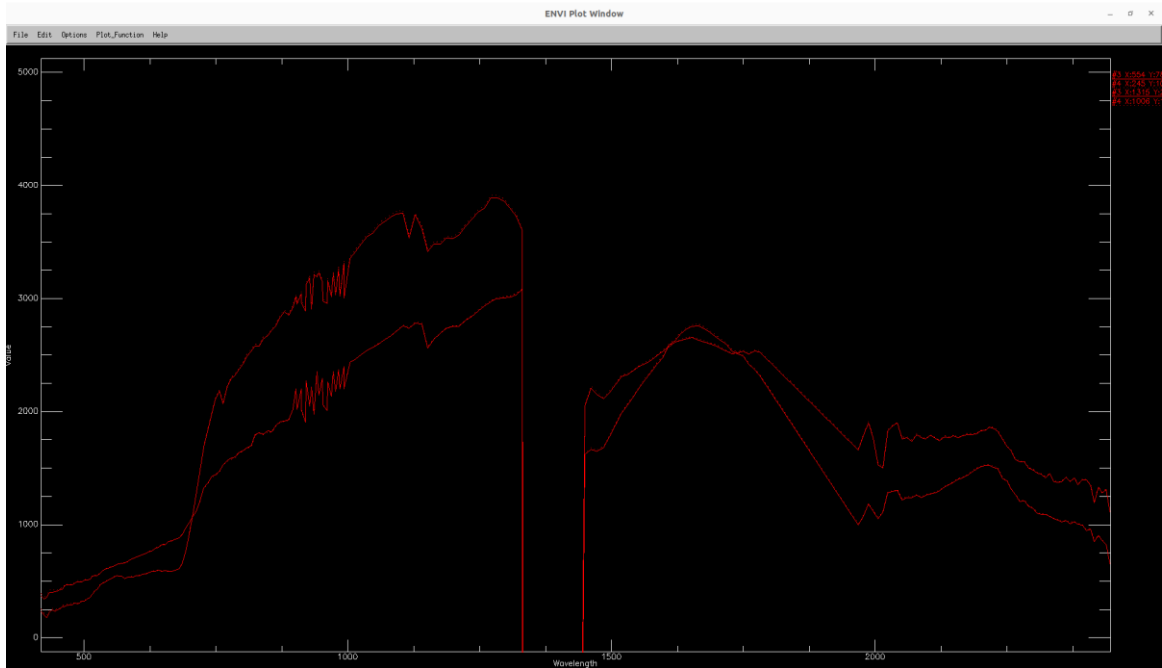


Figure 7-45 Comparison of image spectra of the two neighbouring tiles (scene 43267 Tile 7 and Tile 8, solid and dashed lines resp.)

As the generation of time series is now more in the focus by users, this is also checked for 3 different time steps representing the years 2022, 2023 and 2024, all processed with the latest processor version. As expected, the spectra do vary representing the phenological states and surface covers of land pixels (Figure 7-46). For all scenes and surfaces, the presented vegetation spectra are highly plausible, showing the typical phenological behavior (i.e., changes in vitality and water content). The same also applies to water spectra, as shown in for smaller lakes and ponds within these scenes. So, for these scenes, there are no apparent differences related to the data quality with changing years of data acquisition. Note that the bands in these figures do differ slightly which is expected as the SWIR band configuration was changed in Q3 2023.

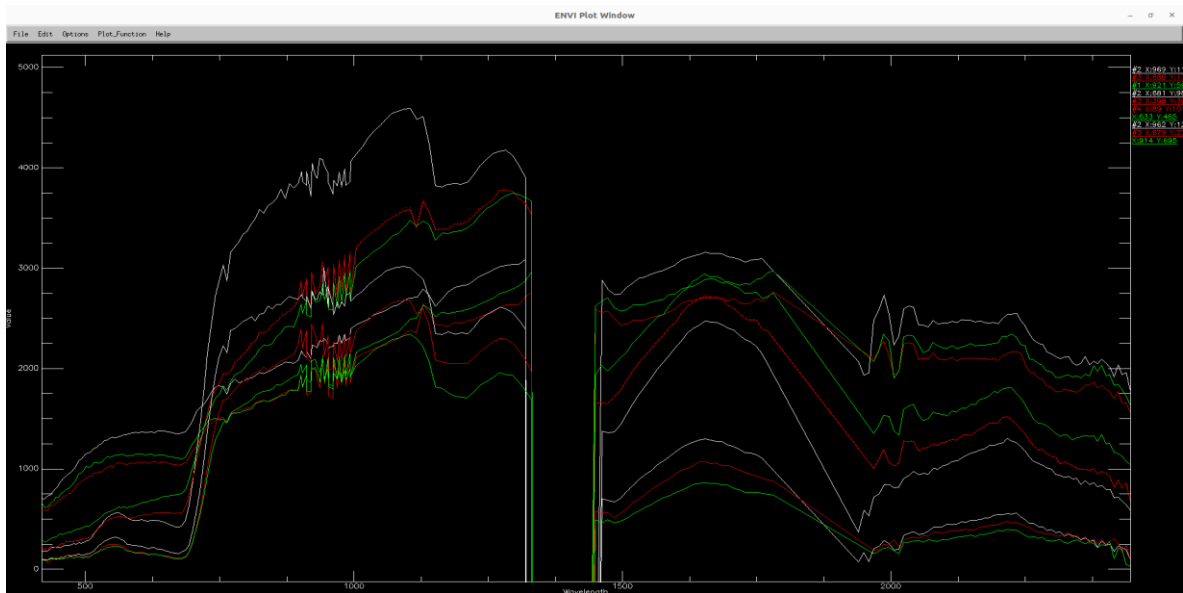


Figure 7-46 Typical image spectra (single pixel) of vegetation of the different years (white=2022, red=2023, green=2024)

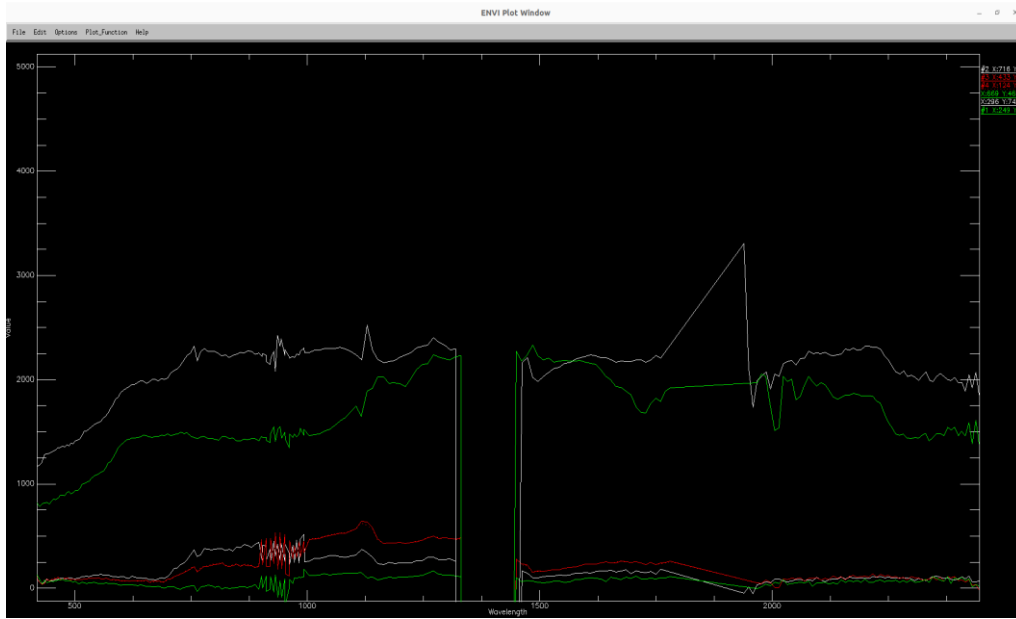


Figure 7-47 Typical image spectra (single pixel) of water bodies of the different years (white=2022, red=2023, green=2024)

When checking the generated cloud and quality layers, the masking and assignment of flags in generally valid. In some cases, the class labels for water and cloud shadows are incorrectly assigned (Figure 7-48), but this behavior is known and due to the high spectral similarity of these classes, especially when cloud shadows occur over dense dark vegetation, as shown for vegetation in Figure 7-48 and water in Figure 7-49.

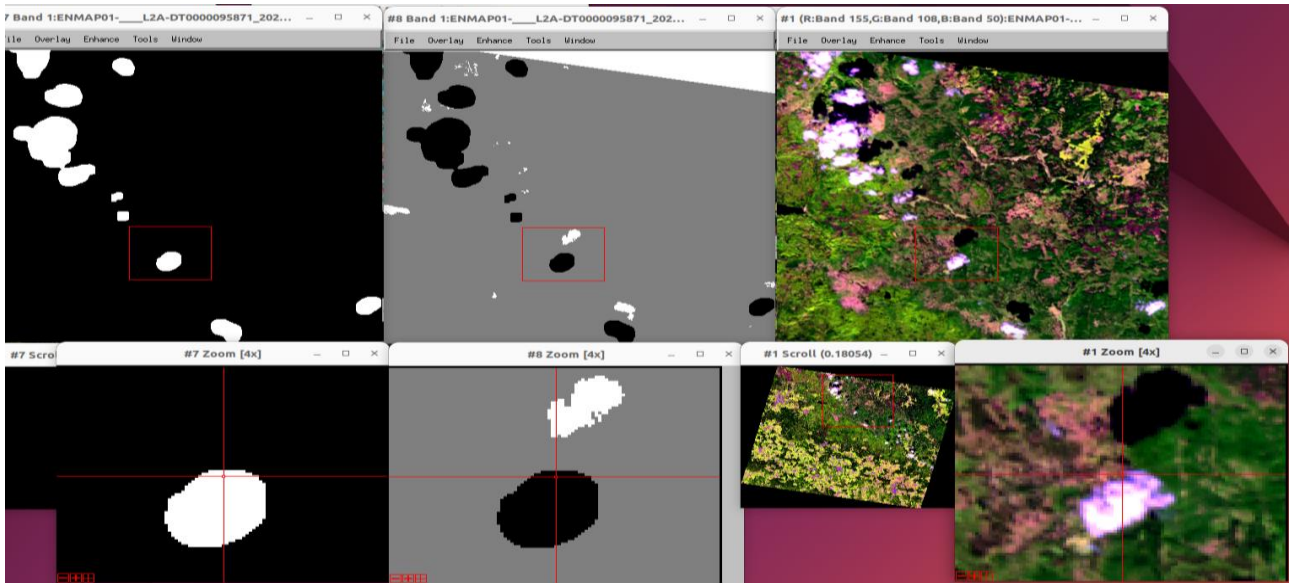


Figure 7-48 Cloud mask, QL quality classes and EnMAP L2A false colour composite (155, 108, 50) of DT95871 Tile 24 showing misclassification of cloud shadow as water bodies (in white in the center image).

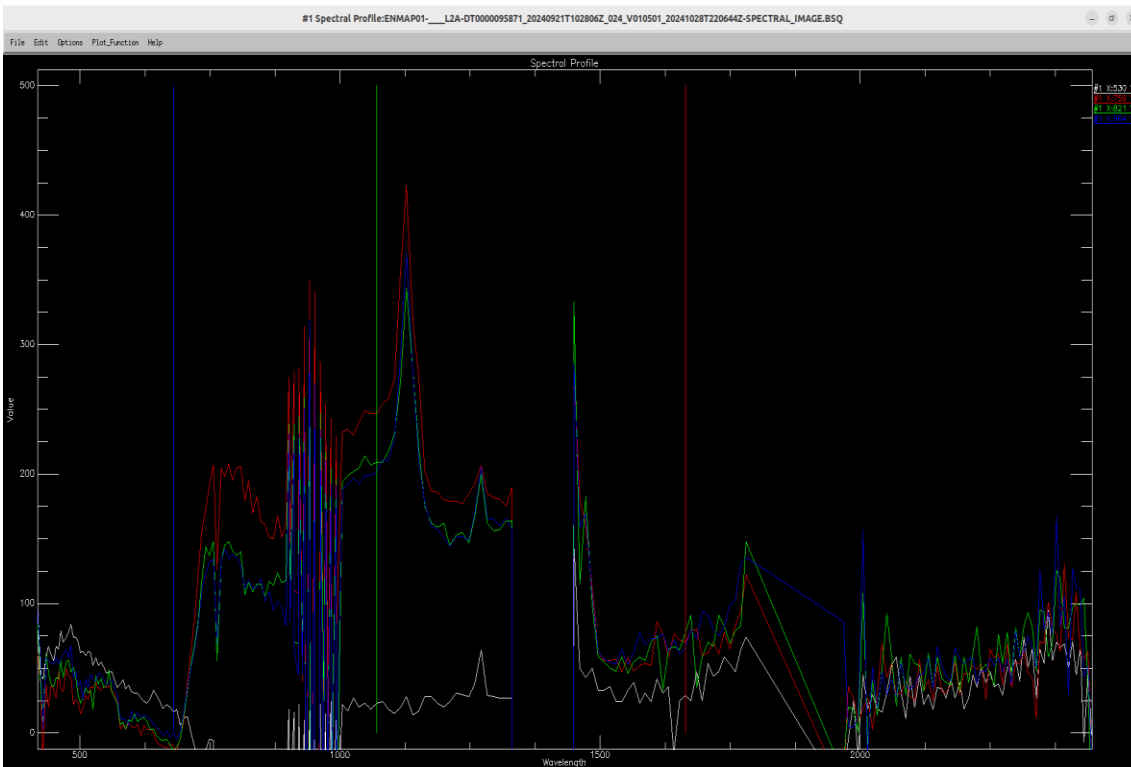


Figure 7-49 Image spectra of classified water bodies (DT95871 Tile 24), whereas only the white spectra corresponds to water, the other three correspond to cloud shadow over dense dark vegetation

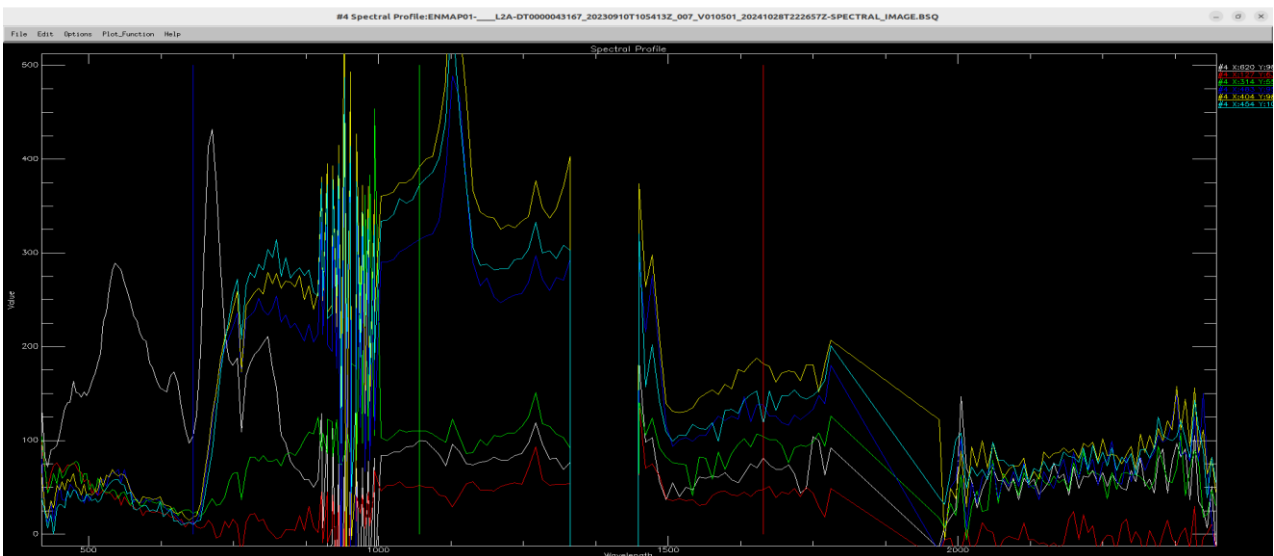


Figure 7-50 Image spectra of classified water bodies (DT43267 Tile 7), whereas only the white, red and green spectra correspond to water, the other three correspond to cloud shadow over dense dark vegetation

Within the QC, a second similar multi-temporal analysis was also conducted for more difficult scenes where some dates were affected by cirrus and haze (in addition to clouds) in order to check the related L2A correction results (Figure 7-51 for scene information). Within the side-by-side analysis using the coordinates, the geometry matches very well so that a pixel-wise analysis can be conducted (Figure 7-51). As shown in Figure 7-52, the spectra of these pixels align well considering the phenological changes. It is worth pointing out that this is still valid considering the different haze and cirrus corrections, as depicted in the masks shown in Figure 7-53, indicating the L2A processing and corrections work well for these multi-temporal scenes. Given these challenging conditions, also the masking shows a general good agreement for flagging clouds and cirrus, noting that the separation of these classes is not easy.

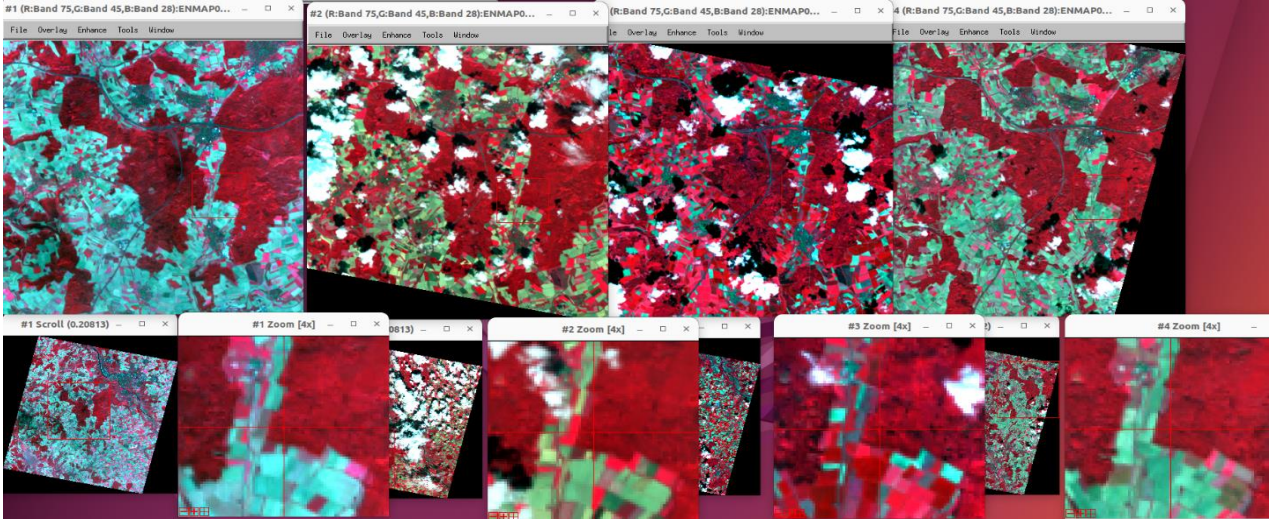


Figure 7-51 Time series of EnMAP L2A CIR colour composites (bands 155-108-50), Wuerzburg area, Germany.

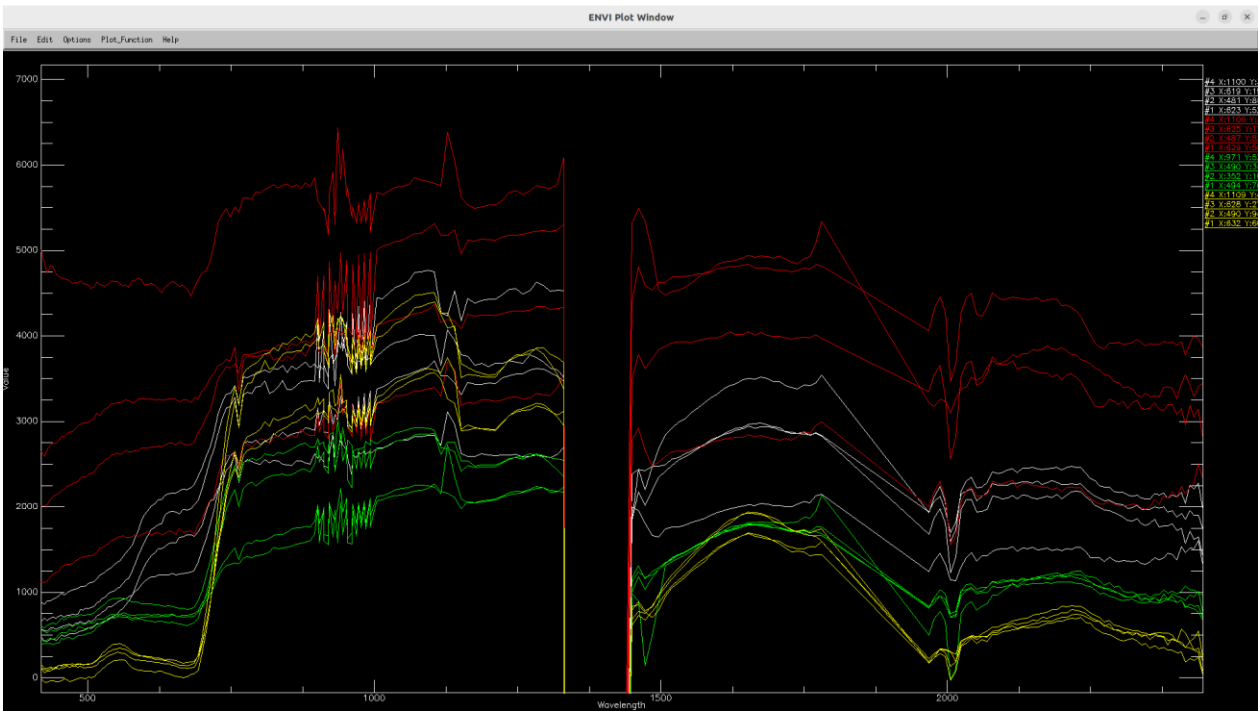


Figure 7-52 Typical image spectra (single pixel) of trees of the different years; each color represents a pixel within the 4 different times.

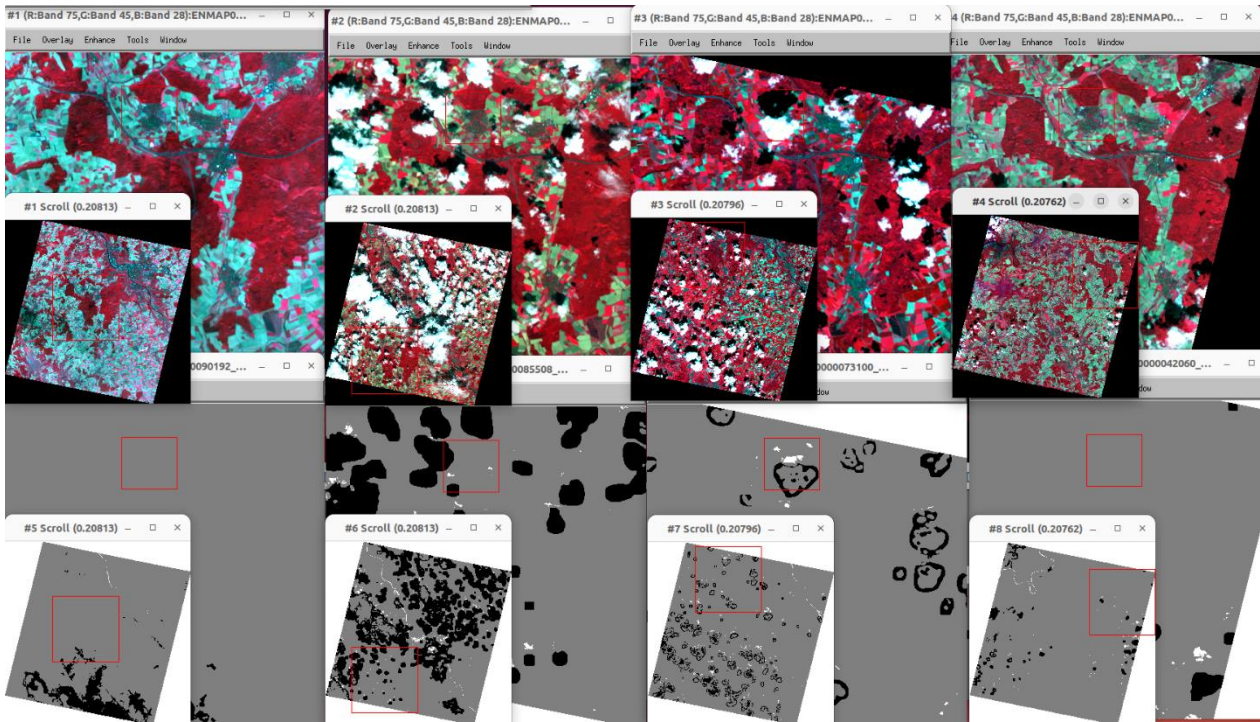


Figure 7-53 Cloud mask, QL quality classes and EnMAP L2A CIR colour composite for the 4 years.

8 External Product Validation

The standard quality parameters were validated in the external product validation process for the reporting period. More than 300 EnMAP products from the latest available processor and archiving versions were downloaded, checked for suitability and finally selected for validation. Some new matchups with reference measurements could be implemented in the reporting period.

8.1 Level 1B

The following validation scenarios were performed to validate Level 1B products:

- TOA Radiance
- Spatially coherent radiometric miscalibration (striping artifacts; along- and across-track)
- Signal-to-Noise Ratio (SNR)
- Spectral validation

The latest TOA radiance comparisons have confirmed that the radiometric deviation for the significant wavelength ranges is still $< 5\%$ RMSE. Minor overshoots in the detector wavelength edge regions and in the water absorption bands cannot be clearly attributed to errors in the EnMAP products, the processing, or the validation data.

No significant anomalies were detected regarding the VNIR and SWIR across-track direction spatially coherent radiometric miscalibration indicating that the implemented correction algorithm works very well. SWIR along-track artifacts at wavelengths with a vital gradient/feature are still visible. However, there are currently no needs to implement a correction, as there are hardly user complaints and a perfect correction is apparently not feasible. The mentioned artifacts are well within the mission requirements of $< 5\%$.

The SNR assessment was updated based on 163 reprocessed tiles (VNIR 93 and SWIR 70) and was found to be very stable (VNIR: 410:1; SWIR: 267:1) compared to the previous evaluations and inside the mission requirements (VNIR $> 343:1$ @495 nm SSD 4.7 nm; SWIR $> 137:1$ @2200 nm & SSD 8.4 nm).

Eight tiles acquired under different atmospheric and angular conditions were used to determine the spectral smile and offset using the O₂ band (761 nm) for the VNIR and CO₂ band (2300 nm) for the SWIR detector. The across-track variations (VNIR: -0.16 nm offset, ~0.35 nm peak to peak and SWIR: 0.4 nm offset, ~0.6 nm peak-to-peak) are always small with respect to the requirements (761 nm: 1.72 nm, 2300 nm: 1.55 nm).

8.2 Level 1C

The following Level 1C validation scenarios have been performed:

- VNIR-to-SWIR spatial co-registration
- Absolute spatial accuracy

For the spatial co-registration between VNIR-to-SWIR for products with an archived version $\geq 01.04.02$ an RMSE of 5.8 m in X and 6.8 m in Y direction is achieved. Thus, the geometric co-registration has reached a stable level, well inside the mission requirements of $< 30\%$ of a pixel.

The quality of the absolute spatial accuracy is also stable. Once again, an RMSE of 10.2 m in X and 12.6 m in Y derived from 32 tiles with an archived version $\geq 01.04.02$ was achieved which is well inside the mission requirements (< 30 m with GCPs in the image, < 100 m without GCPs).

8.3 Level 2A

Ten new in-situ matchups were added to the L2A land and water quality assessment during the last quarter.

Land

Two new matchups increased the total number of successful matchups to 47. The results stabilized the uncertainty pattern and thus confirmed the fulfillment of mission requirements for BOA reflectance. Similar to the TOA radiance product, at the beginning (< 500 nm) and ending (> 2400 nm) of the wavelength domain, slightly higher residuals (up to 3% RMSE, accuracy, and precision) can be identified. The majority is around 2% for the rest of the wavelength domain. All measures are generally well inside the mission requirements

for BOA reflectance of 5%. Another explanation besides the inaccuracy of field spectrometers in these wavelength ranges seems to be that there are often not enough dark, dense vegetation pixels in the available validation tiles, so that in these cases no AOT retrieval was possible and the default value had to be used.

Water

Seven new valid matchups of normalized water leaving reflectance could be integrated into the statistics of this report. Accordingly, the result was further stabilized and continues to show a clear fulfillment of the requirements.

8.4 Summary of External Product Monitoring

No anomalies or non-compliance with the mission requirements were identified. All validation and quality monitoring efforts during the reporting period indicated that the EnMAP product quality is stable and respective mission requirements are fulfilled.

9 Others

EnMAP Mission Operations and Status Publications:

EnMAP Mission Operations and Status Presentations:

- Presented at IGARSS 2024 Workshop (7–12 July 2024. Athens, Greece):
 - “EnMAP Operations Status“ (E. Carmona et al.)
 - “EnMAP German Imaging Spectroscopy Spaceborne Mission: Status and Update two Years after Launch” (S. Chabrilat et al.)